PHOTO-EXCITATION AND DISSOCIATION OF SMALL MOLECULAR CLUSTERS

BEN HEIJMEN

PHOTO-EXCITATION AND DISSOCIATION OF SMALL MOLECULAR CLUSTERS

PHOTO-EXCITATION AND DISSOCIATION OF SMALL MOLECULAR CLUSTERS

EEN WETENSCHAPPELIJKE PROEVE OP HET GEBIED VAN
DE WISKUNDE EN NATUURWETENSCHAPPEN

PROEFSCHRIFT

TER VERKRIJGING VAN DE GRAAD VAN DOCTOR
AAN DE KATHOLIEKE UNIVERSITEIT TE NIJMEGEN,
VOLGENS BESLUIT VAN HET COLLEGE VAN DECANEN
IN HET OPENBAAR TE VERDEDIGEN
OP WOENSDAG 22 JUNI 1988,
DES NAMIDDAGS TE 3.30 UUR

door

BERNARDUS JOHANNES MARIA HEIJMEN

geboren op 22 mei 1959
te Westervoort

Krips repro Meppel
1988

Promotor : **Prof. Dr. J. Reuss**

Co-referent : **Dr. S. Stolte**

Graag wil ik iedereen bedanken die heeft bijgedragen aan het tot stand komen van dit proefschrift, in het bijzonder:

- Alle medewerkers en oud-medewerkers van de afdeling molekuul en laserfysika voor de prettige samenwerking en de stimulerende diskussies.

- Derek Lainé for helpful discussions during his many visits to Nijmegen.

- Peter Verhoeve, Theo Spiertz, Loni Jansen en Gerrit van de Sanden die als student bij het onderzoek betrokken waren.

- Sjaco de Keyzer voor de hulp bij de opbouw van de bundelmachine.

- Cor Sikkens voor zijn onmisbare bijdrages aan het ontwerp en de ontwikkeling van de bundelmachine en de waveguide laser en voor zijn adviezen en technische assistentie.

- John Holtkamp en Frans van Rijn voor de elektronische ondersteuning en vakkundige adviezen.

- Leo Hendriks voor het vervaardigen van het merendeel van de tekeningen in dit proefschrift.

- Eugène van Leeuwen voor zijn inbreng op technisch gebied.

- De medewerkers van de dienstverlenende afdelingen, o.a. de (service) instrumentmakerij, de glasblazerij, vloeibare gassen, fotografie en illustratie.

- Albert van Etteger voor zijn ondersteuning bij de drie-laser experimenten.

- Andreas Rudolph, Lisa Kastner, Christian Lauenstein und Prof. Buck für die schöne Zeit in Göttingen.

- Annette van der Heijden voor haar hulp bij het voltooien van het manuskript.

- Alessandra voor haar ondersteuning en haar bijdrages op wetenschappelijk gebied en Heidi voor haar medeleven bij geboekte successen en bij tegenspoed.

aan mijn ouders

CONTENTS page

CHAPTER 1

INTRODUCTION

1. IR-EXCITATION OF MOLECULAR CLUSTERS AND THEIR PREDISSOCIATION

Clusters can be excited by putting energy (a photon) into a monomer vibrational mode of the molecules within the complex. If the photon energy exceeds the binding energy of the clusters vibrational excitation leads to the rupture of the van der Waals bond (predissociation). The situation is schematically indicated in fig. 1 for a cluster consisting of a diatomic molecule AB and an atom C. The potentials in this figure represent the (dominant) isotropic part of the intermolecular potential. For the lower curve AB is in its vibrational ground state, whereas for the top curve AB is vibrationally excited (indicated by the *). The displacements of the atoms A and B in the vibrationally excited AB-molecule are small in comparison with the distance between AB and C. Consequently, the potentials for AB+C and AB*+C have essentially equal shapes.

In zero order approximation (Hamiltonian H_0) $|\phi_1\rangle$ (see fig. 1) is a bound-state eigenfunction of the excited complex (potential-curve AB*+C) and $|\beta E\rangle$ is a continuum eigenfunction belonging to the lower potential, describing the fragments AB and C flying apart. In the following it is assumed that there is a non-zero transition dipole moment for a transition starting from ground state levels (potential-curve AB+C) to $|\phi_1\rangle$. For the state $|\beta,E\rangle$ this transition dipole moment is assumed to be zero. Predissociation occurs due to a coupling potential W between the vibrational motion in AB* and motions involving changes in the intermolecular distance. In the following the predissociation process will be described in two complementary ways, a "time-picture" and an "energy-picture".

2. A "TIME-PICTURE" OF A PREDISSOCIATION PROCESS

This picture of a predissociation process is adopted from [2,3] in which the decay of a discrete state resonantly coupled to a continuum of final states is treated.

At time t=0 the cluster is assumed to be in $|\phi_1\rangle$, a non-eigenstate of H_0+W (see fig. 2). Preparation of the complex in $|\phi_1\rangle$ can be performed by means of a very short (broad banded in the frequency domain) light pulse [5]. An interesting quantity is the average lifetime τ of the cluster after its preparation in $|\phi_1\rangle$. To simplify the calculations some assumptions about the unperturbed Hamiltonian H_0 are made. The spectrum of H_0 (see fig. 2) includes

(i) the ground state $|\phi_0\rangle$; $H_0|\phi_0\rangle = E_0|\phi_0\rangle$;

(ii) an excited discrete bound state $|\phi_1\rangle$; $H_0|\phi_1\rangle = E_1|\phi_1\rangle$;

(iii) a set of unbound continuum states $|\beta,E\rangle$; $H_0|\beta,E\rangle = E|\beta,E\rangle$. The set of continuous parameters β and the energy E characterize the different states $|\beta,E\rangle$.

The eigenstates of H_0 satisfy the following relations

$$\langle\phi_i|\phi_j\rangle = \delta_{ij} \qquad i=0,1;\ j=0,1$$
$$\langle\phi_i|\beta,E\rangle = 0 \qquad i=0,1$$
$$\langle\beta,E|\beta',E'\rangle = \delta(E-E')\delta(\beta-\beta')$$

It is assumed that the coupling potential W is not explicitly time-dependent and that it has zero diagonal matrix elements. The only non-zero matrix elements are $\langle\beta,E|W|\phi_1\rangle$, representing a coupling between the excited state $|\phi_1\rangle$ and the continuum states $|\beta,E\rangle$, describing the fragments flying apart.

As is demonstrated in [2,3] the probability $|b_1(t)|^2$ of finding the cluster in the bound state $|\phi_1\rangle$ at a time t>0 is given by

$$|b_1(t)|^2 = e^{-\Gamma t}\ , \qquad \Gamma = \frac{2\pi}{\hbar}\int d\beta\ |\langle\beta,E=E_1|W|\phi_1\rangle|^2\ \rho(\beta,E=E_1)$$

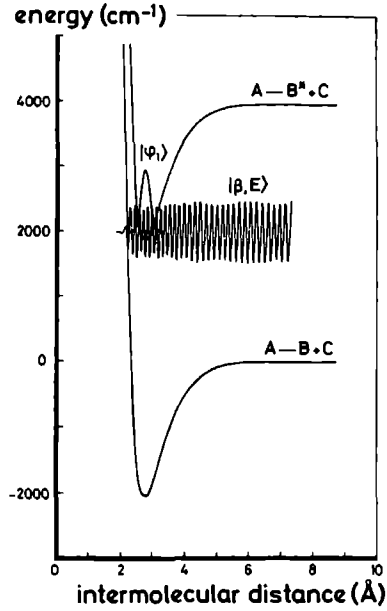

Figure 1: potentials and wavefunctions for the dimer AB+C (adapted from [1]).

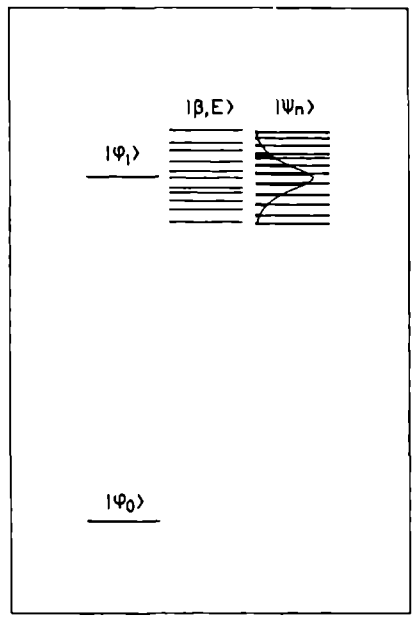

Figure 2: energy levels involved in predissociation processes.

where $\rho(\beta,E)$ stands for the density of the continuum states $|\beta,E\rangle$. These expressions show that due to the coupling W between the bound state $|\phi_1\rangle$ and the unbound states $|\beta,E\rangle$ the excited cluster has a finite average lifetime τ,

$$\tau = \frac{1}{\Gamma} \quad \text{with} \quad \Gamma = \frac{2\pi}{\hbar} \int d\beta \; |\langle \beta, E=E_1 | W | \phi_1 \rangle|^2 \; \rho(\beta, E=E_1)$$

3. AN "ENERGY-PICTURE" OF THE PREDISSOCIATION PROCESS

Due to the coupling potential W $|\phi_1\rangle$ and $|\beta,E\rangle$ (see fig. 2) are not eigenstates of the cluster. The eigenfunctions are linear combinations of $|\phi_1\rangle$ and the functions $|\beta,E\rangle$. A similar problem is treated in [4,5] in which it is assumed that the levels $|\beta_i,E_i\rangle$ are discrete, non-degenerate and uniformly spaced (spacing ε) and that the matrix elements $\langle \beta_i,E_i|W|\phi_1\rangle$ are equal for all $|\beta_i,E_i\rangle$. The eigenfunctions $|\psi_n\rangle$ can be expanded in the functions $|\phi_1\rangle$ and $|\beta_i,E_i\rangle$,

$$|\psi_n\rangle = a_1^n \, |\phi_1\rangle + \sum_i \alpha_i^n \, |\beta_i,E_i\rangle$$

As is demonstrated in [4]

$$|a_1^n|^2 = w^2[(E_n-E_1)^2+w^2+(\frac{\pi w^2}{\varepsilon})^2]^{-1}$$

with $w = \langle \beta_i,E_i|W|\phi_1\rangle$ and E_n the energy belonging to state $|\psi_n\rangle$.

$|a_1^n|^2$ has a Lorentzian shape with a FWHM-width $\Delta E = 2[w^2+(\frac{\pi w^2}{\varepsilon})^2]^{\frac{1}{2}}$.

As stated before, it is assumed that only the state $|\phi_1\rangle$ has a non-zero transition dipole moment with the ground state $|\phi_0\rangle$. Consequently, with a narrow banded laser transitions can be made to a band (FWHM-width ΔE) of final states $|\psi_n\rangle$ with transitions strengths proportional to $|a_1^n|^2$. Energy-levels belonging to functions $|\psi_n\rangle$ are indicated in fig. 2. The lengths of the thick parts of the levels belonging to the functions $|\psi_n\rangle$ in fig. 2 are proportional to the $|a_1^n|^2$-values.

For $\varepsilon \to 0$ (continuum states) $\Delta E \simeq 2 \cdot \frac{\pi W^2}{\varepsilon}$, yielding $\Delta\nu = \frac{W^2}{\hbar\varepsilon}$ in the frequency domain.

To compare with the "time-picture" of predissociation we can replace $\frac{W^2}{\varepsilon}$ by $\int d\beta \; |\langle \beta, E=E_1 | W | \phi_1 \rangle|^2 \; \rho(\beta, E=E_1)$ ($\frac{1}{\varepsilon} \to \int d\beta \; \rho(\beta, E=E_1)$), yielding

$$\Delta\nu = \frac{\Gamma}{2\pi} \quad \text{with as before} \quad \Gamma = \frac{2\pi}{\hbar} \int d\beta \; |\langle \beta, E=E_1 | W | \phi_1 \rangle|^2 \; \rho(\beta, E=E_1)$$

As a consequence we find

$$\Delta\nu \cdot \tau = \frac{1}{2\pi}$$

This relation shows that there is a direct connection between the linewidth $\Delta\nu$ of the "energy-picture" and the lifetime τ of the "time-picture".

The experiments described in the following chapters are all performed with cw, narrow-banded lasers. For $(C_2H_4)_2$ (Chapters 2 and 3), $(SF_6)_2$ (Chapters 4 and 5), $(SF_6)_3$ and $(SiF_4)_2$ (Chapter 5), $(NH_3)_2$ (Chapter 6) and $ArNH_3$ (Chapter 7), predissociation spectra have been studied. For ammonia trimers and some heavier ammonia clusters excitation of the ν_2-monomer mode does not lead to dissociation (Chapter 6). However, for these complexes absorption of a second (red-shifted) photon does yield a rupture of the van der Waals bond.

REFERENCES

[1] G.E. Ewing, Faraday Disc. Chem. Soc. 73 (1982) 325

[2] V.F. Weisskopf and E. Wigner, Z. Phys. 63 (1930) 54

[3] C. Cohen-Tannoudji, B. Diu and F. Laloë, "Quantum Mechanics", Vol. II (John Wiley and Sons, New York, 1977)

[4] M. Bixon and J. Jortner, J. Chem. Phys. 48 (1968) 715

[5] M. Bixon and J. Jortner, J. Chem. Phys. 50 (1969) 4061

High Resolution Measurements of IR Predissociation of C_2H_4 Dimers

B. Heijmen, C. Liedenbaum, S. Stolte, and J. Reuss
Fysisch Laboratorium, Katholieke Universiteit Nijmegen,
Nijmegen, The Netherlands

Received April 6, 1987

The narrow lines on top of the broad homogeneous background of the $(C_2H_4)_2$ predissociation spectrum are studied. The high resolution spectra are measured tuning the length of a CO_2 waveguide laser by means of a PZT yielding a frequency scan of 230 MHz around the CO_2 laser lines. In the absense of power broadening a minimum non-instrumental linewidth of 3.5 MHz fwhm is found, corresponding to a lower limit for the predissociation lifetime of 45 ns From the power broadening of the strongest sharp line a transition dipole moment of 0.14 Debye has been determined. To this transition corresponds a saturation fluence $F_{sat} = 3\ \mu J/cm^2$, in strong contrast with $F_{sat} = 20\ mJ/cm^2$ for the broad background. The dependence of the ratio structure/background on the concentration of C_2H_4 in He, on the source temperature and on the stagnation pressure, yields insight in the origin of the co-existence of the broad background and the narrow lines. Evidence is found that the sharp lines are due to dimers with low internal energies, whereas the background originates mainly from dimers with higher internal energy. By means of a two-laser experiment it is shown that the sharp peaks are inhomogeneous. Moreover, the first laser can significantly diminish the background predissociation signal produced by the second laser without consequences for the height of the sharp peaks.

PACS: 36.40, 33.20E; 33.80G

1. Introduction

$(N_2O)_2$ was the first dimer to be studied by infrared predissociation spectroscopy [1]. Shortly afterwards, $(C_2H_4)_2$ was observed to dissociate when irradiated by CO_2-laser photons [2]. Since then, $(C_2H_4)_2$ has often been studied, using pulse CO_2-lasers [3], *cw* CO_2-lasers [4–7] and FC-lasers [8]. The dimer predissociation results have been reviewed in [9–12].

The challenge came from the first observed broad excitation profiles with fwhm $\Delta\tilde{\nu} > 10\ cm^{-1}$, which led to predissociation lifetimes $\tau = 1/(2\pi\Delta\nu) < 1$ ps. Because of the large mismatch between the excitation energy (about $950\ cm^{-1}$) and the v.d. Waals mode energies (about $30\ cm^{-1}$) this short lifetime has stimulated theoretical work [13–15] which led from the prediction of much longer lifetimes to the question whether important coupling mechanisms might have been overlooked.

In Table 1, some experimental results with respect to linewidth are summarized. It seems that the different systems investigated can be divided into four groups – short lived ones like $(SF_6)_2$, long lived ones like $(C_2H_2)_2$, systems with mode-specific predissociation times like $(HF)_2$ and finally the system $(C_2H_4)_2$, which shows evidence of ambivalent behaviour [6, 7] as will be discussed in detail in the present paper.

Before entering this discussion, the important contributions of the Göttingen group have to be mentioned. Their method of time-resolved differential scattering permits a definite means of distinguishing between dimer- and higher multimer-signals yielding e.g predissociation spectra for $(C_2H_4)_n$ with $2 \leqq n \leqq 6$ [26–30]. Moreover, the method allows predissociation of either cold [26] or hot clusters [27, 28]. In the latter case the energy deposited into the clusters comes from the collision with the scattering partner He used to deflect the complexes before they are dissociated by exposing them to the radiation of a line-tunable pulsed CO_2-laser.

In Fig. 1 the laser conditions are summarized, with which the various investigators have attacked the

Table 1. Ir-excited dimers with short and long lifetimes The excited mode and its frequency are shown in column 2 and 3 The homogeneous linewidth is obtained by double resonance measurements, for the upper-section The next section contains the observed long living dimers The third section shows two examples where different mode-specific linewidths have been observed In the bottom section $(C_2H_4)_2$ shows an ambiguous behaviour The homogeneous width yields the width-time (lifetime) $\tau = 1/(2\pi\Delta\nu)$

Dimer	Transition	Frequency [cm^{-1}]	Homogeneous width	Width time	Reference
$(SF_6)_2$	ν_3	948	0 8 cm^{-1}	6 6 ps	[16, 17]
$(NH_3)_2$	ν_2	950	1 cm^{-1}	5 5 ps	[17]
$(SiF_4)_2$	ν_3	1031	3 cm^{-1}	2 ps	[17]
$(C_2H_2)_2$	$\nu_3(\nu_2+\nu_4+\nu_5)$	3295(3282)	2 MHz	80 ns	[18, 19]
$(C_3H_4)_2$	ν_1	3334	375 MHz	0 4 ns	[19]
$(N_2O)_2$	$\nu_1+\nu_3$	3481	16 MHz	10 ns	[20]
$(CO_2)_2$	$\nu_1+\nu_3$	3716	$\leqq$3 MHz	$\geqq$50 ns	[20]
$(HF)_2$	H-bonded/free $H-F$ vibration			1 ns/22 ns	[21-24]
$(NO)_2$	symm/asymm vibration			880 ps/39 ps	[25]
$(C_2H_4)_2$	ν_7	948	12 cm^{-1}	0 4 ps	[3-5, 23]
$(C_2H_4)_2$	ν_7	948	3 5 MHz	50 ns	[6, 7] present work

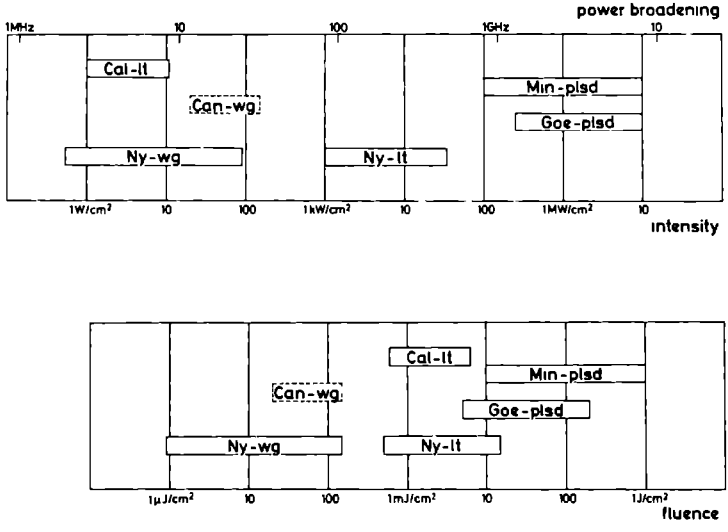

Fig. 1. In the lower (upper) part, the experimental conditions are summarized with respect to laser fluence (laser intensity) for the Minneapolis and Göttingen pulsed lasers [3, 27], the Caltech and Nijmegen line tunable lasers [4–6] and the Canberra and Nijmegen waveguide lasers [7] The pulse length of [3] was assumed to be 10^{-7} s, the pulse length of [27] is stated to have been 20 ns, the waveguide laser of Nijmegen had a focus diameter of $D=2.4$ mm ∅ (here $f=75$ cm is taken, see Sect 2) i e an interaction time of $\tau = 2\ 10^{-6}$ s, the Nijmegen-line tunable laser had four times smaller τ and D values The power-broadening Δ (fwhm $= 2\nu_{Rabi}$) has been calculated from $\Delta = 2.56\sqrt{I}$ [MHz], I in W/cm² This corresponds to a space averaged transition dipole moment of $0.16/\sqrt{3}$ Debye

$(C_2H_4)_2$ problem. In this figure the laser intensity, the laser fluence and its power-broadening ($2\nu_{Rabi} = 2\mu_{01}E/h$) are displayed, where for the transition dipole moment μ_{01} of the dimer the Göttingen result has been used [23], $\mu_{01} = 0.16 \pm 0.04$ Debye. The differences in interaction time due to laser pulse duration or focusing conditions are stated in the caption.

2. Experimental

The measurements were performed using the bolometer apparatus described in detail elsewhere [6]. In brief, a bolometer detects energy. Irradiation of a molecular beam by a CO_2-laser dissociates the clusters in the beam. The fragments leave the molecular beam so that a reduction of the energy flux to the bolometer is obtained, resulting in a change of the bolometer signal. By modulating the CO_2-laser intensity by a chopper, phase-sensitive detection can be used. The sensitivity of the bolometer in these experiments was such that we could see changes of $1:10^6$ of the total beam energy (i.e. NEP $= 8 \cdot 10^{-14}$ W/Hz$^{\frac{1}{2}}$).

Most of the measurements were done with a 5% C_2H_4 in He mixture, stagnation pressure $P_0 = 5$ atm,

source temperature 293 K. In case of deviating conditions these will be indicated in the text. The nozzle consisted of a platinum-iridium electron microscope diaphragm (Siemens) with a diameter of 30 micron.

There was a choice between three laser sources.

1) A homebuilt 62.5 cm CO_2 waveguide laser with output power up to 5 W and a tunability of 230 MHz around the CO_2-laser lines.

2) A homebuilt 2 m line tunable CO_2-laser with more power (50 W), but less tunability (75 MHz).

3) A modified version of *2)* to create an intracavity set-up with a power up to 400 W. The normal end-mirror ($r = 10$ m) of the CO_2-laser has been replaced by the combination of a ZnSe lens ($f = 40$ cm) and a partially reflecting ($R = 95\%$) curved end mirror ($r = 40$ cm), producing a focused laser beam of high intensity. This focal point was placed on the intersection with the molecular beam. The distance lens to end mirror was 80 cm. The power and mode structure could be monitored by detecting the radiation transmitted through the end mirror. Care was taken to keep the laser as much as possible in the TEM_{00} mode. Due to mechanical instabilities of the laser cavity the laser linewidth was equal to the free spectral range of 30 MHz (cavity length = 5 m).

To focus the waveguide laser on the molecular beam two lenses could be used. The lenses had focal lengths of 75 cm and 40 cm, resulting in a spot diameter of 2.4 mm and 1.3 mm, respectively. The intracavity laser focus had a diameter of 0.6 mm.

The effective molecular beam diameter for the intracavity laser (waveguide laser) was 0.3 mm (0.6 mm). The distance between source and bolometer was 50 cm. The dimensions of the bolometer were 2×5 mm^2, resulting in an acceptance angle for the molecular beam smaller than 0.6°.

Scanning the waveguide laser was performed by putting a high voltage ramp on a PZT that controlled the length of the cavity. The power was monitored via a beam splitter by a pyro-electric detector. No attempt was made to keep the waveguide laser power constant during a scan. The power was varied by attenuating the laser beam with a dual brewster plate assembly. Over a period of about 100 s the frequency stability of the waveguide laser was better than 1 MHz.

3. Results

3.1. General Aspects

The main feature of the present work is the systematic study of laser intensity and source condition dependence of the narrow transitions in the predissociation spectra of $(C_2H_4)_2$. These narrow spectral structures have been observed for all CO_2-laser lines near to the maximum absorption at 952 cm^{-1} (10P6 ÷ 10P16) (Fig. 2) and near to the center of the combination band at 986 cm^{-1} (10R32 ÷ 10R40) (Fig. 3). The further away from these center frequencies the less pronounced the narrow sectral features become. For the line 10P18, sharp peaks are at least a factor 20 weaker than for the strongest peak of the 10P12 transition. Narrow peaks have been reported before [6, 7]. Here we have reduced the linewidth to 3.5 MHz by employing a very stable laser at low power.

For monomer absorption (4, 1, 3) → (5, 0, 5), an (instrumental) linewidth of 1 MHz fwhm has been observed, see Fig. 2d. The narrow dimer peaks are always significantly broader, showing minimum widths of 3.5 MHz fwhm. The maximum, not power broadened width (see 3.2) we measured was 6.5 MHz.

All these peaks near 952 cm^{-1} are superimposed on a broad background, the relative strength of which dramatically depends on laser power, C_2H_4-source concentration in He, source temperature and pressure (see Fig. 5, 6 and 7) as will be discussed below. At CO_2-laser transitions further away from 952 cm^{-1} (e.g. 10P4 (957.8 cm^{-1}) and 10P20 (944.19 cm^{-1}), see Fig. 2a) only this broad structureless background is observed if the waveguide laser is scanned over its tuning range of 230 MHz. The combination band near 986 cm^{-1} shows little of this background; the observed background can be attributed to the blue tail of the main transition centered at 952 cm^{-1}.

As a side-remark we mention the fact that the monomer transition (4, 1, 3) → (5, 0, 5) does not exhibit power broadening. From Fig. 1 it is clear that sizeable power broadening was to be expected for the highest laser power used, i.e. about 20 MHz. This phenomenon has been observed before and was attributed to multiphoton transition, accidentally and strangely unaccompanied by spectral shifts [31]. The bolometer signal, however, shows saturation at low intensity already (300 mW/cm^2). This result renders the multiphoton hypothesis even more questionable and interesting since it would require that a highly excited C_2H_4 molecule deposits only one ν_7-photon as energy on the bolometer, independent of the level of excitation.

3.2. Laser Intensity Effects

The continuously scanned spectra around the different CO_2-laser transitions 10P4 – 10P8 depend very much on the applied laser power. At the lowest intensity the background is almost gone and only the strongest sharp peaks remain, see Fig 5. At an intensi-

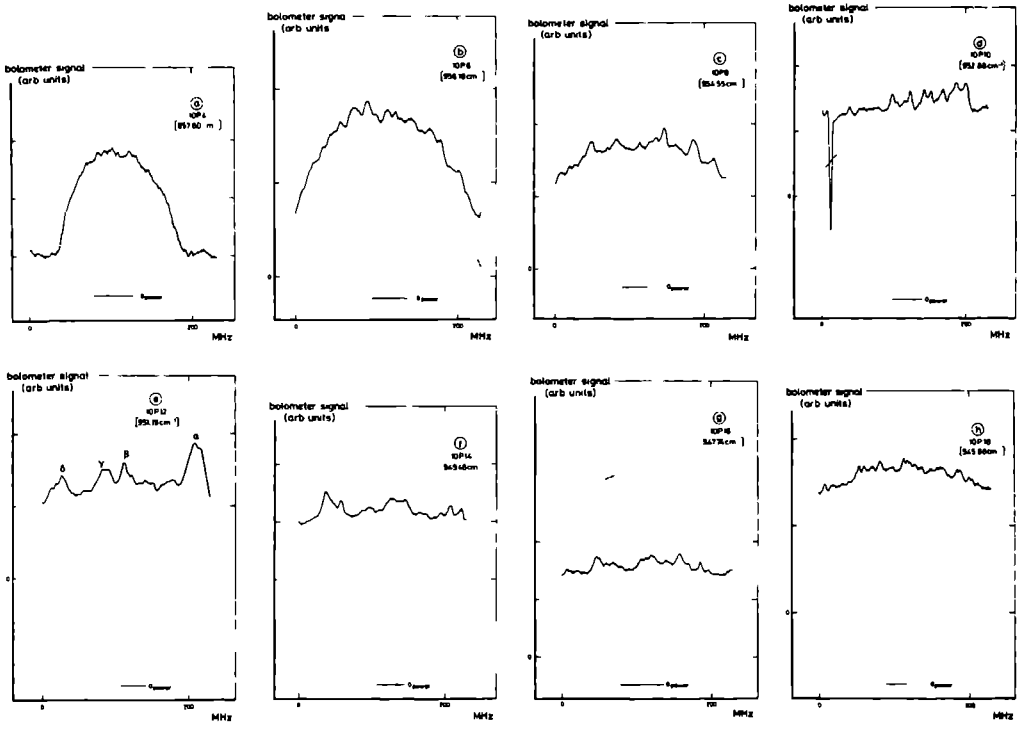

Fig 2a–h. High resolution spectra around several CO_2 laser lines in the neighbourhood of the centre of the main peak (952 cm^{-1}) of the $(C_2H_4)_2$ predissociation spectrum The source conditions are $P_0 - 5$ atm $T_0 = 293$ K $C = 5\%$ C_2H_4 in He The figures which are numbered from a to h are respectively taken around the 10P4 10P6 10P8 10P10 10P12 10P14 10P16 and 10P18 CO_2 laser lines The maximum applied laser intensity is respectively 22 W/cm^2 42 W cm^2 51 W/cm^2 62 W cm^2 64 W/cm^2 67 W/cm^2 67 W/cm^2 69 W/cm^2 The interaction time with the laserfield is 1 6 μs The dashed lines represent a monitor of the power during the different frequency scans. The absolute height of the different lines should not be compared In d the strong negative peak is due to the (4 1 3)→(5 0 5) monomer transition

ty of 20 W/cm^2 must of the narrow lines are saturated and broadened due to power broadening, while the background signal is still increasing linearly with laser fluence At higher laser intensity the saturation of the narrow peaks yields a smooth predissociation spectrum At a laser power for which the background is also saturated, the ratio structure to background becomes of the order 10^{-3}, for the 10P12 laser line To measure the power dependence of the background signal two experiments were performed In one the waveguide laser was scanned around the 10P12 CO_2 laser line with and without a high power laser pumping on the 10P10 CO_2 laser line (see Sect 3 4) In this way the attenuation of the background signal in the waveguide laser spectrum has been measured as a function of pump laser power The remaining fraction of the background signal shows an exponential decay with increasing fluence resulting in a e [1] remaining fraction for $F_{sat} = 20$ mJ/cm^2 ($I_{sat} = 50$ kW/cm^2) The power dependence of the background signal was also determined in a one laser experiment by measuring the dissociation signal of the high power intracavity laser at the 10P12 laser line as a function of fluence (even at rather low powers the contribution of a few narrow lines can be neglected), yielding a saturation bolometer signal B_{sat} The sharp structures saturate already at some W/cm^2, the strongest one observed (peak α of Fig 5) at $I_{sat} = 2$ W/cm^2 ($F_{sat} = 3$ μJ/cm^2), with a corresponding bolometer signal $b_{sat} = 5\ 10^{-3} B_{sat}$, with $P_0 = 5$ atm, $C = 5\%$ and $T_0 = 293$ K Here C stands for the concentration of C_2H_4 in He

At low laser intensities the width of the sharp spectral structures depends only on the lifetime and is independent of the applied laser power For higher laser powers the width of the lines is proportional

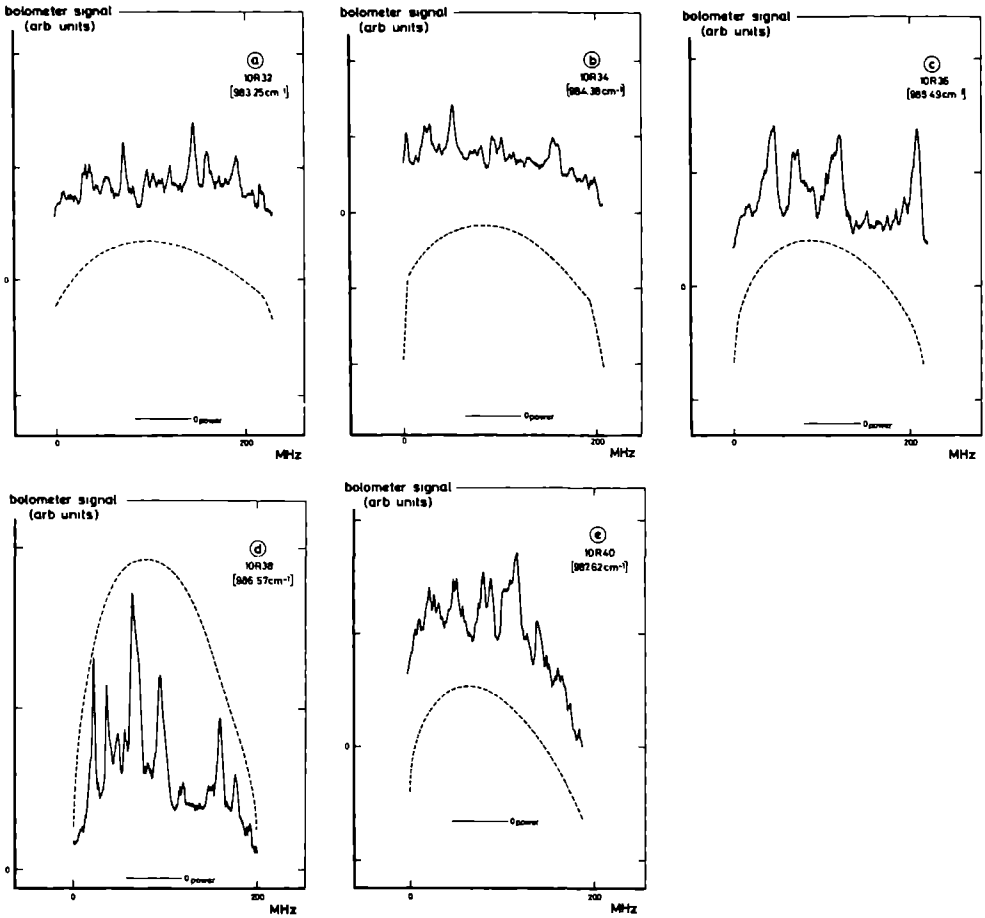

Fig. 3a–e. High resolution spectra around several CO_2 laser lines in the neighbourhood of the combination band (986 cm^{-1}) of the $(C_2H_4)_2$ predissociation spectrum The source conditions are $P_0 = 5$ atm, $T_0 = 293$ K, $C = 5\%$ C_2H_4 in He The spectra numbered from a to e are taken respectively around the 10R32, 10R34, 10R36, 10R38 and 10R40 CO_2 laser lines. The maximum applied laser intensity is respectively 56 W/cm^2, 56 W/cm^2, 44 W/cm^2, 44 W/cm^2, 33 W/cm^2 The interaction time with the laserfield is 1 6 μs The dashed lines represent a monitor of the power during the different frequency scans The absolute height of the different lines should not be compared

to $\sqrt{I}$; here I is the applied laser intensity (see Fig. 4). For example, for peak α in Fig. 5 we found: $\Delta = 3.8\sqrt{I}$ (fwhm in MHz, I in W/cm^2). According to $\Delta = 2\nu_{Rabi} = (2\sqrt{2}\mu_{01}/h(\varepsilon_0 c)^{\frac{1}{2}})\sqrt{I}$, the transition dipole moment μ_{01} corresponding to peak α is determined to be 0.14 Debye, in agreement with the value 0.16 Debye for the broad background as observed by [26]. For different peaks the value of I_{sat} varies by at least a factor of 20.

The combination band around 986 cm^{-1} shows sharp peaks which saturate for $I_{sat} \geqq 80$ W/cm^2 ($F_{sat} \geqq 65$ μJ/cm^2), i.e. $\mu_{01} \leqq 0.03$ Debye. These peaks are apparently without background. The fwhm of the frequency band around 986 cm^{-1} where predissociation is observed is 5.5 cm^{-1} [6]. For 10R42 and 10R30, the maximum predissociation signal has at least been 20 times weaker than that observed around the 10R38 line to escape from observation.

The little background appearing under the sharp spectral structures of the combination band is attributed to the blue tail of the main band lorentzian.

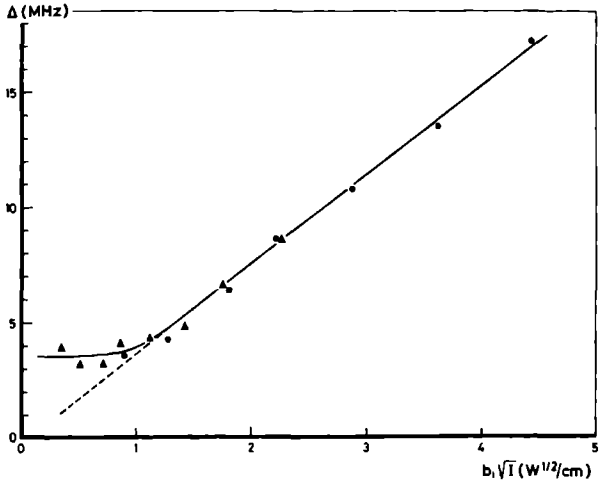

Fig. 4. The linewidths of the peaks α and δ (see Fig. 5) as a function of laserpower For high laser power we find $\Delta_\alpha = a_\alpha\sqrt{I}$ with $a_\alpha = 3.8$ MHz W$^{-\frac{1}{2}}$ cm, $a_\delta = 1.5$ MHz W$^{-\frac{1}{2}}$ cm $b_\alpha = 1$, $b_\delta = a_\delta/a_\alpha$ which is proportional to the quotient of the transition dipole moments of the two lines The symbols ● and ▲ correspond to peaks α and δ, respectively

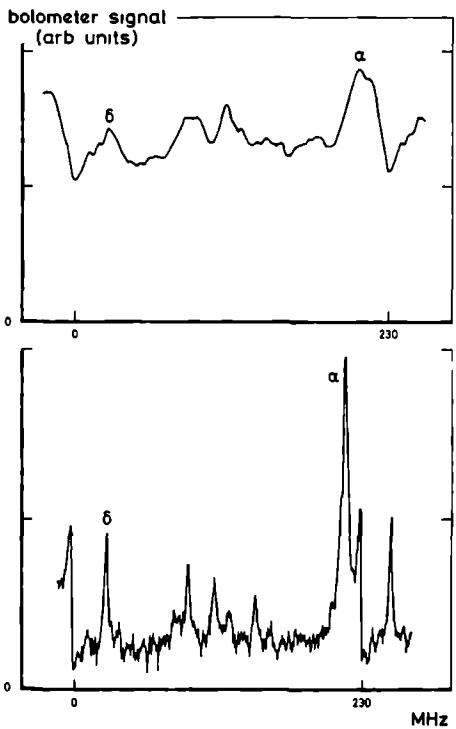

Fig. 5. High resolution spectra around the 10P12 CO_2 laser line (951.2 cm^{-1}) The source conditions are $P_0 = 5$ atm, $T_0 = 293$ K, $C = 5\%$ C_2H_4 *in He The upper (lower) spectrum is measured with* a laser intensity of 67 W/cm^2 ($F = 100$ μJ/cm^2) (3 W/cm^2, ($F = 5$ μJ/cm^2)) One can clearly notice the power broadening and the appearance of the background for high power

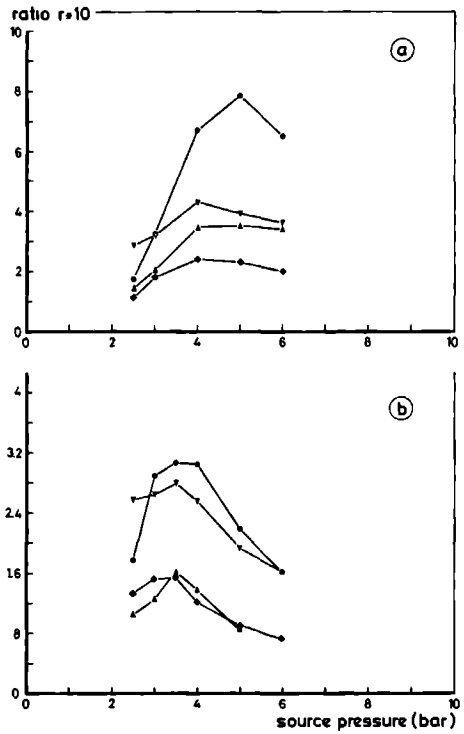

Fig. 6a and b. The structure to background ratio r as a function of stagnation pressure for four narrow lines of the $(C_2H_4)_2$ predissociation *spectrum around the 10P12 CO_2-laser transition*, **a** $C = 5\%$ C_2H_4 in He, **b** $C = 12.5\%$ C_2H_4 in He One can clearly see that the relative intensity of the lines changes as a function of stagnation pressure The laser intensity for both **a** and **b** is 50 W/cm^2 ($F = 30$ μJ/cm^2) The source temperature is 293 K The symbols ●, ◆, ▼ and ▲ correspond respectively to the lines α, β, γ and δ in Fig 2e

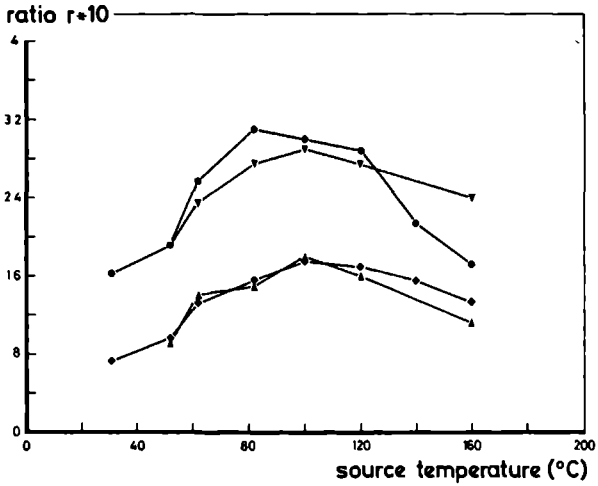

Fig. 7. The structure to background ratio r as a function of source temperature for four narrow lines of the $(C_2H_4)_2$ predissociation spectrum around the 10P12 CO_2-laser transition, $C = 12.5\%$ C_2H_4 in He The stagnation pressure is 6 bar The laser intensity is 50 W/cm^2 ($F = 40$ μJ/cm^2) The symbols ●, ◆, ▼ and ▲ correspond respectively to the lines α, β, γ and δ in Fig 2e

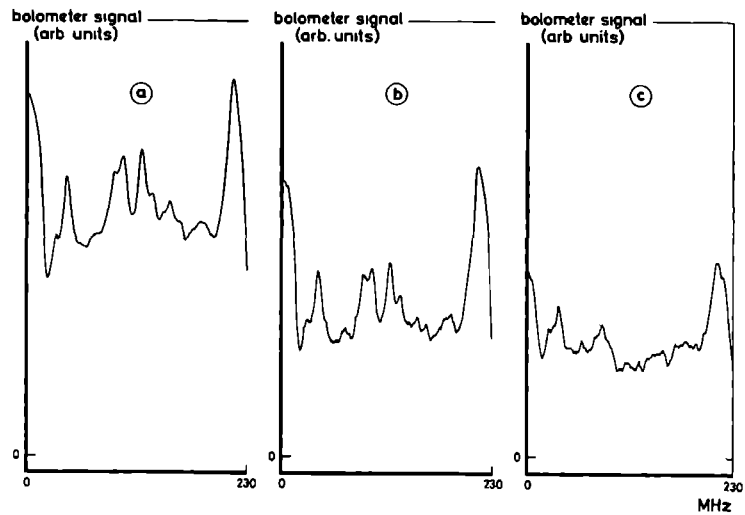

Fig. 8a–c. **a** High resolution spectra around the 10P12 CO_2 laser line The source conditions are $P_0 = 5$ atm, $T_0 = 293$ K, $C = 5\%$ C_2H_4 in He. The laser intensity is 24 W/cm^2 ($F = 65$ μJ/cm^2) **b** The same spectrum while pumping with a second laser on the 10P10 laser line with an intensity of 35 kW/cm^2 ($F = 14$ mJ/cm^2). **c** Again the same spectrum but now pumping on the 10P12 laser line with an intensity of 35 kW/cm^2 ($F = 14$ mJ/cm^2)

3.3. Stagnation Condition Effects

To get clues concerning the origin of the sharp predissociation peaks and the broad background, the source conditions were varied. Measurements were performed for $2.5\ \text{atm} \leqq P_0 \leqq 6\ \text{atm}$, $293\ \text{K} \leqq T_0 \leqq 433\ \text{K}$, $0.5\% \leqq C \leqq 25\%$.

The peak/background ratio r diminishes for increasing C. For example $(C; r) = (0.5\%; 0.8)$, $(5\%; 0.4)$ and $(12.5\%; 0.1)$ has been found, for $T_0 = 293$ K and $P_0 = 6$ atm and a laser intensity of 50 W/cm^2.

The results for various source pressures P_0 are displayed in Fig. 6, for $C = 5\%$ and 12.5% and $T_0 = 293$ K. There exists an optimum P_0-value, where r is at a maximum. Similarly, for $P_0 = 6$ atm and $C = 12.5\%$ we found an optimum T_0-value (Fig. 7). For higher source temperatures (lower stagnation pressures) the dimers are produced with higher internal energies, apparently yielding smaller r-values. At lower temperatures (higher stagnation pressures) the beam contains heavier clusters in addition to dimers and monomers, accompanied by smaller r-values.

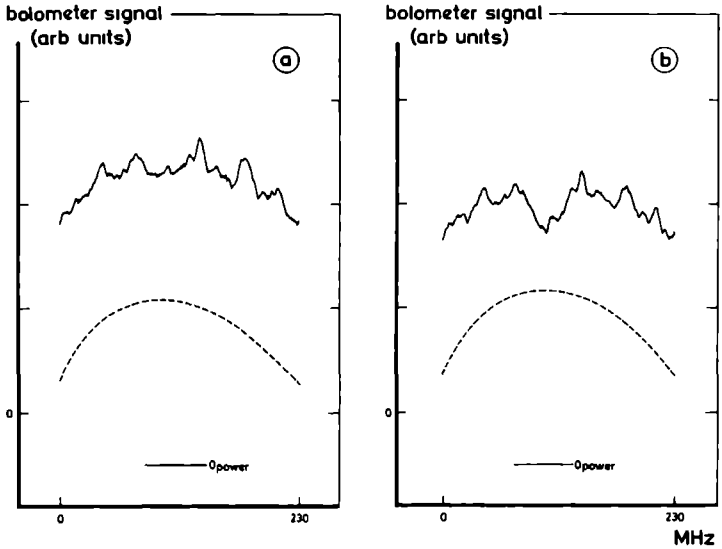

Fig. 9a and b. a High resolution spectra around the 10P8 CO_2 laser line The maximum laser intensity is 50 W/cm^2 ($F = 80$ μJ/cm^2) The source conditions are $P_0 = 5$ atm, $T_0 = 293$ K, $C = 5\%$ C_2H_4 in He b The same spectrum while pumping with a second laser on the 10P8 laser line The pump laser intensity is 12 kW/cm^2 ($F = 5$ mJ/cm^2)

Both these results of Figs 6 and 7 play a key role in our understanding of the predissociation process as will be discussed below

3 4 Two-Laser Excitation

To check whether the measured predissociation spectra were homogeneous or inhomogeneous two-laser experiments have been performed The waveguide laser served as a probing device over its 230 MHz free spectral range while the line-tunable laser was set at the various center frequencies of the CO_2-transitions to pump the $(C_2H_4)_2$ up to predissociative states In Fig. 8a and Fig 8b is shown the spectrum obtained around the 10P12 line (951 20 cm ^{1}) with and without pumping at the 10P10 transition (952 88 cm^{-1}) A homogeneous reduction of the background signal is observed whereas the sharp peaks remain unaltered In this measurement the intensity of the pump (probe) laser was 35 kW/cm^2 (20 W/cm^2) Setting the pump-laser, too, on the 10P12 transition led, in addition to the reduction of the background signal, to the disappearance of two sharp peaks, corresponding to frequencies close to the pump frequency, which is near the center of the scanning range of the waveguide laser (Fig 8c). The other sharp peaks are diminished in agreement with the expected power broadening at the intensity of the pump-laser (35 kW/cm^2, see Fig 1)

If both pumping and probing occurs at the 10P8 (954 55 cm^{-1}), the 10P16 (947 74 cm^{-1}), the 10P20 (944 19 cm^{-1}) or the 10P22 (942 38 cm^{-1}) CO_2-transitions (at 10P20, 10P22, 10P24 and 10P26 no sharp peaks have been observed) a small inhomogeneous hole (width of about 3 MHz) is burned into the background signal, which shows also a homogeneous overall reduction as before (Fig 9) Note that the width of 30 MHz is considerably smaller than the power broadening calculated above for the applied laser intensity, 250 MHz fwhm at 12 kW/cm^2, see Fig 1

These experiments clearly demonstrate that there are homogeneous and inhomogeneous contributions to the predissociation spectrum The strength of the homogeneous part follows the broad line shape of the main peak (fwhm about 12 cm^{-1}) that has been observed formerly in experiments with line-tunable lasers [4, 5]

Against all odds we tried, in vain, to find correlation between at least some of the sharp peaks, depleting one and attempting to observe a diminution in the other In this unsuccessful search the sharp peaks of the combination band (around 986 cm^{-1}) were also included

4. Discussion

4.1 The Co-Existence of Broad and Narrow Spectral Structures

Remarkably the spectral features fall into two groups either they are extremely narrow or they are extreme-

ly broad No continuous distribution over various linewidths is found

We are convinced that dimers are responsible for both the narrow peaks and at least part of the broad background The peak to background ratio r does not increase continuously if the stagnation conditions are changed such that the dimer to heavier cluster proportion definitely increases (by lowering P_0 or rising T_0, see Sect 3 3) Therefore the background cannot be attributed exclusively to higher clusters But also the opposite cannot be true, for example that the trimers are responsible for the narrow structures and the dimers produce nothing but broad background Then, at lower C_2H_4 concentrations C lower values of r would be expected, contrary to our experimental findings (see Sect 3 3) Moreover, mass-spectrometer measurements (Baldwin and Watts [7]) show no narrow line predissociation on ion-masses which can be attributed exclusively to neutral trimers and heavier clusters

It is hard to estimate quantitatively the fraction of the dimers that produces the sharp and inhomogeneous spectral structures We put the inhomogeneous fraction proportional to the sum of all the signals due to the sharp peaks, measured at a power for which peak α (see Fig 5, the measured peak with the lowest I_{sat}) has the signal $b^{(\alpha)}$ and is not saturated, multiplied by $b^{(\alpha)}_{sat}/b^{(\alpha)}$ Here $b^{(\alpha)}_{sat}$ stands for the saturated bolometer signal of peak α Due to the limited scanning range of the waveguide laser only a part of the sharp peaks could be measured From these measurements an average inhomogeneous signal per frequency interval was deduced, which multiplied by the frequency range in which sharp peaks are to be expected leads to the total inhomogeneous contribution The homogeneous fraction is proportional to B_{sat} (see 3 2) if the contribution of heavier clusters is neglected Thus the (slightly overestimated) ratio "homogeneous" dimers/"inhomogeneous" dimers becomes of the order of 1 Both the Minneapolis group [3] and the Gottingen group [26] find a remaining, non-dissociable fraction in their molecular beams Especially the remaining fraction of 10^{-3} of [3], which was attributed to an impurity in the beam or to an incomplete overlap of the laser beam with the molecular beam, seems to be in contradiction with our observation that a substantial part of the dimers belongs to the inhomogeneous fraction However, the Minneapolis experiments have been performed at intensity levels 5 orders of magnitude higher than the Nijmegen waveguide laser measurements and 2 orders of magnitude higher than the line-tunable laser measurements (see Fig 1) Thus, high laser intensity effects could be responsible for the apparent discrepancy (see 4 2) A large contribution of heavier clusters present in the Minneapolis experiments could also reduce the discrepancy The Gottingen group assumes that their remaining fraction of 24% is an artifact and completely due to newly formed dimers by dissociation of heavier clusters [26]

The transition dipole moment derived in [26], $\mu_{01} = 0\,16 \pm 0\,04$ Debye, is in agreement with our observations of line broadening, see Sect 3 2 Actually the saturation behaviour for both the strong sharp spectral structure and the broad background can be explained with the same value of the transition dipole moment The value I_{sat} for the broad background is $0\,25\ 10^5$ times higher than for the strongest sharp feature, in accordance with a fwhm, which is 10^5 times larger ($12\ cm^{-1}$ vs $3\,5$ MHz)

The width, within which strong narrow peaks are observed extends from the 10P8 to the 10P14 transition of the CO_2-laser, i e over about $5\ cm^{-1}$ This width is definitely smaller than the fwhm of the broad lorentzian background ($12\ cm^{-1}$) It is comparable to the width of the combination tone at $986\ cm^{-1}$ [6]

Next we shall discuss various hypotheses by which the co-existence of broad and narrow structure can be explained

A The "ν_{10} Dissociation Threshold" Hypothesis In this model, the broad background in our measurements is produced by dimer transitions where the final state containing still one ν_{10} monomer excitation lies above the dissociation limit, i e above the ν_{10} dissociation threshold The arguments in favour are that the structure to background ratio r starts to increase at very low stagnation pressures P_0 and/or high temperatures T_0 (i e for relatively warmer dimers) and that a distinct change in lifetime is expected for dimers excited to levels above and below the ν_{10} dissociation threshold in agreement with our experimental findings

A counter-argument might be that the estimated well-depth of $350\ cm^{-1}$ [32] excludes any dimers to be excited above the ν_{10} dissociation threshold, in view of the measured beam temperature of 10 K [34] However, this argument has to be handled with care First, by fast internal $\nu_7 \rightarrow \nu_{10}$ relaxation an energy of $125\ cm^{-1}$ can be disposed of to overcome the dissociation energy Secondly, a considerable amount of zero-point energy has to be taken into account, for the six v d Waals modi According to Beswick [33], the total zero-point energy amounts to $150\ cm^{-1}$, i e only $200\ cm^{-1}$ of energy is needed for dissociation, of which $125\ cm^{-1}$ is furnished by the $\nu_7 \rightarrow \nu_{10}$ relaxation Thirdly, the well depth is not known accurately It is quite possible that it is overestimated by $50\ cm^{-1}$ But then the counter-argument turns around into an

argument in favour of hypothesis *A*. Finally it is not at all sure that during the expansion all dimers are cooled down to the configuration of minimum energy. A sizable fraction may remain in a metastable state of significantly higher energy. The source conditions influence the cooling process and thus this metastable fraction

Since we observe narrow lines for the combination tone we may conclude that 30 cm^{-1} extra energy does not suffice to overcome the ν_{10} dissociation threshold. The fact that around 986 cm^{-1} no clear background has been observed yields no further hint. The reason can be that we had not enough laser power to excite these background transitions which are more than 10 times weaker than the background transitions around 950 cm^{-1}. The latter produce a background tail at 986 cm^{-1}.

B. The "High Density of States" Hypothesis. To produce a homogeneously broadened line a high density of final states suffices distributed over an energy interval corresponding to the observed linewidth of 12 cm^{-1}. To be in agreement with our observation, about 10^5 upper levels with a width of 3.5 MHz have to be postulated, accessible for each lower state level which, being excited, yields a contribution to the observed broad background. We consider this improbably large number as a counter-argument, since it seems incompatible with selection rules. A second counter-argument is derived from the experimental fact that two classes of transitions, with 3.5 MHz fwhm and with 12 cm^{-1} fwhm, have been observed, whereas one expects from hypothesis *B* that there are ground state levels from where single upper states and the maximum number of upper states (10^5) can be reached, but that also intermediate cases occur, producing linewidths of e.g. 25 MHz, etc.

However improbably Hypothesis *B* looks to explain our results, it can play a role for high intensity measurements [10, 28], where two-level power broadening to about 5 GHz occurs (see Fig. 1) and therefore a much smaller number of accessible upper levels is needed (about 70 at 5 MW/cm^2). This point will be discussed below, see 4.2.

C. The "IVR" Hypothesis. The co-existence of narrow structures and a broad background in the $(C_2H_4)_2$ predissociation spectrum has been explained by using a model which includes fast intramolecular vibrational relaxation (IVR) [35]. According to this model for $(C_2H_4)_2$ $\Gamma_D \ll \Gamma_I$ and $\Gamma_D \ll \varepsilon$. Here Γ_D (Γ_I) is the decay width associated with dissociation (IVR) and ε is the spacing between the "bath" states. However, our two-laser experiments show no correlation between the several narrow peaks, nor between the narrow peaks and the broad homogeneous background. These observations are in contradiction with the implication of homogeneity of the IVR hypothesis Moreover, the broad background and the narrow peaks show a completely different saturation behaviour

In general, we adhere to a discussion remark made by W. Klemperer in a Nato-ARW 1986 Klemperer demands that IVR should be considered mainly as an emergency brake in case all other possibilities are exhausted to explain the experimental facts. In our case Hypothesis *A* still seems to yield a working model and thus we reject IVR for the time being.

4.2. *High Laser-Intensity Measurements*

The problem remains how to reconcile the high laser-intensity measurements on cold dimers with the insight gained from the present work. At 5 MW/cm^2 (100 mJ/cm^2), at least 60% of all dimers are dissociated (uncorrected value) [26]. This result is not in contradiction with our order of magnitude estimate of dissociable/non-dissociable dimers. For hot dimers larger dissociation rates have been observed [27], but those results should not be compared with the present measurements on cold clusters

However, the 10^{-3} fraction of non-dissociable cold clusters of [3] seems incompatible with our measurements. The high laser intensities applied (2 MW/cm^2 average intensity) do not permit to exclude multiphoton processes entirely in [3]. For instance, at 50 MW/cm^2 two-photon excitation should already be significant This estimate is based on

$$\Omega^{(2)}_{\mathrm{Rabi}} = \frac{[\Omega^{(1)}_{\mathrm{Rabi}}]^2}{4\pi\Delta}$$

and

$$P_2 = (1 - \cos \tfrac{1}{2}\, \Omega^{(2)}_{\mathrm{Rabi}}\, t)/2,$$

where $\Omega^{(1)}_{\mathrm{Rabi}}$ ($\Omega^{(2)}_{\mathrm{Rabi}}$) stands for the circular one-(two-) photon Rabi-frequency, P_2 for the population probability of the final levels and Δ for the detuning of the intermediate level put equal to the width of the homogeneous background. Peak intensities of 50 MW/cm^2 can have occurred in the fluctuating laser pulses of [32].

Besides multiple photon excitation high dissociation rates e.g. at $I = 50$ MW/cm^2 can also be partially be due to another mechanism. There is something wrong with our estimates of power broadening. The conventional $2\Omega^{(1)}_{\mathrm{Rabi}}$, fwhm, is based on two and only two levels participating in the excitation process. However, with all those closely spaced transitions ob-

served, power broadening increases significantly If about 400 closely spaced initial levels are coupled to an equal number of closely spaced final levels in such a way that each initial one allows transitions to 10 final ones, with equal probability, then the power broadening is enhanced by about a factor 10 with respect to the case of large level spacing and resolved individual lines. A symmetric top has 9 transitions for a hybrid band, starting from a single initial state If combination and difference bands are taken into account, our assumed 10 transitions of equal strength surely are not unrealistic. Still, the power broadening thus obtained is smaller than the full observed band of 12 cm^{-1}.

The inhomogeneous holes, burned into the broad background if high laser intensities are applied (see Fig 8) are attributed to a congestion of weak transitions possessing a much smaller transition dipole moment and therefore they do not show the power-broadening observed for the strong transitions.

4.3 The Lifetime Limit

As the new lower limit for the predissociation of the υ_7-excited $(C_2H_4)_2$ can be safely derived $\tau = 45$ ns, following directly from the observed non-instrumental minimum line-width of 3 5 MHz. In comparison to recent calculations [12], this τ-value is smaller by more than an order of magnitude, however, theoretical and experimental values were never as close as they are now The difference is such that every new decay mechanism may narrow the gap.

Without the permanent and skilful help of C Sikkens the described measurements would not have been possible We thank Prof A v d Avoird for many helpful discussions This work was financially supported by the Stichting voor Fundamenteel Onderzoek der Materie (FOM/ZWO) A NATO grant made it possible to collaborate with D C Laine on improving the design of the CO_2 waveguide laser We are greatly indepted to Prof U Buck and Dr F Huisken for their constructive comments on earlier drafts of this paper

References

1 Gough, T E, Miller, R E, Scoles, G J Chem Phys. **69**, 1588 (1978)
2 Hoffbauer, M A, Gentry, W R, Giese, C F In Laser induced processes in molecules Kompa, K, Smith, S D (eds), Vol 6, p 252 Berlin Heidelberg New York Springer 1978
3 Hoffbauer, M A, Liu, K, Giese, C F, Gentry, W R J Chem Phys **78**, 5567 (1983)
4 Casassa, M P, Bomse, D S, Janda, K C J Chem Phys **74**, 5044 (1981)
5 Geraedts, J PhD-Thesis, Katholieke Universiteit Nijmegen 1983
6 Snels, M Fantoni R, Zen, M Stolte, S, Reuss, J Chem Phys Lett **124** 1 (1986)
7 Baldwin, K G H, Watts, R O Chem Phys Lett **129**, 237 (1986)
8 Fischer, G, Miller, R E, Watts, R O Chem Phys **80**, 147 (1983)
9 Janda, K C Adv Chem Phys **60**, 201 (1985)
10 Gentry, W R Am Chem Soc Symp Ser **263**, 289 (1984)
11 Miller, R E J Phys Chem **90**, 3301 (1986)
12 Celii, F G., Janda K C Chem Rev **86** 507 (1986)
13 Ewing, G E Faraday Discuss Chem Soc **73**, 325 (1982)
14 Peet, A C, Clary, D C, Hutson, J M Chem Phys Lett **125**, 477 (1986)
15 Peet, A C, Clary, D C, Hutson, J M Faraday Discuss Chem Soc **81**, 19 (1986)
16 Gough, T E, Knight, D G, Rowntree, P A, Scoles, G J Phys. Chem **90**, 4026 (1986)
17 Heijmen, B, Liedenbaum, C Private Communications
18 Miller, R E, Vohralik, P F, Watts, R O J Chem Phys **80**, 5453 (1984)
19 Fischer, G, Miller, R E, Vohralik, P F, Watts, R O J Chem Phys **83**, 1471 (1985)
20 Miller, R E, Watts, R O Chem Phys Lett **105**, 409 (1984)
21 Pine, A S, Lafferty, W J J Chem Phys **78**, 2154 (1983)
22 Pine, A S, Lafferty, W J, Howard, B J J Chem Phys **81**, 2939 (1984)
23 DeLeon, R L, Muenter, J S J Chem Phys **80**, 6092 (1984)
24 Miller, R E Private Communications
25 King, D S Private Communications, Far Wisc Chem Soc **82** (1986) (in press)
26 Huisken, F, Pertsch, T J Chem Phys **86**, 106 (1987)
27 Huisken, F, Meyer, H, Lauenstein, Ch, Sroka, R, Buck, U J Chem Phys **84**, 1042 (1986)
28 Buck, U, Huisken, F, Lauenstein, Ch, Meyer, H, Sroka, R J Chem Phys (to be published)
29 Buck, U, Lauenstein Ch, Meyer, H, Sroka, R J Chem Phys (to be published)
30 Buck, U, Huisken, F, Lauenstein, Ch, Pertsch, T, Sroka, R In Structure and dynamics of weakly bound molecular complexes NATO Advanced Research Workshop Weber, A (ed) 1986
31 Knyazev, I N, Kuzmina, N P, Letokhov, V S, Lobko, V V, Sarkisyan, A A Appl Phys **22**, 429 (1980)
32 van der Avoird, A, Wormer, P E S, Mulder, F, Berns, R M Top Curr Chem **93**, 1 (1980)
33 Beswick, A Private Communications
34 Dam, N, Liedenbaum, C, Stolte, S, Reuss, J Chem Phys Lett **136**, 73 (1987)
35 Gentry, W R In Structure and dynamics of weakly bound complexes NATO Advanced Research Workshop Weber, A (ed) 1986

B Heijmen
C Liedenbaum
S Stolte
J Reuss
Fysisch Laboratorium
Katholieke Universiteit Nijmegen
Toernooiveld
NL-6525 ED Nijmegen
The Netherlands

CHAPTER 3

High resolution infrared photodissociation spectra of C_2H_4 dimers

U. Buck, Ch. Lauenstein and A. Rudolph,

Max-Planck-Institut für Strömungsforschung, 3400 Göttingen,

Fed. Rep. of Germany

B. Heijmen, S. Stolte and J. Reuss, Nijmegen

Fysisch Laboratorium, Katholieke Universiteit Nijmegen,

Nijmegen, The Netherlands

Abstract

Vibrational predissociation spectra of C_2H_4 dimers have been measured near the ν_7 absorption band of the monomer by combining high resolution waveguide lasers with a bandwidth of 1MHz and a tuning range of 230MHz around the lasing transitions and the scattering analysis of cluster beams. The dimers are labelled either by the scattering process itself or the measured fragmentation pattern obtained by electron bombardment ionisation. The results clearly show that both the narrow fine structure and the broad background are due to dimers confirming two different time scales of the dimer predissociation rates of 45ns and 0.5ps.

1. Introduction

The photodissociation of weakly bound van der Waals clusters following the excitation with an infrared photon has attracted much interest in recent years [1]. In particular, ethylene clusters were thoroughly investigated in the spectral range of the CO_2 laser near the absorption frequency of the ν_7-mode of the monomer at 949 cm^{-1}. The width of the dissociation spectrum of the dimer using line tunable CO_2 lasers was reported to be quite broad about 12 cm^{-1}, both for continous wave and pulsed laser excitation [2-4]. If these results are attributed to lifetime broadening only the lifetime corresponds to less than 1 ps. Other processes for broadening could be a contribution from higher clusters, which because of fragmentation cannot be ruled out even if mass spectrometer detection is used, or an unresolved rotational band structure.

To test the first hypothesis the experiments were repeated using a scattering process with He to select the different cluster sizes and a pulsed CO_2 laser for dissociation. The results for cold clusters which are irradiated by CO_2 laser radiation before entering the scattering region confirmed the earlier experiments showing line widths of about 12 cm^{-1} for the dimer and, interestingly enough, also for the larger clusters [5]. For clusters, which are irradiated after the scattering process and which are therefore internally excited, values of 32 cm^{-1} were found for the dimer [6,7]. The second possibility was tested by using a piezoelectrically scanned CO_2 laser with a tunability of 75 MHz around the lasing transitions and a laser bandwidth of 10 MHz [8] and CO_2 waveguide lasers with a tuneability of 230 MHz around the lasing transitions and a laser bandwith of 10 MHz [9,10] and 1 MHz [11], respectively. Resolved structure was

observed both around the maximum of the dissociation spectrum and in a newly observed van der Waals combination band [8-11]. The reported linewidths lay in the range of 10-20 MHz [8-10] and 3.5 MHz [11]. These results correspond to lifetimes of about 10 ns to 45 ns. In all experiments the structure was superimposed on a broad background. By varying the experimental conditions of beam production and detection Baldwin and Watts [10] concluded that the "fine structure is due to dimers and the broad background is attributed to a superposition of inhomogeneous contributions from larger clusters", while Heijmen et al. [11] concluded from a very detailed analysis that "the sharp lines are due to dimers with low internal energies and the background originates mainly from dimers with higher internal energy". It is the purpose of this contribution to verify and clarify these statements by combining the scattering method for selecting single cluster sizes [12] with a high resolution waveguide laser [11] for dissociating the ethylene clusters. Two experiments have been carried out:

1) A direct beam experiment: A molecular beam containing C_2H_4 clusters is irradiated with photons from a waveguide CO_2 laser and detected with a quadrupole mass spectrometer. High resolution dissociation spectra were measured at different masses. The results are analysed using the recently measured fragmentation pattern of ethylene clusters by electron bombardment ionisation [13].

2) A scattered beam experiment: C_2H_4 dimers which are selected in a scattering process are irradiated by the waveguide CO_2 laser.

2. Experimental

2.1 Direct beam experiment

To perform this experiment a molecular beam apparatus which is described elsewhere [14] is used. Irradiation of the beam by a CO_2 laser dissociates the clusters in the beam. Since the fragments leave the molecular beam, the dissociation can be detected as a decrease of the signal at the quadrupole massspectrometer using lock-in techniques. To produce the cluster beams mixtures of 10%, 4% and 2% of C_2H_4 in He were expanded through a 35µm nozzle at room temperature and stagnation pressures between 3 and 12 bar. The beam is collimated by a 0.6 mm diameter skimmer 10 mm downstream from the nozzle. After 70 mm the beam interacts with the radiation of the homebuild CO_2 waveguide laser [11], perpendicular to the beam. The laser which can be scanned about 230 MHz around each CO_2-laserline has a frequency stability better than 1 MHz per minute and an output power up to 5 W. To focus the laser on the beam a lens with a focal length of 25 cm is used, resulting in a spot diameter of 1 mm. Therefore the interaction time of the beam with the laserfield is 0.7µs corresponding to a maximum laserfluence of $450\mu J/cm^2$.

2.2 Scattered beam experiment

The scattering analysis of a cluster beam and its use in infrared photodissociation experiments has been discussed in detail in [5-7]. In the present experiment a 10% mixture of C_2H_4 in He is expanded through a nozzle of 55 µm diameter at a stagnation pressure of 4 bar and scattered by a target beam of He expanded through a 30µm nozzle at 30bar. Only dimers are

detected, if the detector is fixed at a deflection angle of 9° and mass 41 amu. If this deflected beam is irradiated by the CO_2 laser, it is possible to obtain dissociation spectra only for dimers. The spectra are obtained by scanning the laser in small steps and measuring the dissociated fraction of scattered dimers by a lock-in procedure. The smallest fraction of dissociated molecules which could be detected in this way amounts to 0.03. Perpendicular crossing of the waveguide laser with the scattered molecular beam results in a fluence of about $75\mu J/cm^2$, which is a factor of 670 less than the value used in Ref. [7] and which is not large enough to produce a measurable signal. Therefore, the laser in this experiment is collinear with the scattered beam [15] to increase the interaction time to 400μs. In this way a fluence of $5mJ/cm^2$ is achieved corresponding to a laser intensity of 12 W/cm^2.

3. Results and Discussion

3.1. Direct beam

Measurements of the dissociation spectra were carried out for different mixtures of C_2H_4 seeded in He with detection at mass 41amu. The result of tuning the laser around the 10P12 line near the maximum of the ν_7 absorption spectrum is shown in Fig. 1 for 2% and 4% mixtures. The two dissociation spectra exhibit sharp features on top of a background signal which increases with increasing concentration of C_2H_4 in He. The structure is in complete agreement with the results of the two previous experiments [10,11] thus confirming the existence of these lines in a completely different apparatus. In order to test from which cluster the sharp features originate, the measurements were repeated tuning the mass spectrometer to different masses. According to Ref. [13], the most interesting results are expected for the masses m=55 amu and m=56 amu at an electron energy of 100

eV. Due to an intra-cluster ion-molecule reaction the m=55 amu is a dimer mass, while at m=56 amu only trimers and higher cluster are observed. The results are shown in Fig. 2 for the 2% mixture of C_2H_4 in He. The sharp peak is only present in the dimer spectrum and completely absent in the trimer spectrum. This analysis is confirmed by comparing the dissociation signals measured at different masses with the results obtained by the fragmentation analysis of size selected clusters [13], as is given in Tab. 1. Within the experimental errors the peak intensities follow nicely the fragmentation pattern of the dimer. Thus we conclude, in agreement with the two previous measurements [10,11], but on a better basis that the sharp structure results only from dimers. The analysis also shows that the fragmentation pattern can be easily used as a finger print to identify cluster sizes. If we apply, therefore, the same procedure to the background signal, we get, after a correction of a small amount of trimers in the beam [16], the result that also the background is caused by the dimer. This analysis is, of course, only valid for the source conditions of the beam used in the experiment, 2% C_2H_4 in He, 8 bar, d=35 µm. A similar analysis for the 4% mixture clearly revealed that higher clusters are present in the beam. The pressure dependence of the peak and the background structure are displayed in Fig. 3 for different concentrations. All signals increase with increasing pressure according to a power law p^{α} with $\alpha>2$ in agreement with what was published previously [13]. As was already visible in Fig. 1, at low concentration (2%) the peak and the background are of comparable intensity, while for larger concentrations (4%) the background is much larger. The peak to background ratio, however, depends on the laser fluence [11], which is in the present experiment 300µJ/cm^2. Since we already know that the 2% mixture consists mainly of dimers, the large increase of the background signal for the 4% mixture is attributed to larger clusters. It is interesting to note that the peak intensity of the 4% mixture levels off at higher pressure and reaches the value found for the 2% mixture, a

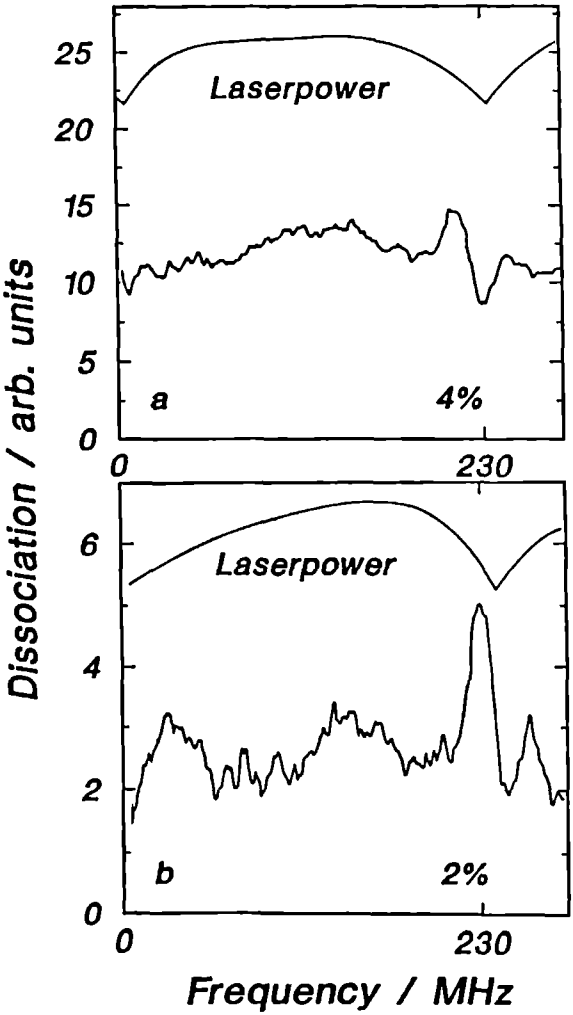

Fig. 1: High resolution dissociation spectrum around the 10P12 CO_2 laserline at a detection mass of 41 amu. The maximum of the monitored laserpower (upper curves) is 450 W/cm^2. a) shows the spectrum of a 4% mixture of C_2H_4 in He at a stagnation pressure of 6 bar. b) corresponds to a 2% mixture at a stagnation pressue of 8 bar.

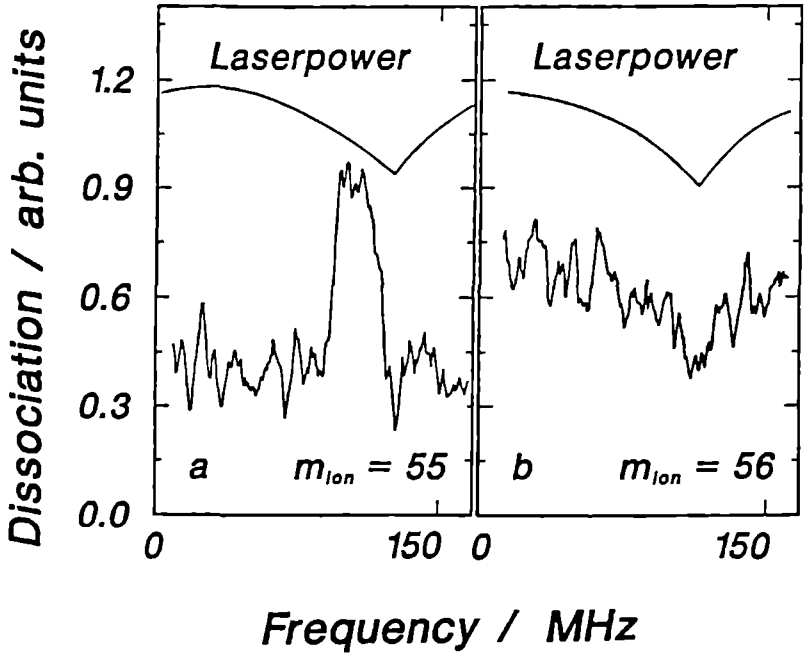

Fig. 2: Dissociation spectra observed by a frequency scan of 230MHz around the 10P12 CO_2 laserline for a 2% mixture of C_2H_4 seeded in He at 8 bar for different detection masses. The maximum of the monitored laserpower (upper curves) is 450 W/cm^2. a) shows the spectrum for m_{ion}=55, where mainly dimers appear. b) is a spectrum for m_{ion}=56 where only trimers and higher cluster can be detected.

	29	41	55	56
Ref. 13	5.6	10	2.2	0.0
Peak	4.0	10	1.9	0.0
Background[a]	5.6	10	2.4	0.0

[a] corrected for a small amount (0.05) of trimers.

Table 1: Fragmentation pattern by electron bombardement ionisation of ethylene dimers normalized to m=41amu.

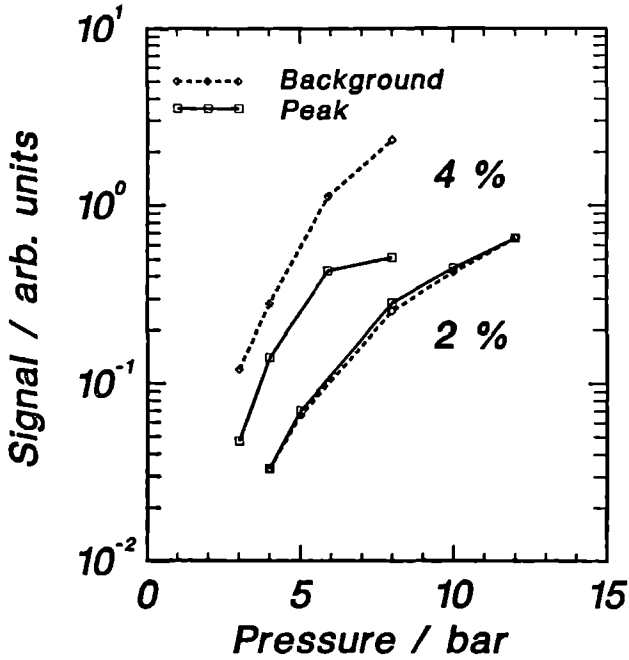

Fig. 3: Intensity of the peak and the background of the dissociation spectra as a function of the stagnation pressure for a 4% mixture of C_2H_4 in He (upper curves) and a 2% mixture (lower curves). The laserfluence is fixed at 3000μJ/cm^2.

further indication that the peak is only caused by dimers. For the ratio of structure to background we found a qualitatively similar behaviour as Heijmen et al. [11].

3.2. Scattered beam

In this experiment the dimers are dissociated after the scattering process. A dissociation spectrum for these internally excited dimers is shown in Fig. 4. It is taken by scanning the waveguide laser across the 10P12 CO_2 laser line and measuring the loss of scattered signal at the detector. A broad background of 10% dissociation signal is seen following roughly the laser power. Superimposed structures are barely visible outside the signal fluctuation. Because the laser is collinear with the scattered beam, the spectrum is Doppler shifted by about 150 MHz with respect to the results in Fig. 1. Thus, the largest peak is shifted out of the tuning range of the laser. In addition, the sharp peaks are Doppler broadened. The main reason, however, for the lack of structure is that these features are already saturated at about $30\mu J/cm^2$, whereas the background increases proportional to the fluence. In the 2% mixture which contains only dimers the peak to background ratio is about 1 for a laser fluence of $300\mu J/cm^2$. In the present experiment with a laser fluence of $5mJ/cm^2$ we expect a peak to background ratio of 0.06. This means that any structure is not detectable within our signal fluctuations. Nevertheless, the present results clearly show that dimers are also responsible for the background signal, in contrast to the statement made in Ref. [10].

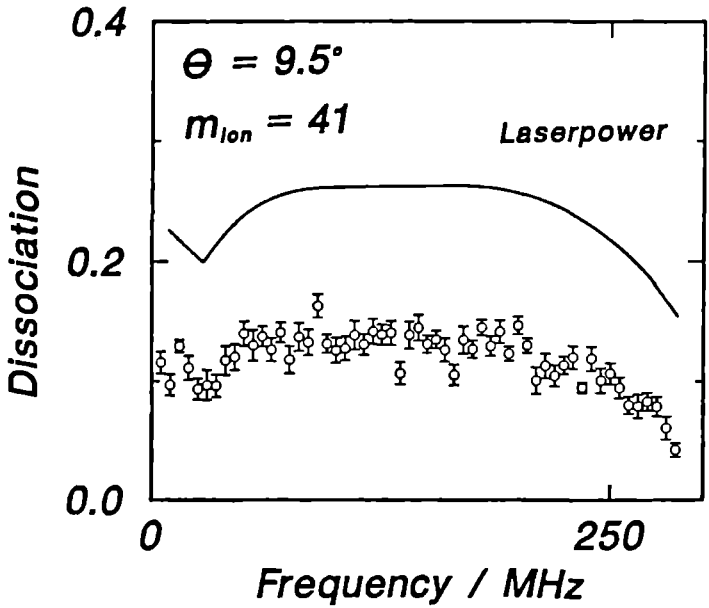

Fig. 4: Dissociated fraction of scattered dimers measured by scanning the laser around the 10P12 laserline (at a deflection angle of 9° and mass 41). The maximum of the monitored laser power (upper curve) is 12 W/cm^2 and corresponds to a fluence of 5mJ/cm^2.

3.3. Conclusions

The present experiments clearly demonstrate without any assumption or speculation that

(1) the sharp structure with linewidths smaller than 10 MHz (about 10^{-4} cm^{-1}) results only from dimers,
(2) there is always a broad background signal present which is also due to dimers.

If we attribute the linewidth of 12 cm^{-1} measured by the linetunable lasers to the broad feature - and there is convincing evidence for doing so [7,11] - we conclude that the same species, the ethylene dimer, dissociates on two different time scales which differ by 5 orders of magnitude. Whether this behaviour is caused by two different structures, two different degrees of internal excitation [11] or different dynamical processes, is still a matter of controversy which can only be solved in cooperation with theoretical calculations.

Acknowledgement

The authors from Göttingen acknowledge support of the Sonderforschungsbereich 93 (Photochemie mit Lasern).

References

[1] R.E. Miller, J. Phys. Chem. 90 (1986) 3301

[2] M.P. Casassa, D.S. Bomse, and K.C. Janda, J. Chem. Phys. 74 (1981) 5044

[3] J. Gereadts, Ph. D. Thesis, Katholieke Universiteit, Nijmegen (1983)

[4] M.A. Hoffbauer, K. Liu, C.F. Giese, and W.R. Gentry, J. Chem. Phys. 78 (1983) 5567

[5] F. Huisken and T. Pertsch, J. Chem. Phys. 86 (1987) 106

[6] F. Huisken, H. Meyer, Ch. Lauenstein, R. Sroka, and U. Buck, J. Chem. Phys. 84 (1986) 1042

[7] U. Buck, F. Huisken, Ch. Lauenstein, H. Meyer, and R. Sroka, J. Chem. Phys. 87 (1987) 6276

[8] M. Snels, R. Fantoni, M. Zen, S. Stolte, and J. Reuss, Chem. Phys. Lett. 124 (1986) 1

[9] K.G.H. Baldwin and R.O. Watts, Chem. Phys. Lett. 129 (1986) 237

[10] K.G.H. Baldwin and R.O. Watts, J. Chem. Phys. 87 (1987) 873

[11] B. Heijmen, C. Liedenbaum, S. Stolte, and J. Reuss, Z. Phys. D. 6 (1987) 199

[12] U. Buck, and H. Meyer, J. Chem. Phys. 84 (1986) 4854

[13] U. Buck, Ch. Lauenstein, H. Meyer, and R. Sroka, J. Phys. Chem..... (1987)

[14] D. Otten, Doctoral Thesis, Göttingen (1984); J. Kesper, Doctoral thesis, Göttingen (1987).

[15] U. Buck, Ch. Lauenstein, and A. Rudolph, to be published.

[16] The amount of trimers is determined from the signal measured at m=56 amu and the trimer fragmentation pattern.

CHAPTER 4

HOLE BURNING IN THE IR PREDISSOCIATION SPECTRUM OF SF_6-DIMERS

B. Heijmen, C. Liedenbaum, S. Stolte and J. Reuss
Fysisch Laboratorium
Katholieke Universiteit Nijmegen
Toernooiveld, 6525 ED Nijmegen, The Netherlands

ABSTRACT

Hole burning experiments with two CO_2 lasers have been performed to obtain insight in the predissociation mechanism of SF_6-dimers. For the well known double peak predissociation spectrum, always two correlated holes are observed. Strongly enhanced widths of the holes are found for dimers with higher internal energy.

The SF_6-dimer IR predissociation spectrum in the neighbourhood of the ν_3 vibrational mode of the SF_6 monomer has been studied in detail [1,2,3,4]. This spectrum consists of two peaks, one blue shifted and the other red shifted with respect to the monomer ν_3-absorption frequency (948.0 cm^{-1}), see fig. 2a. The shifts and also the relative intensities of the two peaks can be explained by means of a resonant dipole-dipole interaction [2,3]. The interacting dipoles are the transition dipole moments of the two SF_6 monomers in the dimer. According to this model the red shifted peak corresponds to two in-phase transition dipole moments parallel to the dimer axis, whereas the blue shifted peak is due to in-phase transition dipole moments perpendicular to the dimer axis. Recently the above mentioned model has been refined by including induction effects into the interaction hamiltonian [5].

The model discussed up to this point produces a stick spectrum. To account for the experimental width of the two lines in the dimer spectrum, an extension has been proposed in which is assumed that a dimer consists of two freely rotating molecules in the vibrational groundstate with rotational quantum numbers J_1 and J_2, respectively [4]. The groundstate of the dimer is given by $|v=0, J_1\rangle|v=0, J_2\rangle$. Only transitions with ΔJ_1, ΔJ_2 = 0,-1 or +1 can occur. According to this extension of the dipole-dipole interaction model each of the two dimer peaks consists of a P-, a Q- and a R-branch. The low frequency side, the centre and the high frequency side of the two observed peaks are respectively due to $\Delta J=-1$, $\Delta J=0$ and $\Delta J=+1$ transitions in one of the monomers forming the dimer. In this case J stands for J_1, or J_2. As a further refinement the end over end rotation of the dimer is considered, which gives an extra broadening of the peaks.

The present work describes a two laser experiment which gives insight in the origin of the width of the two peaks in the dimer predissociation spectrum. The new experimental results cannot be reconciled with the assumptions of the extended model [4].

2. EXPERIMENTAL

The measurements have been performed using the molecular beam apparatus described in detail elsewhere [4]. The molecular beam is detected by means of a bolometer that monitors its energy content. Irradiation with CO_2- laser photons leads to dissociation of dimers. The fragments leave the molecular beam, yielding a diminution of the energy content of the beam and hence a change in bolometer signal. For a schematic picture of the apparatus see fig.1.

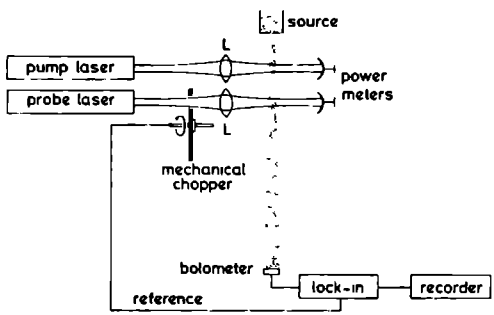

Figure 1

Schematic picture of the apparatus. The lens of the pump laser (probe laser) has a focal length of 37.5 cm (75 cm), resulting in a spot diameter of 0.6 mm (1.2 mm). For both lasers there is a more than complete overlap with the molecular beam. The bolometer, which consists of a 1x1 mm^2 doped Ge detector on a 2x5 mm^2 substrate of sapphire (Infrared laboratories), is operated at 4.2K. The N.E.P at this temperature is $8 \cdot 10^{-14}$ $WHz^{-\frac{1}{2}}$, the responsitivity is $5 \cdot 10^{4}$ V/W and the response time is 2.5 ms. The distance nozzle bolometer is about 50 cm.

Both the pump and the probe laser are cw CO_2-lasers. The probe laser, with fixed frequency and power, is modulated with a mechanical chopper. The dissociation due to this laser is measured by means of phase-sensitive detection of the bolometer signal. The pump laser, which is not modulated and constant in power, is tuned from laser-line to laser-line. Irradiation by the pump laser, on a frequency which leads to dissociation of dimers which contribute to the probe laser dissociation signal, yields a reduction of this signal. Thus, if pump and probe laser excite dimers in the same initial state, pumping leads to a reduction of the probe laser dissociation signal. The attenuation of the probe laser dissociation signal is measured as a function of pump laser frequency.

The distance between the intersection points of the two lasers with the molecular beam is 7.5 cm. The measurements have been performed with a 1% SF_6 in helium mixture. The stagnation pressure P_0 was 5 atm. and the source temperature T_0 was 293K. The nozzle consisted of a platinum iridium electron microscope diaphragm (Siemens) with a diameter of 30 μm.

3. RESULTS

The experimental results are presented in fig. 2 and fig. 3. Figure 2a shows the one-laser dissociation spectrum as it has been measured by Snels et al [4]. The two main peaks (A and B) are assigned to the dimer $^{32}SF_6$ ---- $^{32}SF_6$. The bumps around 950 cm^{-1} and 960 cm^{-1} are respectively due to $^{32}SF_6$---- $^{34}SF_6$ and $(SF_6)_3$.

Figure 2b demonstrates that the dimer peak around 934.4 cm^{-1} (peak A) is inhomogeneous: The probe laser dissociation signal on the red wing of this peak is much more reduced by pumping at the red side of the peak than by pumping at the blue side. In addition, this figure shows that the red wing of peak A is correlated with the blue wing of peak B.

The figures 2c and 2d show that the blue side of peak A is correlated to the red side of peak B. Comparison of fig. 2b with fig. 2c shows that the red wing of peak A is more inhomogeneous than the blue wing of this peak and the red wing of the other peak.

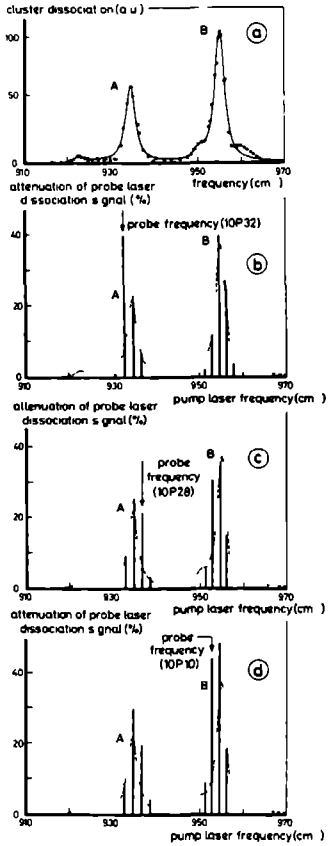

Figure 2

Fig. 2a shows the dissociation spectrum of SF_6-dimers, as it was measured by Snels et al [4]. Figs. 2b, 2c, and 2d show the results of the two laser experiments. The probe laser frequencies for 2b, 2c and 2d are, respectively, 932.96 cm^{-1}, 936.80 cm^{-1}, and 952.88 cm^{-1}. The indications for the probe frequencies in the figures refer to the used CO_2 laser lines. The pump laser fluence (intensity) is always 0.4 mJ/cm^2 (1 kW/cm^2). For figs. 2b and 2c the probe laser fluence is 0.4 mJ/cm^2, for 2d this fluence is 0.1 mJ/cm^2. The dashed lines in 2b, 2c and 2d indicate the one laser predissociation spectrum [4].

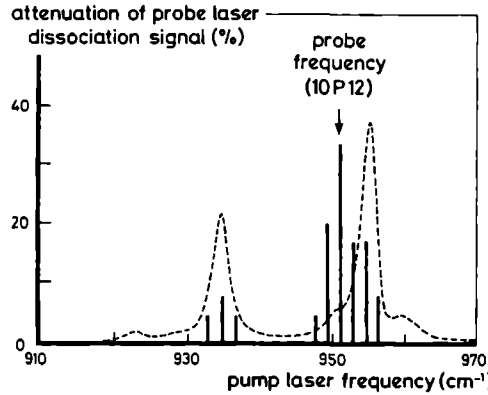

Figure 3

Results of a two laser experiment in which the probe laser irradiates at a transition frequency of the $^{34}SF_6$---- $^{32}SF_6$- dimer. The picture shows that at this frequency there is also dissociation of $(^{32}SF_6)_2$. This is explained by the fact that the homogeneous lineshapes of these dimers have a tail at the probe frequency (951.20 cm $^{-1}$, the 10P12 CO_2-laser transition). The pump laser fluence is 0.4 mJ/cm^2, the probe laser fluence is 0.1 mJ/cm^2.

High resolution measurements with a CO_2-waveguide laser have been performed to look for narrow lines on top of the broad spectral structures. (Such lines with a width of 3.5 MHz have been found for C_2H_4- dimers [6,7,8].) No narrow structures were observed for SF_6-dimers.

4. DISCUSSION

The inhomogeneity of the SF_6-dimer spectrum demonstrates that the coupling of excited states to the continuum of dissociated states is weaker than suggested by the width of the two peaks. For the red wing of peak A we find a width smaller than about 1 cm^{-1}, corresponding to a minimum lifetime longer than 5 ps. For the blue wing of this peak we find a significantly larger width of about 3 cm^{-1}, corresponding to a minimum lifetime of 1.5 ps.

According to the extension of the dipole-dipole interaction model of Snels and Fantoni [4], as described briefly in the introduction, the red wings of the two peaks consist of P-transitions, whereas the blue wings consist of R-transitions. This means that for all four wings the transitions should originate from the same initial levels. As a result pumping on a blue wing should have the same effect on the probe laser dissociation signal as pumping on the corresponding red wing.The figures 2b and 2c clearly demonstrate that our observations are not in agreement with the above mentioned consequences of the extended model. The figures 2c and 2d show that the blue wing of peak A is more correlated with the red wing of peak B than with the blue wing of peak B, again in contradiction with the extended model.

According to the stick-model of Geraedts et al [2,3] peak A (peak B) is situated 2λ (λ) to the red (blue) of the ν_3 monomer transition (948.0 cm^{-1}), with λ = 6.8 cm^{-1}. λ is given by:

$$\lambda = (\mu_{01})^2(4\pi\epsilon_0)^{-1}\langle\frac{1}{R^3}\rangle,$$

in which μ_{01} is the transition dipole moment for a ν_3~ transition in a SF_6 monomer and R is the distance between the monomers in the dimer. The brackets around $\frac{1}{R^3}$ indicate the average value of this quantity for a certain dimer state. From our measurements we conclude that not all the dimers have the same average intermolecular distance. Dimers with a relatively big average distance, and hence a small λ, are related to the blue wing of peak A and to the red wing of peak B, a correlation observed in the measurements shown in figure 2c and figure 2d. A bigger average distance stems from a higher internal energy, supposedly yielding a stronger coupling to the continuum after vibrational excitation. The dimers of high internal energy display a larger width (about 3 cm^{-1}, see fig. 2c and 2d) than those of low internal energy (about 1 cm^{-1}, see fig. 2b), in agreement with the expectation. Further measurements are in progress.

ACKNOWLEDGEMENTS

The authors wish to thank Cor Sikkens, Frans van Rijn and John Holtkamp for their technical and electronical advice and assistance. This work is financially supported by the Stichting voor Fundamenteel Onderzoek der Materie (FOM) and the Nederlandse Organisatie voor Wetenschappelijk Onderzoek (NWO).

REFERENCES

[1] J. Geraedts, S. Setiadi, S. Stolte and J.Reuss, Chem. Phys. Lett. 78 (1981)277

[2] J. Geraedts, S. Stolte and J. Reuss, Z. Phys. A 304 (1982)167

[3] J. Geraedts, M. Waayer, S. Stolte and J. Reuss, Faraday Discuss. Chem. Soc., 73 (1982)375

[4] M. Snels and R. Fantoni,Chem. Phys. 109 (1986)67

[5] M. Snels and J. Reuss, Chem. Phys. Lett. 140 (1987)543

[6] M. Snels, R. Fantoni, M. Zen, S. Stolte and J. Reuss, Chem. Phys. Lett. 124 (1986)1

[7] B. Heijmen, C. Liedenbaum, S. Stolte and J. Reuss, Z. Phys. D 6 (1987)199

[8] K.G.H. Baldwin and R.O. Watts, Chem. Phys. Lett. 129 (1986)237

CHAPTER 5

IR-IR DOUBLE RESONANCE EXPERIMENTS ON SF_6 AND SiF_4 CLUSTERS

B. Heijmen, A. Bizzarri, S. Stolte and J. Reuss
Fysisch Laboratorium
Katholieke Universiteit Nijmegen
Toernooiveld, 6525 ED Nijmegen, The Netherlands

ABSTRACT

By means of IR-IR double resonance experiments with CO_2-lasers insight is obtained in the origin of the widths of the peaks in the predissociation spectra of $(^{32}SF_6)_2$ and $(^{28}SiF_4)_2$. The observed correlations in the dimer spectra reflect a distribution in the average intermolecular distance for the dimer states. A model, based on centrifugal distortion, yielding a distribution in intermolecular distance is proposed. We demonstrate that Coriolis interaction yields extra broadening only for one of the two peaks in the dimer spectra, in agreement with the observations. The observed dimer-double-resonance-spectra are independent of the relative polarization of the two lasers. By applying the double resonance technique, predissociation spectra of $^{32}SF_6$-trimers and of $(^{32}SF_6)_n{}^{34}SF_6$ (n=1,2) have been determined. These spectra are compared with the predictions of a model concerning excitation of a three-fold degenerate monomer mode in a cluster.

IR-predissociation has been observed for many molecular clusters [1,2,3,4]. Most of the experiments were performed in a molecular beam machine. Since the van der Waals complexes are held together by weak intermolecular forces a low temperature and a collisionless environment are favourable for cluster measurements. Both requirements are met in a supersonic molecular beam. By expansion of gas through a nozzle into vacuum low temperatures are achieved and large amounts of clusters are produced. Due to the low density downstream of the expansion region the clusters can proceed on their way without collisions.

Often the observed IR-predissociation spectra display broad, rather poorly structured peaks. The absence of resolved lines can be due to a complicated rotation-vibration structure of the spectrum yielding a congestion of lines, or due to line-broadening because of lifetime effects. Thus, structural information concerning the cluster can hardly be deduced from these spectra. The situation is even more complicated if dimers and higher clusters absorb in the same frequency region. Due to fragmentation in the ionizer, mass-selective detection is of no great help in this case. Recently, Buck and Meyer introduced a new technique to overcome the problem of fragmentation [5]. In order to select the cluster-size, the molecular beam is deflected by means of scattering with a secondary (rare gas) beam. By choosing the proper detection-angle and detection-mass or by means of a TOF-analysis IR-predissociation experiments can be performed on a single cluster-species. In this way the overlapping predissociation spectra of ethylene clusters ($(C_2H_4)_n$, n=2-5) have been unravelled [6,7]. Recently, the fragmentation-pattern of C_2H_4-clusters obtained by means of this scattering technique was used to confirm that fine-structure (3.5 MHz FWHM) on top of the broad (12 cm^{-1}) homogeneous $(C_2H_4)_2$ dissociation spectrum is due to dimers [8].

To reduce the problems of congestion of lines and partially overlapping cluster spectra, two-laser experiments can be performed. In these "pump and probe" experiments the fixed-frequency probe laser labels cluster levels of a certain cluster-species and the pump laser is scanned to find IR-predissociation frequencies connected with the labelled cluster-states. We applied this technique to measure the $(^{32}SF_6)_3$-, the $^{32}SF_6{}^{34}SF_6$-, and the $(^{32}SF_6)_2{}^{34}SF_6$-IR-predissociation spectra. For $(^{32}SF_6)_2$ and $(^{28}SiF_4)_2$ the method revealed new aspects of the known spectra [9,10,11,12].

The three-fold degenerate ν_3-vibrations of SF_6 and SiF_4 can be excited by CO_2 laser radiation. For $^{32}SF_6$ and $^{34}SF_6$ the band centres are situated at 948.0 cm^{-1} and 930.8 cm^{-1}, respectively. The transition dipole moment μ_{01} amounts to 0.387 debye. The infrared active ν_3-modes of $^{28}SiF_4$, $^{29}SiF_4$ and $^{30}SiF_4$ have band centres at 1031.4 cm^{-1}, 1022.4 cm^{-1} and 1014.0 cm^{-1}, respectively. The transition dipole moment μ_{01}=0.276 debye.

The observed spectra for SF_6- and SiF_4-clusters are in rather good agreement with the predictions of a model concerning excitation of a three-fold degenerate monomer mode in a cluster [9,10]. In this model the observed spectra are explained by means of a resonant dipole-dipole interaction between the monomers in the complex. This interaction predicts the shifts of excited cluster levels with respect to the ν_3 monomer frequency. In the following the model will be summarized for the $^{32}SF_6$-dimer.

The dipole-dipole operator H_{dd} is given by

$$H_{dd} = \frac{1}{4\pi\varepsilon_0} \cdot \left[\vec{\mu}_1 \cdot \vec{\mu}_2 - 3(\vec{\mu}_1 \cdot \hat{R})(\vec{\mu}_2 \cdot \hat{R})\right] \cdot \left\langle \frac{1}{R^3} \right\rangle$$

where $\vec{\mu}_1$ and $\vec{\mu}_2$ stand for the dipole moment operators belonging to the two monomers and R for the intermolecular distance coordinate. For convenience the dimer fixed z-axis is chosen along the line connecting the two sulphur atoms ($\hat{R}$). In the absence of interaction the ν_3 level is six-fold degenerate. As a basis we adopt $|x_1\rangle$, $|y_1\rangle$, $|z_1\rangle$, $|x_2\rangle$, $|y_2\rangle$ and $|z_2\rangle$. $|x_1\rangle$ stands for the wavefunction in case of excitation of monomer 1 along the x-direction, while monomer 2 is in its ground vibrational state. The matrix of H_{dd} is given in fig. 1. The energy shifts with respect to the monomer ν_3-frequency are calculated by means of diagonalization. Of course the ground vibrational level is not affected by H_{dd}. The energy level scheme is depicted in fig. 2.

To compare the transition strengths of the four possible transitions, the following matrix elements have to be calculated: $\langle\phi_i|\vec{\mu}_1+\vec{\mu}_2|0\rangle$, with $|\phi_i\rangle$ (i=1,...,6) the ν_3-excited eigenstates. Transitions to the levels $-\lambda$ and $+2\lambda$ appear to be not allowed. Due to the degeneracy of the $+\lambda$-level the transition strength for this level is twice that of the -2λ-level. The allowed transitions are indicated in fig. 2 by means of arrows. The predicted spectrum is in good agreement with the observed IR-predissociation spectrum.

To account for the width of the two peaks in the experimental spectrum an extension of the above mentioned model has been proposed [12]. As reported before [13] this extension appears to be in contradiction with some

	$\|x_1\rangle$	$\|x_2\rangle$	$\|y_1\rangle$	$\|y_2\rangle$	$\|z_1\rangle$	$\|z_2\rangle$
$\|x_1\rangle$	0	λ				
$\|x_2\rangle$	λ	0				
$\|y_1\rangle$			0	λ		
$\|y_2\rangle$			λ	0		
$\|z_1\rangle$					0	-2λ
$\|z_2\rangle$					-2λ	0

Figure 1

Matrix of the dipole-dipole interaction operator, $\lambda = \frac{1}{4\pi\varepsilon_0}(\mu_{01})^2\langle\frac{1}{R^3}\rangle$.

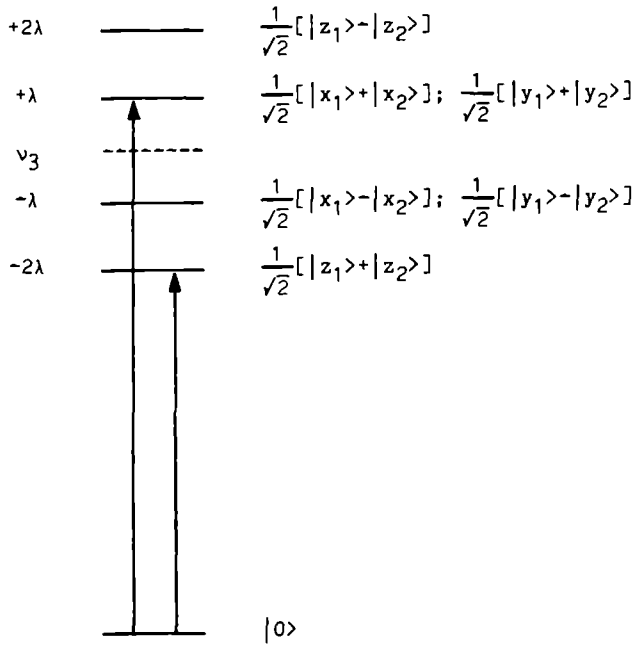

Figure 2

Energy level scheme for the $^{32}SF_6$-dimer, $\lambda = \frac{1}{4\pi\varepsilon_0}(\mu_{01})^2\langle\frac{1}{R^3}\rangle$. The arrows indicate allowed transitions.

frequency laser 1	frequency laser 2	$\vec{E}_1:\vec{E}_2$	double-resonance signal
R	R	//	$\frac{6}{5} - \frac{6}{5}(\frac{K}{J})^2 + \frac{9}{5}(\frac{K}{J})^4$
R	R	$\perp$	$\frac{9}{10} + \frac{3}{5}(\frac{K}{J})^2 - \frac{9}{10}(\frac{K}{J})^4$
R	B	//	$\frac{9}{5} + \frac{3}{5}(\frac{K}{J})^2 - \frac{9}{5}(\frac{K}{J})^4$
R	B	$\perp$	$\frac{21}{10} - \frac{3}{10}(\frac{K}{J})^2 + \frac{9}{10}(\frac{K}{J})^4$
B	B	//	$\frac{21}{5} - \frac{3}{5}(\frac{K}{J})^2 + \frac{9}{5}(\frac{K}{J})^4$
B	B	$\perp$	$\frac{39}{10} + \frac{3}{10}(\frac{K}{J})^2 - \frac{9}{10}(\frac{K}{J})^4$

Table 1

For a rigid dimer with $J>>1$ the IR-IR double-resonance-signals are proportional to the given expressions. In case of laser frequency R(B) the laser is tuned to the red (blue) peak of the dimer spectrum. $\vec{E}_1:\vec{E}_2$ = //($\perp$) indicates that the polarization of laser 1 is parallel (perpendicular) to that of laser 2. The results are valid in the limit of low laser fluences.

preliminary two-laser measurements.

As shown in fig. 2 the final state wavefunction belonging to the red peak of the $^{32}SF_6$-dimer spectrum is given by $1/\sqrt{2}[|z_1\rangle+|z_2\rangle]$, i.e. this peak is due to a parallel transition. For the blue peak the final state wavefunctions are linear combinations of $1/\sqrt{2}[|x_1\rangle+|x_2\rangle]$ and $1/\sqrt{2}[|y_1\rangle+|y_2\rangle]$, yielding perpendicular transitions. As a consequence the laser polarization plays a role in the photodissociation process; for a fixed laser polarization some $\hat{R}$-orientations will contribute more to the red peak, others more to the blue peak. Suppose the electric field $\vec{E}$ of the laser is pointed along the space-fixed Z-axis. The rotational wavefunction of a rigid dimer is given by $|JKM_J\rangle$ with M_J and K respectively the projections of $\vec{J}$ on the space fixed Z-axis and on the dimer fixed z-axis. Consider first only K=0 states, $|J0M_J\rangle$. If $M_J=\pm J$ and J>>1 the intermolecular axis is perpendicular to the polarization vector of the laser field. Consequently only perpendicular transitions are possible. For $|J00\rangle$-states only parallel transitions are allowed. If K≠0 the above described laser polarization effect is reduced. However, the B and the A constants for a rigid SF_6-dimer differ by a factor of 5. B was derived from the intermolecular distance [12], B=0.26 GHz; $A=\frac{1}{2}B_0$ with B_0=2.79 GHz, the rotational constant for the SF_6 molecule. As a consequence $|JKM_J\rangle$-states with high K-values will not be populated in the molecular beam.

To look for these polarization effects we performed two-laser experiments with linear polarized lasers; for $(^{32}SF_6)_2$ and $(^{28}SiF_4)_2$ two-laser spectra were measured both with parallel and with perpendicular polarization-vectors. Table 1 predicts double resonance signals in case of a rigid dimer both for mutually parallel and perpendicular polarization-vectors. The given expressions are valid in the limit of low laser fluences and J>>1.

2. EXPERIMENTAL

The measurements were performed with a molecular beam apparatus, described in detail in [14]. The apparatus is sketched in fig. 3. The molecular beam is produced by supersonic expansion of a gas mixture through a platinum-iridium electron microscope diaphragm (Siemens) with a diameter of 30 μm. In the laser chamber interaction with three home-built cw CO_2 lasers is possible. Finally the molecular beam is detected by a semi-conductor bolometer, operated at 4.2 K.

In all experiments the probe-laser-beam is mechanically chopped (67 Hz). Irradiation of the molecular beam by the probe laser yields dissociation of clusters. The fragments leave the molecular beam, yielding a reduction of energy flux onto the bolometer, which results in a change in bolometer signal. This probe-laser-dissociation-signal is measured by means of phase-sensitive detection. If the pump and the probe lasers dissociate clusters of the same initial state, irradiation with the unchopped pump laser(s) leads to a reduction of probe-laser-dissociation-signal (hole burning).

Several concentrations of SF_6 and SiF_4 in the seeding gas helium were used. The stagnation pressure was always 5 atm and the source temperature was chosen between 230 K and 295 K. The lasers were operated on gas mixtures containing $^{12}CO_2$, $^{13}CO_2$ and N_2O.

Most of the experiments described below are two-laser experiments. In these cases pump laser 1 is not used (see fig. 3). Three-laser experiments will be indicated explicitly in the text.

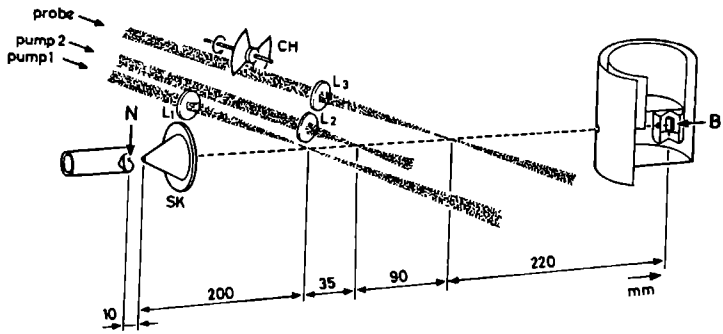

Figure 3

A schematic picture of the apparatus. The lenses L_1, L_2 and L_3 have focal lengths of 37.5 cm, 25 cm and 37.5 cm, respectively. Pump laser 1, pump laser 2 and the probe laser have spot diameters of, respectively, 0.8 mm, 0.5 mm and 0.8 mm at the molecular beam. N=nozzle (30 μm), SK=skimmer, B=bolometer, CH=chopper. The bolometer is shielded by screens at 4.2 K and 77 K, respectively. The nozzle temperature can be varied between 100 K and 300 K.

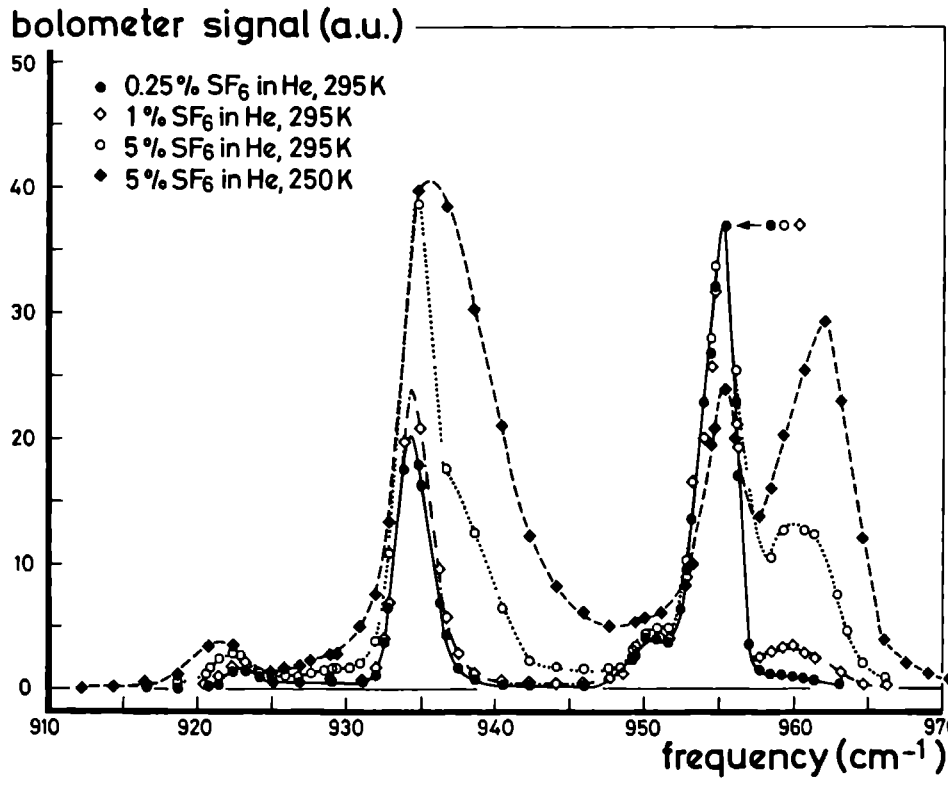

Figure 4

One-laser predissociation spectra of SF_6-clusters for different source conditions. The laser power was 1 Watt and the spot diameter at the molecular beam was about 0.5 mm. For purpose of clarity smooth curves are drawn through the measured points. All spectra except that for 5% SF_6 in He, 250 K, are normalized at 955.54 cm^{-1}.

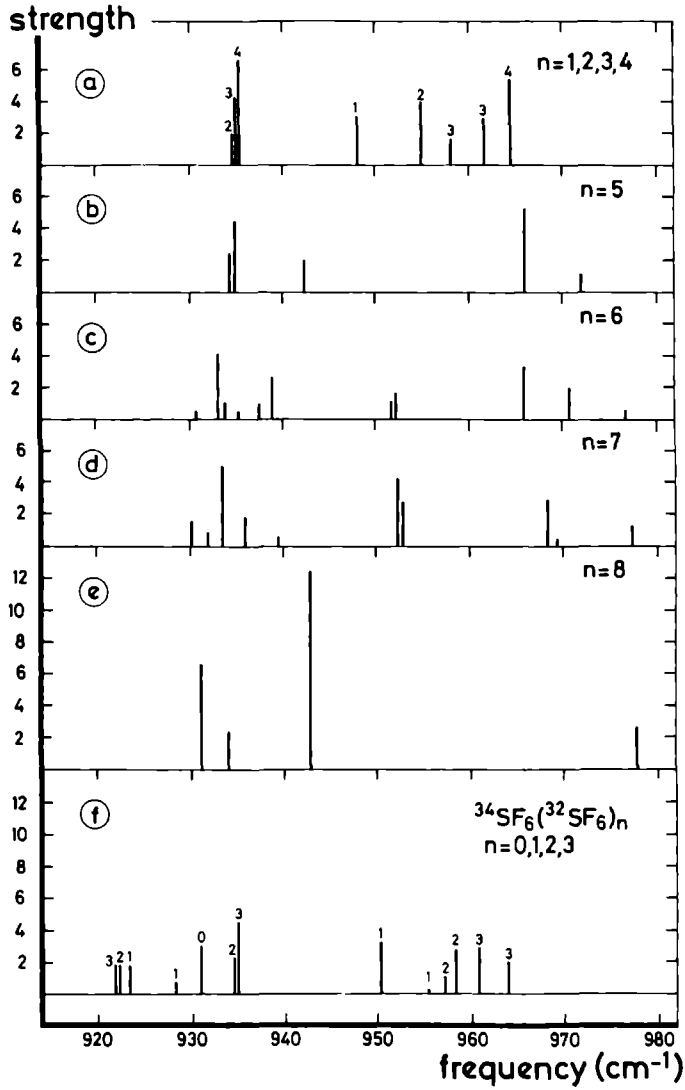

Figure 5

Stick spectra of SF_6-clusters according to the resonant dipole-dipole interaction model (λ=6.8 cm^{-1}) [9,10]. Figs. 5a, 5b, 5c, 5d and 5e display $(^{32}SF_6)_n$-spectra. In fig. 5f the spectra of $^{34}SF_6(^{32}SF_6)_n$ are depicted; for n=2 and n=3 only the most intense peaks (strength $\geq$ 0.5) are included. The height of each bar corresponds to the transition strength times degeneracy. The natural abundances of $^{32}SF_6$ and $^{34}SF_6$ are, respectively, 95.02% and 4.21%.

3. EXPERIMENTAL RESULTS

3.1. SF_6-CLUSTERS

3.1.1. GENERAL ASPECTS

Fig. 4 displays one-laser predissociation spectra of SF_6 clusters for different source conditions. For the lowest concentration of SF_6 in He (0.25%) one expects to measure a rather pure dimer spectrum, $(^{32}SF_6)_2$ and $^{32}SF_6{}^{34}SF_6$. For higher concentrations and lower source temperatures the contribution of higher clusters becomes more important. Fig. 5 displays the calculated SF_6-cluster spectra based upon the resonant dipole-dipole interaction (H_{dd}) [9,10]. These calculations are in rather good agreement with the experimental observations of fig. 4, e.g. for 0.25% SF_6 in He, 295 K, only dimer peaks appear. The behaviour of the experimental spectra around 920 cm^{-1} and 950 cm^{-1} is also well predicted; the predissociation signal in these frequency regions is due to isotopically mixed SF_6-clusters, $^{34}SF_6(^{32}SF_6)_n$, see fig. 5f.

The $(^{32}SF_6)_2$-peaks are situated at 934.5 cm^{-1} and 955.0 cm^{-1} (see fig. 4). Their widths are, respectively, 2.8 and 2.6 cm^{-1} FWHM. According to the dipole-dipole interaction model the distance between the dimer peaks is 3λ (see introduction). From the measured line positions we derive $\lambda = 6.8$ cm^{-1}, in agreement with [9,10,12]. The central frequency ([955.0 $-\lambda$] cm^{-1}) is 948.2 cm^{-1}, which is within the experimental error equal to the ν_3 excitation frequency of a free SF_6-molecule (948.0 cm^{-1}).

Henceforth, for simplicity, the red peak (blue peak) in the $(^{32}SF_6)_2$-spectrum will be called peak R (peak B).

3.1.2. $(^{32}SF_6)_2$

Two-laser spectra

For the two-laser spectra depicted in figs. 6 and 7 the conditions were such that the beam contained mainly dimers. Fig. 6 demonstrates that the blue side of peak R is correlated to the red side of peak B. According to the spectra of fig. 7 the red side of peak R is correlated to the blue side of peak B. Note that in fig. 7a the small structure at the blue side of peak B at

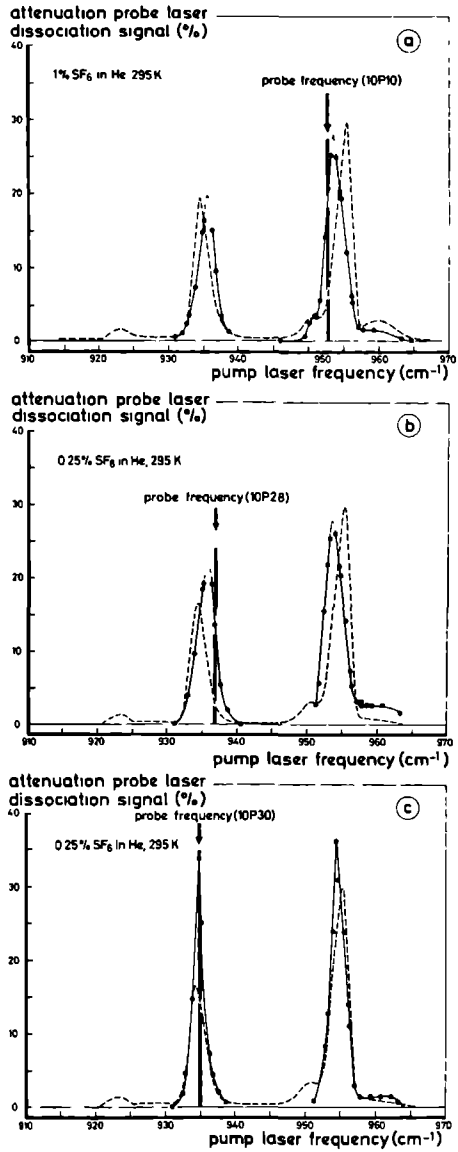

Figure 6

Two-laser spectra of $(^{32}SF_6)_2$. The pump laser power was 1 Watt. The fixed-frequency probe laser was operated at about 2 Watt. The solid curves represent smooth interpolations through the measured points of the two-laser spectra. The dashed curves indicate the relevant (equal source conditions) one-laser spectra.

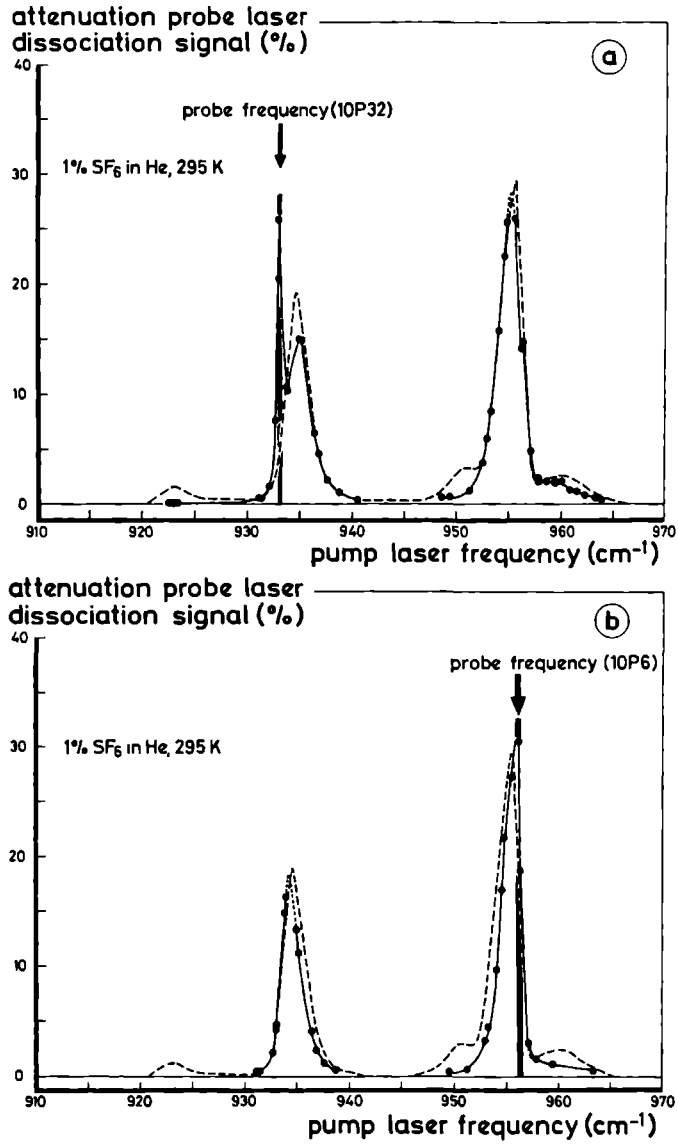

Figure 7

Two-laser spectra of $(^{32}SF_6)_2$. The pump laser power was 1 Watt. The solid curves represent smooth interpolations through the measured points. The dashed curves indicate the relevant (equal source conditions) one-laser spectra.

about 957 cm^{-1} is significant. This feature shows up more clearly in fig. 10a, which was measured with a different laser power. The structure around 960 cm^{-1} is due to trimers as will be discussed in section 3.1.3.

As explained in the introduction, the positions of the two peaks of the dimer spectrum are determined by the parameter λ defined as

$$\lambda = \frac{1}{4\pi\varepsilon_0} (\mu_{01})^2 \left\langle \frac{1}{R^3} \right\rangle$$

According to this formula dimers with a relatively big average intermolecular distance have a small λ and hence absorb at the blue side of peak R and the red side of peak B. Dimers with a relatively small average R have a big λ and absorb at the red side of peak R and the blue side of peak B. This explanation of the widths of the peaks R and B is in agreement with the correlations found in the two-laser spectra (see figs. 6 and 7). A model yielding a distribution in the average intermolecular distance, based on centrifugal distortion, is discussed in section 4.1. Such an explanation for the widths of the peaks in the dimer spectrum implies a width for peak R (shift = -2λ) twice as big as the width for peak B (shift = $-\lambda$). The observed widths are 2.8 cm^{-1} (peak R) and 2.6 cm^{-1} (peak B). A mechanism yielding an extra broadening only for peak B, based on Coriolis interaction, is discussed in section 4.2.

Double resonance experiments around peak R (figs. 6b and 7a) were simulated assuming a simplified spectrum (see fig. 8a) and low laser fluences. Peak R is composed of three Lorentzian lines with different central frequencies. The lines are assumed to belong to different initial levels (1, 2 and 3) of the dimer. The line-shapes are given by

$$L_i(\nu) = \frac{\gamma_i/\pi}{(\nu_i-\nu)^2+\gamma_i^2} \qquad i=1,2,3$$

with $2\gamma_i$ the FWHM linewidths and ν_i the central frequencies. For weak laser power, the one-laser dissociation signal is proportional to $I(\nu)$ with

$$I(\nu) = \sum_{i=1}^{3} N_i L_i(\nu)$$

N_1 is the number of dimers in level i. For the simulation we took $N_1:N_2:N_3 = 50:1:8$, ν_1=935 cm^{-1}, ν_2=933 cm^{-1} and ν_3=937 cm^{-1}, $2\cdot\gamma_1$=1.5 cm^{-1}, $2\cdot\gamma_2$=0.5 cm^{-1} and $2\cdot\gamma_3$=2.5 cm^{-1}. $I(\nu)$ is depicted in fig. 8a.

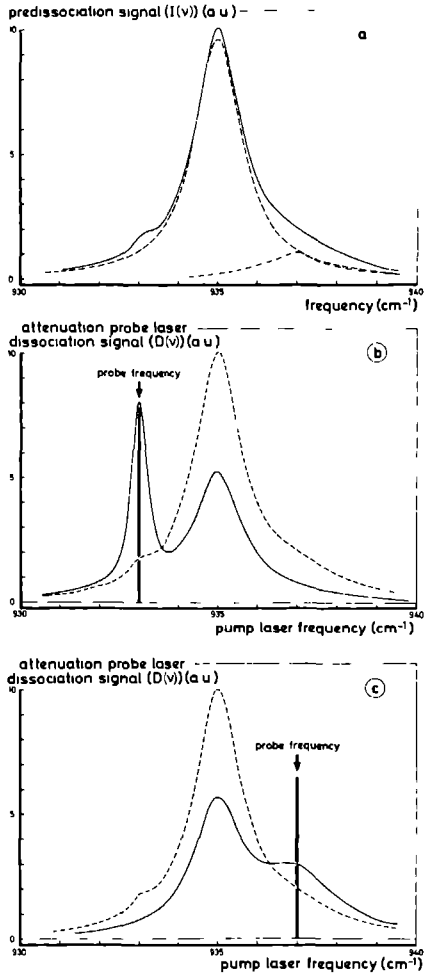

Figure 8

Simulated one-laser (8a, solid line) and two-laser (8b and 8c, solid lines) spectra of $^{32}SF_6$-dimers around peak R. The dotted and dashed curves in 8a are the Lorentzians forming the simulated one-laser predissociation spectrum. The dashed curves in 8b and 8c represent the simulated one-laser spectrum.

In a two-laser experiment with pump and probe laser frequencies ν_{pu} (scanned) and ν_{pr} (fixed), respectively, the double-resonance-signal is proportional to $D(\nu_{pu})$ with (again for weak laser power)

$$D(\nu_{pu}) = \frac{\sum_{i=1}^{3} N_i L_i(\nu_{pu}) \cdot L_i(\nu_{pr})}{I(\nu_{pr})}$$

Figs. 8b and 8c display $D(\nu_{pu})$ for $\nu_{pr}=\nu_2$ and $\nu_{pr}=\nu_3$. Figs. 6b, 7a, 8b and 8c demonstrate a qualitative agreement between the measurements and the simulated spectra. A quantitative agreement is not expected because of the assumed simplified composition of Lorentzians. The simulation shows that the broad structure in fig. 7a around 935 cm^{-1} is due to tails at the probe frequency of relatively strong lines centered around 935 cm^{-1} (see figs. 8a and 8b). Qualitative agreement is also observed between figs. 6b and 8c.

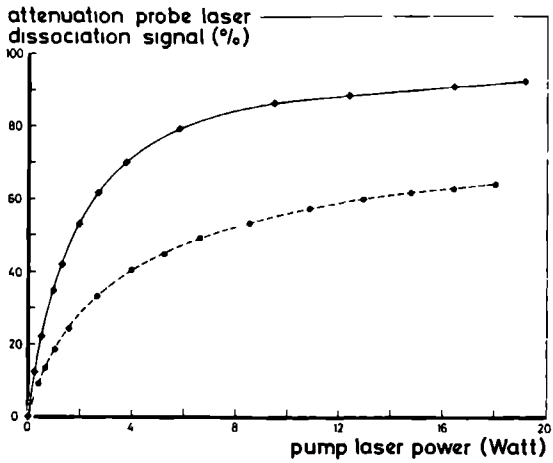

Figure 9

The attenuation of probe-laser-dissociation-signal as a function of pump laser power. Smooth curves have been drawn through the measured points. For the solid curve both the pump laser and the probe laser are tuned to the 10P30 CO_2-laser transition (934.90 cm^{-1}). For the dashed curve the probe laser is tuned to the 10P32 laser line (932.96 cm^{-1}) and the pump laser is operated at the 10P30 laser line.

The inhomogeneity in the $(^{32}SF_6)_2$-predissociation spectrum is also clear from fig. 9. Probing and pumping at the 10P30 laser transition (934.90 cm^{-1}) yields a more than 90% reduction in the probe-laser-dissociation-signal for the highest pump laser powers. However, pumping at the 10P30 laser line while probing at the 10P32 line (932.96 cm^{-1}) only attenuates the probe-laser-dissociation-signal by about 60% even at the highest pump laser powers.

Three-laser spectra

To test the just described ideas we have performed some three-laser experiments (see fig. 3). The results are displayed in fig. 10. In figs. 10a and 10c two-laser spectra (pump laser 1 off) are depicted. These spectra were remeasured with pump laser 1 switched on and tuned close to the top of peak R (see figs. 10b and 10d). The main effect of pump laser 1 is clear; a deep, narrow hole is burnt into the two-laser spectra at the position of pump laser 1. This observation is in agreement with the proposed concept of superposition of Lorentzians (see the last section). In terms of the 3-Lorentzian simulation, pump laser 1 dissociates more than 90% of the dimers belonging to level 1, reducing N_1 to about 10% of its original value (see figs. 8a and 9). This means that the number of these dimers probed at 933 cm^{-1} or 937 cm^{-1} diminishes to about 10% of their original values, yielding a reduction in double-resonance-signal (i.e. attenuation of probe-laser-dissociation-signal due to pump laser 2) if $\nu_{pu1}=\nu_{pu2}$; ν_{pu1} and ν_{pu2} are, respectively, the frequencies of the scanned pump laser 2 and the frequency-fixed pump laser 1.

Irradiation with pump laser 1 yields an increase in double-resonance-signal if $\nu_{pr}=\nu_{pu2}=932.96$ cm^{-1} (10P32) (compare fig. 10a with fig. 10b). If $\nu_{pr}=\nu_{pu2}=936.80$ cm^{-1} (10P28) the double-resonance-signal is reduced by the action of pump laser 1 (compare fig. 10c with fig. 10d). These observations are in agreement with the assumed distribution of linewidths in the simulation described in the last section. The linewidth increases from a relatively small value (0.5 cm^{-1}) at the red side of peak R to a relatively large one (3 cm^{-1}) at the blue side of this peak (compare also fig. 10b with fig. 10d). In terms of our simulation-model switching on pump laser 1 yields mainly a reduction in N_1, the number of dimers in level 1. Thus, for probing at the 10P32 laser transition (932.96 cm^{-1}), pump laser 1 operating at the 10P30 laser line

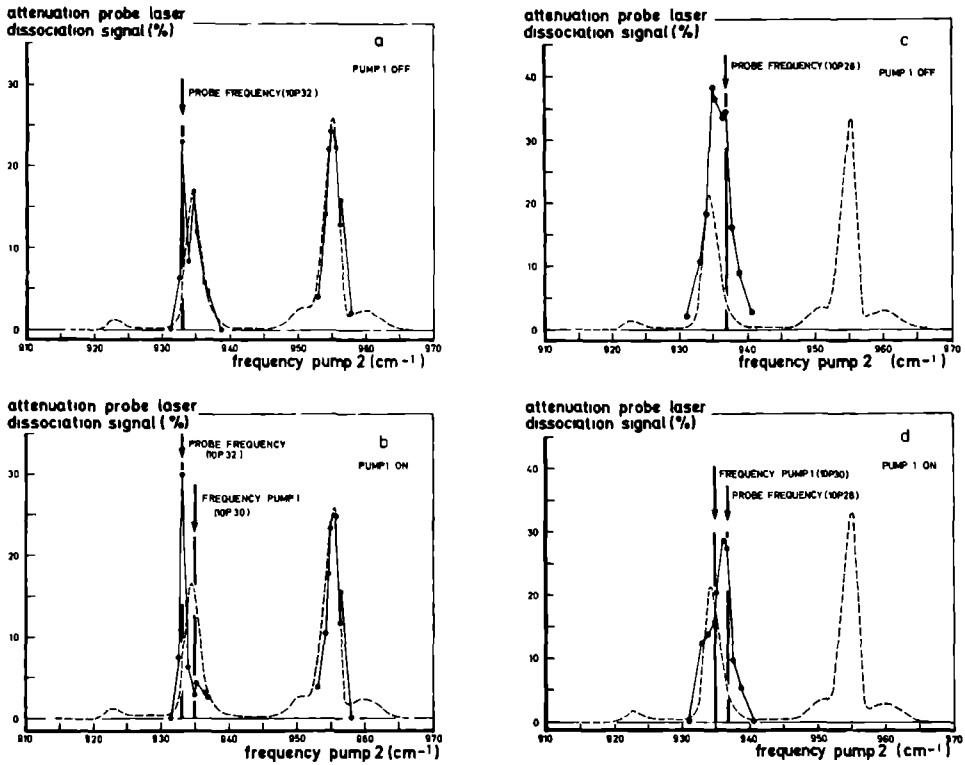

Figure 10

Two-laser (10a and 10c, solid lines) and three-laser (10b and 10d, solid lines) spectra of $^{32}SF_6$-dimers. Pump laser 1 and pump laser 2 were operated at, respectively, 15 Watt and 1 Watt. A mixture of 1% SF_6 in He was used. The dashed curves indicate the relevant one-laser spectrum. In case of three-laser experiments the attenuation of probe-laser-dissociation-signal indicated in the figures is the percentual attenuation due to pump laser 2 of the probe-laser-dissociation-signal left after irradiation by pump laser 1. For probing at 932.96 cm^{-1} (936.80 cm^{-1}) pump laser 1 alone yielded an attenuation of 60% (85%).

(934.90 cm^{-1}) has the effect that the number of probed dimers in level 2 (narrow line and hence relatively easily dissociable) increases with respect to the number of probed dimers in level 1 (relatively broad line and hence more difficult to dissociate). Consequently, switching on pump laser 1 at the 10P30 laser transition yields an increase in double-resonance-signal for $\nu_{pu2}=\nu_{pr}=932.96$ cm^{-1}. Similarly, because of the larger linewidth of dimers in level 3 with respect to the linewidth of dimers in level 1, the double-resonance-signal for $\nu_{pu2}=\nu_{pr}=936.80$ cm^{-1} decreases if pump laser 1 is switched on at the 10P30 laser transition.

According to fig. 6c the 10P30 CO_2 laser frequency (934.90 cm^{-1}) is correlated to the red side of peak B. This correlation is also clear from comparison of figs. 10a and 10b; irradiation with pump laser 1 at the 10P30 laser line yields a narrow hole around 935 cm^{-1}, but also the red side of peak B is influenced. The reduction in double-resonance signal around 954 cm^{-1} is much smaller than the reduction around 935 cm^{-1}. This feature could be due to Coriolis interaction which smears out the $+\lambda$-level (peak B), but (in first order) does not affect the -2λ-level (peak R). This interaction will be discussed in section 4.2.

Laser polarization effects

The two-laser spectra depicted in figs. 6 and 7 were measured with linear-polarized lasers with parallel polarization vectors. The polarization was perpendicular to the molecular beam. To look for laser polarization effects some of the spectra were remeasured with perpendicular polarization vectors. The probe-laser-polarization was along the molecular beam whereas the pump laser was polarized perpendicular to the beam. In contradiction with the expectations no polarization effects were observed; within the relatively small experimental error the spectra were equal to those displayed in figs. 6 and 7. Also, if the pump and the probe laser spatially overlapped no laser polarization effects in the two-laser spectra were observed. The absence of these effects is attributed to coupling between internal motions in the dimer and the rotational angular momentum of the complex.

3.1.3. $(^{32}SF_6)_n$ (n>2)

As is clear from the spectra in fig. 4, the peak around 960 cm^{-1} originates from higher SF_6 clusters.

Fig. 11 displays two-laser IR-predissociation spectra with probe frequencies around 960 cm^{-1}. For figs. 11a and 11b the conditions were such that the beam was expected to contain mainly dimers and trimers. Hence probing around 960 cm^{-1} yields trimer spectra. As predicted by the dipole-dipole interaction model the trimer spectrum consists of three peaks (see fig. 5a). For the prediction of this spectrum an equilateral triangle configuration was assumed. Other (less symmetric) configurations would yield five lines. (The peaks around 935 cm^{-1} and 955 cm^{-1} are doubly degenerate for an equilateral configuration). The peak-positions and the peak-intensities are indicated in table 2.

According to the dipole-dipole interaction model, the peak positions are determined by the parameter λ. For all peaks in the spectrum the shift with respect to the monomer ν_3 frequency (948.0 cm^{-1}) is proportional to λ. Consequently, the peak with the largest shift is most sensitive to this parameter. For the SF_6-trimer this peak is situated around 935 cm^{-1}. As is clear from table 2, the position of this peak is in good agreement with the predicted position for λ=6.8 cm^{-1}, the average value of λ found for the SF_6-dimers. For the peak around 955cm^{-1} there is a slight discrepancy between the measured and the predicted position.

	frequency (cm^{-1}) / intensity (a.u.)		
fig. 11a	935.5 / 4.2	955.2 / 1.8	959.4 / 3
fig. 11b	934.9 / 4.7	955.2 / 2.2	963.3 / 3
H_{dd}	934.9 / 4.3	957.7 / 1.7	961.6 / 3

Table 2

Measured and calculated $(^{32}SF_6)_3$-predissociation-frequencies and peak-intensities, λ=6.8 cm^{-1}.

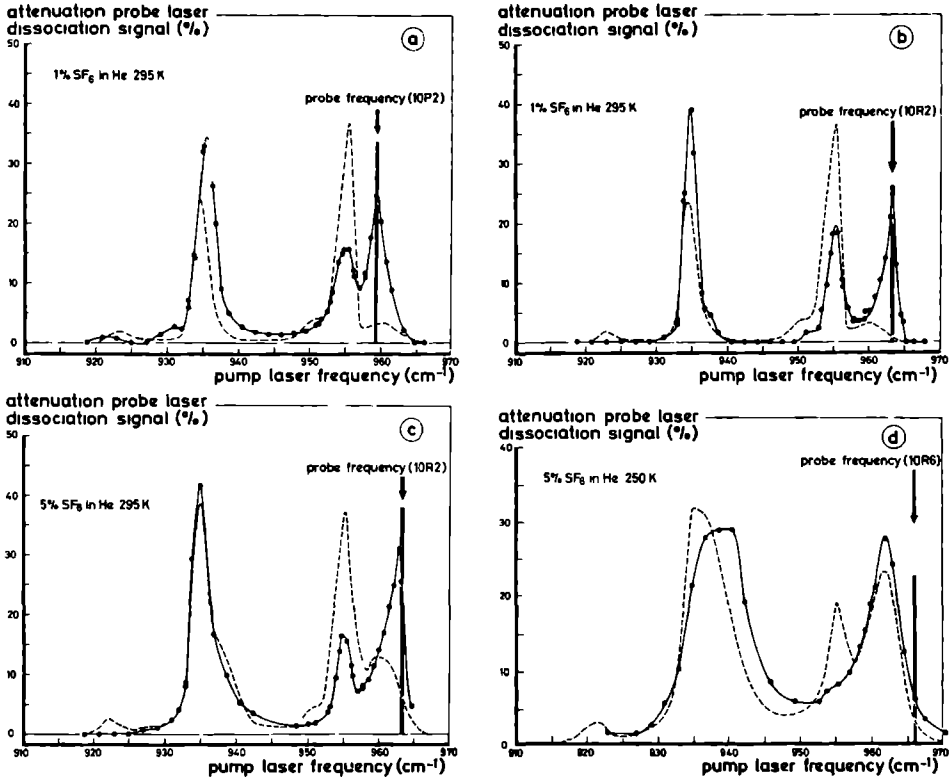

Figure 11

Two-laser spectra of $(^{32}SF_6)_n$-clusters ($n \geq 3$). The pump laser was operated at 1 Watt. Smooth curves have been drawn through the measured points. The dashed curves indicate the relevant one-laser spectra.

As was pointed out in section 3.1.2. for $(SF_6)_2$, a small shift of probe frequency means a change of the probed λ-value. For the SF_6-trimer changing the probe frequency by about 4 cm^{-1} hardly affects the other peaks in the spectrum (see table 2 and figs. 11a and 11b); the peak around 960 cm^{-1}, however, shifts considerably. We have not yet found an explanation for this intriguing behaviour. Geometrical modifications e.g. from the equilateral to isosceles forms did not yield a solution for this problem. Possibly an underlying van der Waals mode around 960 cm^{-1} could be responsible for the observations.

The spectra of figs. 11c and 11d were taken under source conditions favourable for the production of heavier clusters. In the spectrum displayed in fig. 11c the peak around 955 cm^{-1} is smaller than in fig. 11b, indicating that not only trimers but also higher clusters were probed. In fig. 11d this peak is completely absent; mainly higher clusters were probed. The linewidth for the higher clusters is much larger than the linewidth for the trimers (compare e.g. figs. 11b and 11d). In contrast, for C_2H_4-clusters the observed linewidth is essentially independent of cluster-size [6].

3.1.4. $(^{32}SF_6)_n{}^{34}SF_6$

For the two-laser spectra depicted in figs. 12a and 12b the probe laser was tuned to the 10P42 CO_2 laser transition (922.9 cm^{-1}). According to the dipole-dipole interaction model isotopically mixed clusters absorb in the frequency region around 922 cm^{-1} (see fig. 5). For fig. 12a mainly dimers are expected to contribute to the spectrum, whereas for fig. 12b also higher clusters were present in the molecular beam. The figures clearly indicate that the peaks around 935 cm^{-1} and 955 cm^{-1} originate from higher clusters. For the $^{32}SF_6{}^{34}SF_6$-dimer three peaks remain (see fig. 12a). The predicted and measured positions and intensities given in table 3 show at least qualitative agreement. The dimer peak around 955 cm^{-1} could not be observed because of the expected low transition strength (see table 3) and overlap with higher clusters.

The assignment of the peaks around 935 cm^{-1} and 955 cm^{-1} to higher clusters is in agreement with the predictions of the dipole-dipole interaction model; around 922 cm^{-1}, 935 cm^{-1} and 955 cm^{-1} strong peaks are predicted for $(^{32}SF_6)_2{}^{34}SF_6$ (see fig. 5).

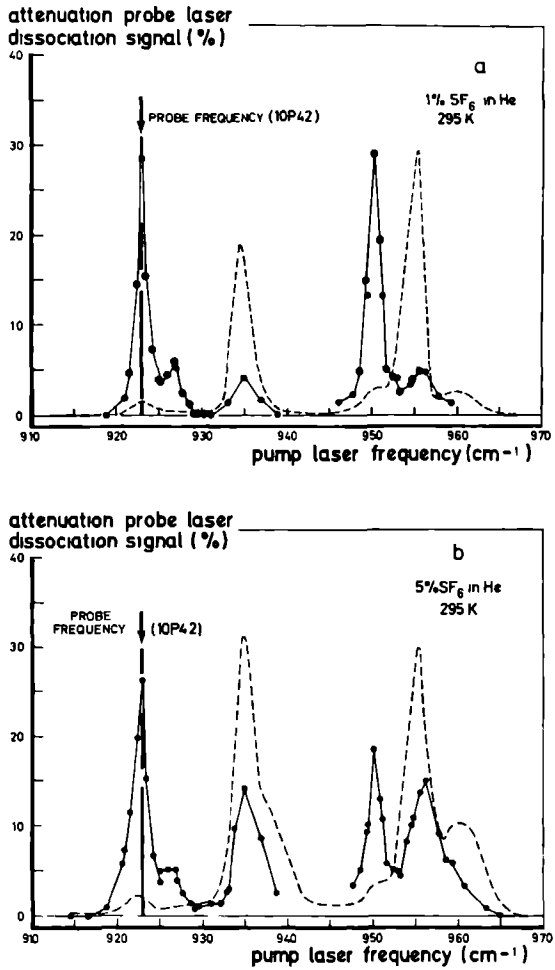

Figure 12

Two-laser spectra of $^{34}SF_6(^{32}SF_6)_n$ (n=1,2). The pump laser was operated at 1 Watt. Smooth curves have been drawn through the measured points. The dashed curves indicate the relevant one-laser spectra.

	frequency (cm^{-1}) / intensity (a.u.)			
experiment	922.9 / 3.3	927.0 / 0.61	950.1 / 3.3	-
H_{dd}	923.3 / 1.9	928.4 / 0.7	950.4 / 3.3	955.5 / 0.15

Table 3

Experimental and theoretical (λ=6.8 cm^{-1}) peak-positions and intensities in the $^{32}SF_6{}^{34}SF_6$-dimer spectrum.

3.2. SiF_4-CLUSTERS

3.2.1. GENERAL ASPECTS

Fig. 13 displays one-laser predissociation spectra of SiF_4-clusters. For the 0.5% SiF_4 in He mixture, source temperature 295 K, mainly dimers contribute to the spectrum. In case of the higher concentration (2%) and lower source temperature (230 K) higher cluster contributions appear.

In fig. 14 peak-positions predicted by the dipole-dipole interaction model [12] are indicated. For the dimers the predicted positions are in agreement with the observations of fig. 13. The $(^{28}SiF_4)_2$-peaks are situated at 1016.4 cm^{-1} and 1037.1 cm^{-1} (see fig. 13). Their widths are, respectively, 7.6 cm^{-1} and 6.0 cm^{-1} FWHM. From the measured line-positions we derive λ=6.9 cm^{-1}, which is slightly smaller than the value of [12] (7.2 cm^{-1}). The central frequency ([1037.1-λ] cm^{-1}) is 1030.2 cm^{-1}, which is (1.2 ± 0.3) cm^{-1} shifted towards the red with respect to the ν_3 excitation frequency of a free $^{28}SiF_4$-molecule (1031.4 cm^{-1}). This shift is in agreement with the result of [12].

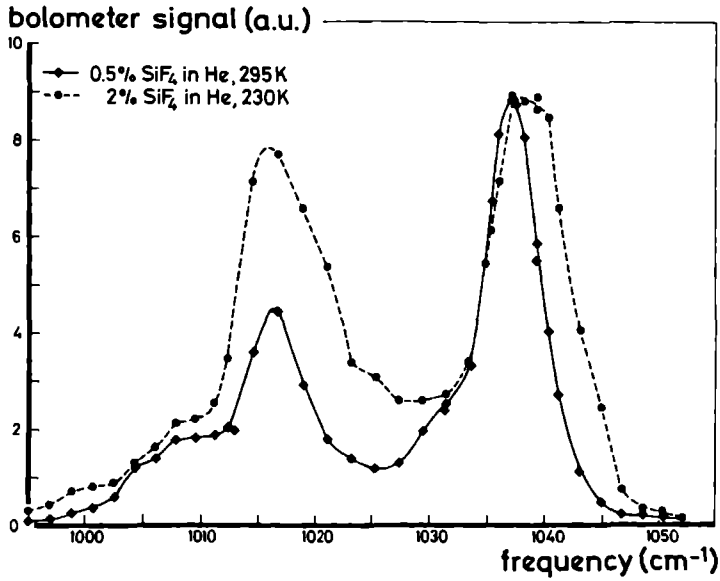

Figure 13

One-laser predissociation spectra of SiF_4-clusters for different source conditions. Smooth curves have been drawn through the measured points. The spectra are normalized at 1036 cm^{-1}. The laser power was 1 Watt and the spot-diameter at the molecular beam was about 0.5 mm.

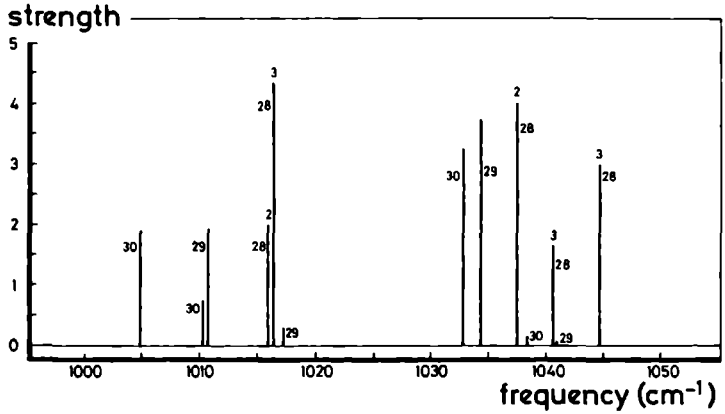

Figure 14

Stick spectra of SiF_4-clusters according to the resonant dipole-dipole interaction model [12]. The height of each bar corresponds to the transition strength times degeneracy. The numbers 29 and 30 indicate transitions of, respectively, $^{29}SiF_4{}^{28}SiF_4$ and $^{30}SiF_4{}^{28}SiF_4$. Sticks indicated by the numbers 28 2 (28 3) belong to $(^{28}SiF_4)_2$ $((^{28}SiF_4)_3)$. The natural abundances of $^{28}SiF_4$, $^{29}SiF_4$ and $^{30}SiF_4$ are 92.21%, 4.70% and 3.09%, respectively.

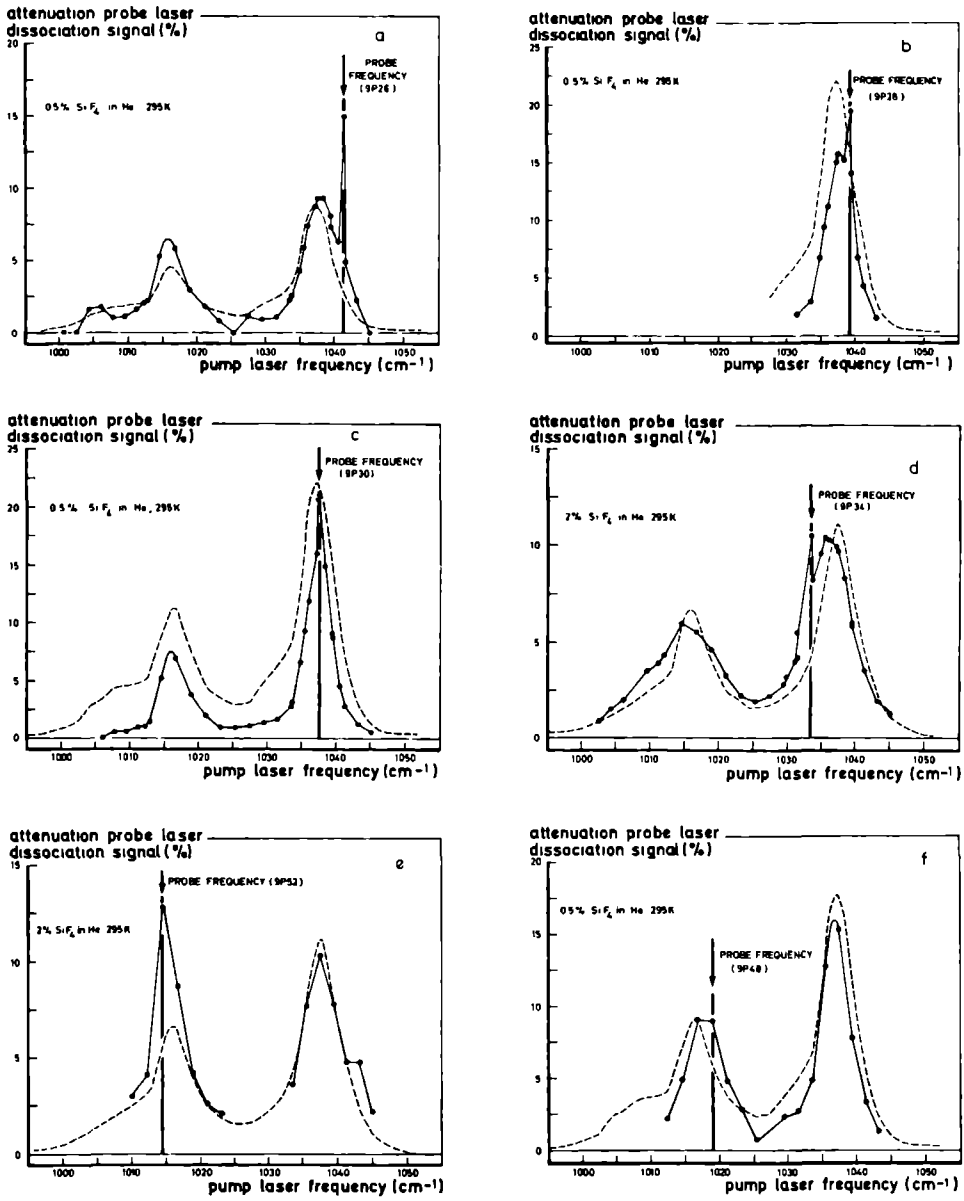

Figure 15

Two-laser spectra of SiF_4-dimers. The pump laser power was 1 Watt. The dashed curves indicate the relevant one-laser spectrum.

3.2.2. $(^{28}SiF_4)_2$

The two-laser spectra of fig. 15 reveal a behaviour of the $^{28}SiF_4$-dimer similar to that of $(^{32}SF_6)_2$. The narrow peak on top of a broad maximum in figs. 15a, 15b, 15c and 15d is comparable to the sharp spectral feature in fig. 7a. As explained in section 3.1.2. the appearance of the broad structure is due to a congestion of Lorentzians around the central frequencies of the two dimer peaks. The concept of a distribution of Lorentzians was again tested by means of three-laser experiments (see fig. 3). The results are displayed in fig. 16. For figs. 16a and 16b the probe laser was tuned to the 9P26 CO_2-laser transition (1041.3 cm^{-1}). For fig. 16a pump laser 1 was switched off, yielding a two-laser spectrum, similar to the one in fig. 15a. This spectrum was remeasured with pump laser 1 tuned to the maximum of the dimer peak (see fig. 16b). A hole is burnt into the broad structure at the position of pump laser 1 and the narrow peak is more intense than in fig. 16a (see also figs. 10a and 10b).

The FWHM-width of the narrow line in fig. 15a is about 0.4 cm^{-1}. The double-resonance-signal around 1010 cm^{-1} for probing at 1033.5 cm^{-1} (see fig. 15d) is attributed to isotopically mixed clusters (see also figs. 13 and 14).

The spectra of fig. 15 confirm a correlation of the blue (red) side of the dimer peak around 1016 cm^{-1} to the red (blue) side of the peak around 1037 cm^{-1} as observed for $^{32}SF_6$ dimers. Note that the small shoulder in fig. 15e around 1043 cm^{-1} is significant. The spectrum in this figure has similarities with those in figs. 7a and 10a.

As for the SF_6-dimer no polarization effects were observed.

4. THEORETICAL RESULTS

4.1. CENTRIFUGAL DISTORTION

A rotating SF_6-dimer experiences a centrifugal force which stretches the dimer so that the effective equilibrium intermolecular distance increases with J, the end-over-end rotational quantum number. In this section the dimer is considered as a diatomic molecule with equilibrium intermolecular distance R_e for J=0. The effective potential $V_J(R)$ [15] is given by

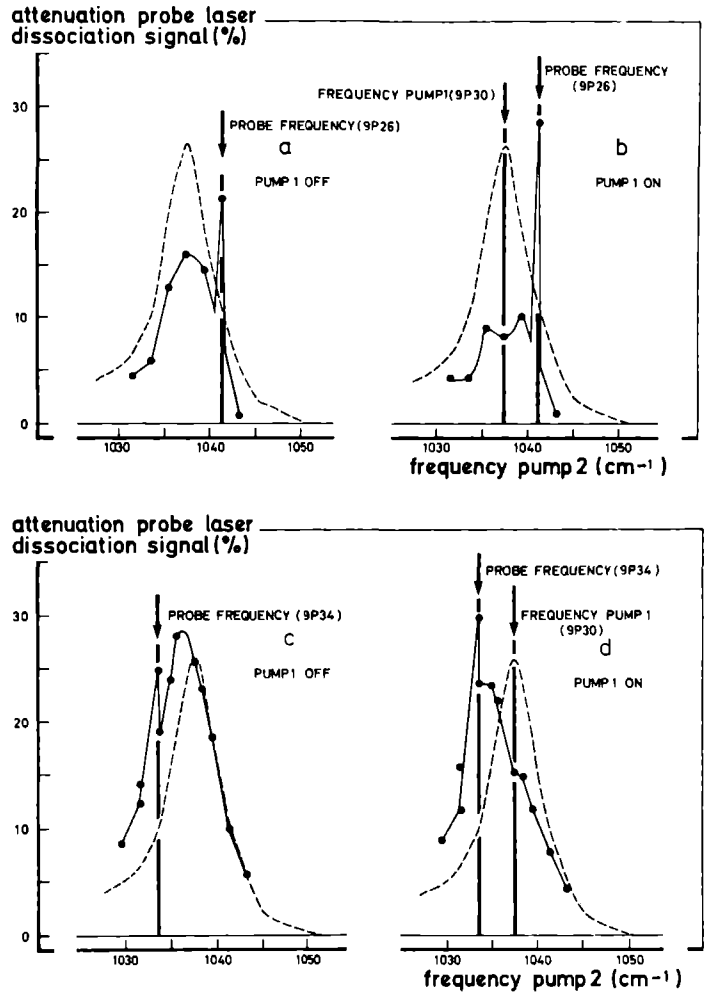

Figure 16

Two-laser (16a and 16c, solid lines) and three-laser (16b and 16d, solid lines) spectra of $(^{28}SiF_4)_2$. Pump laser 1 and pump laser 2 were operated at, respectively, 15 Watt and 1 Watt. The dashed curves indicate the relevant one-laser spectrum. In case of three-laser experiments the attenuation of the probe-laser-dissociation-signal indicated in the figures is the percentual attenuation due to pump laser 2 of the probe-laser-dissociation-signal left after irradiation by pump laser 1.

$$V_J(R) = V(R-R_e) + \frac{J(J+1)\hbar^2}{2\mu R^2}$$

where μ is the reduced mass of the dimer and R the distance between the two monomers in the complex. $V(R-R_e)$ stands for the intermolecular SF_6-potential. According to classical mechanics the equilibrium distance $R_e'(J)$ follows from the relation

$$\left[\frac{dV_J(R)}{dR}\right]_{R=R_e'(J)} = 0$$

For a harmonic potential ($V(R-R_e) = \frac{1}{2}k(R-R_e)^2$) one finds in lowest order

$$R_e'(J) = R_e\left(1 + \frac{J(J+1)4B^2}{(h\nu)^2}\right)$$

Here $B = \frac{\hbar^2}{2\mu R_e^2}$ stands for the end-over-end rotational constant of the complex and $\nu = \frac{1}{2\pi}\sqrt{k/\mu}$ stands for the frequency difference between the vibrational levels of the harmonic potential. As was pointed out in the introduction the position of the two peaks in the $^{32}SF_6$-dimer spectrum is determined by the parameter λ. λ is proportional to $(R_e'(J))^{-3}$, see the introduction. This yields

$$\lambda_e'(J) = \lambda_e\left(1 + \frac{J(J+1)4B^2}{(h\nu)^2}\right)^{-3}, \quad \text{with}$$

$$\lambda_e = \frac{1}{4\pi\epsilon_0}(\mu_{01})^2\frac{1}{R_e^3}.$$

These formulas indicate that the mechanism of centrifugal distortion yields widths for the peaks R and B, which depend on the end-over-end rotational constant B, the energy spacing $h\nu$ between van der Waals stretch vibrational levels and the temperature T of the dimers. $B=0.0087\ cm^{-1}$ was determined in [12]. For $(Ar)_2$ the vibrational spacing $h\nu = 26\ cm^{-1}$ for low lying levels [16,17]. Assuming equal force constants for $(SF_6)_2$ and $(Ar)_2$ the relation $\nu = \frac{1}{2\pi}\sqrt{k/\mu}$ yields $h\nu = 13.6\ cm^{-1}$ for $(SF_6)_2$. The vibrational energy spacing

was also estimated using a Lennard-Jones 12-6 intermolecular potential for SF_6 [18],

$$V(R) = \varepsilon\{(\frac{R_m}{R})^{12} - 2\cdot(\frac{R_m}{R})^6\},$$

with $\varepsilon/k = 200.9$ K and $R_m = 6.18$ Å. The energy spacing between low lying vibrational levels of this potential amounts to 11 cm^{-1}, for a force constant

$$k = (\frac{d^2V}{dR^2})_{R=R_m} = \sqrt{\frac{12\cdot 6\cdot \varepsilon}{R_m^2}}\ .$$

In table 4 the FWHM of the simulated red peak in the dimer spectrum is given as a function of hν and the dimer temperature T. This table indicates that for reasonable temperatures and vibrational spacings the model of centrifugal distortion predicts a linewidth of the correct order of magnitude (1 cm^{-1}). Whether centrifugal distortion alone can explain the observed inhomogeneity can be decided after the dimer temperature and the vibrational spacing are measured properly.

In addition to centrifugal distortion one could also consider the influence on the intermolecular distance of librational modes. From calculations and scattering studies on SF_6-Ar [20] it was concluded that the intermolecular distance for minimum potential energy is strongly dependent on the orientation of the SF_6-molecule. Such an effect can also be expected in the SF_6-dimer. A coupling between the van der Waals stretch and libration modes could be capable to enhance the effects of centrifugal distortion.

4.2. CORIOLIS INTERACTION

The dipole-dipole interaction model discussed in the introduction did not include rotational wavefunctions. In this section rotation of the monomers in the $^{32}SF_6$-dimer will be considered. The Hamiltonian [19] is given by

$$H = H_{dd} + H_{rot1} + H_{rot2} \quad \text{with}$$

$$H_{rot1} = B\vec{J}_1^2 - 2B\zeta\vec{J}_1\cdot\vec{I}_1 \quad \text{and} \quad \vec{J}_1 = \vec{R}_1 + \vec{I}_1,$$

		hν (cm^{-1})				
		2.5	5	10	15	20
	2.5	0.8	0.2	*	*	*
	5.0	1.5	0.4	0.1	*	*
	10	2.8	0.8	0.2	0.1	*
T (K)	15	3.9	1.2	0.3	0.14	*
	20	4.9	1.5	0.4	0.2	0.1
	30	6.5	2.1	0.6	0.3	0.15
	40	7.8	2.7	0.8	0.4	0.2
	50	8.7	3.3	1.0	0.5	0.25

Table 4

The simulated FWHM linewidth in cm^{-1} of the red peak in the $^{32}SF_6$-spectrum as a function of the dimer temperature T and the spacing hν between the vibrational energy levels of the intermolecular potential. A * indicates a width smaller than 0.1 cm^{-1}.

$\hbar\vec{J}_i$ = total angular momentum of monomer i

$\hbar\vec{R}_i$ = rotational angular momentum of monomer i

$\hbar\vec{l}_i$ = vibrational angular momentum of monomer i

B and ζ stand, respectively, for the rotational constant of the monomers and the Coriolis coupling constant. For $^{32}SF_6$ ($^{28}SiF_4$) ζ=0.700 (0.534). For the vibrational ground state l=0, whereas for the ν_3 states l=1. H_{roti} can be written in a more suitable form.

$$H_{roti} = B\vec{R}_i^2 + 2B(1-\zeta)(R_{iz}l_{iz}+\tfrac{1}{2}R_{i+}l_{i-}+\tfrac{1}{2}R_{i-}l_{i+}) + B\vec{l}_i^2(1-2\zeta),$$

with $R_{i\pm} = R_{ix} \pm i R_{iy}$ and $l_{i\pm} = l_{ix} \pm i l_{iy}$.

The vibrational basis-set

$$|1\rangle = \frac{1}{\sqrt{2}}[|x_1\rangle + i|y_1\rangle]$$

$$|2\rangle = \frac{1}{\sqrt{2}}[|x_2\rangle + i|y_2\rangle]$$

$$|3\rangle = \frac{1}{\sqrt{2}}[|x_1\rangle - i|y_1\rangle]$$

$$|4\rangle = \frac{1}{\sqrt{2}}[|x_2\rangle - i|y_2\rangle]$$

$$|5\rangle = |z_1\rangle$$

$$|6\rangle = |z_2\rangle$$

consists of eigenfunctions of the $\vec{l}_i^2$ and the l_{iz} operators.

$$l_{iz}\,|z_i\rangle = 0$$

$$l_{iz}\,\frac{1}{\sqrt{2}}[|x_i\rangle \pm i|y_i\rangle] = \pm\frac{1}{\sqrt{2}}[|x_i\rangle \pm i|y_i\rangle]$$

$$\vec{l}_i^2\,|z_i\rangle = l(l+1)|z_i\rangle$$

$$\vec{l}_i^2\,\frac{1}{\sqrt{2}}[|x_i\rangle \pm i|y_i\rangle] = l(l+1)\,\frac{1}{\sqrt{2}}[|x_i\rangle \pm i|y_i\rangle], \quad l = 1 \text{ in this case.}$$

As is clear from the definition of the functions $|x_i\rangle$, $|y_i\rangle$ and $|z_i\rangle$ (see the introduction) for the states $|1\rangle$, $|3\rangle$ and $|5\rangle$ monomer 2 is in its ground vibrational level, whereas for $|2\rangle$, $|4\rangle$ and $|6\rangle$ monomer 1 is in its ground vibrational state. A more suitable notation for the functions $|1\rangle$ to $|6\rangle$ is given by $|l_1,m_{l1};l_2,m_{l2}\rangle$, i.e.

$$|1\rangle = |1,1;0,0\rangle$$
$$|2\rangle = |0,0;1,1\rangle$$
$$|3\rangle = |1,-1;0,0\rangle$$
$$|4\rangle = |0,0;1,-1\rangle$$
$$|5\rangle = |1,0;0,0\rangle$$
$$|6\rangle = |0,0;1,0\rangle$$

For this basis the matrix of H_{dd} is equal to the matrix given in fig. 1. Consequently, the vibrational eigenfunctions of H_{dd} for the $+\lambda$-level and the -2λ-level are given by

$$+\lambda: \quad |+\lambda_a\rangle = \frac{1}{\sqrt{2}}[|1,1;0,0\rangle+|0,0;1,1\rangle] \quad \text{and}$$

$$|+\lambda_b\rangle = \frac{1}{\sqrt{2}}[|1,-1;0,0\rangle+|0,0;1,-1\rangle]$$

$$-2\lambda: \quad |-2\lambda\rangle = \frac{1}{\sqrt{2}}[|1,0;0,0\rangle+|0,0;1,0\rangle]$$

To determine the energy levels of the vibration-rotation Hamiltonian the following matrix elements have to be considered

$$\langle l_1,m_{l1},R_1,M_{R1};l_2,m_{l2},R_2,M_{R2}|H_{dd}+H_{rot1}+H_{rot2}|l_1',m_{l1}',R_1',M_{R1}';l_2',m_{l2}',R_2',M_{R2}'\rangle$$

The selection rules for H_{rot1} and H_{rot2} are

H_{rot1}	H_{rot2}
$\Delta l_1 = 0$	$\Delta l_1 = 0$
$\Delta R_1 = 0$	$\Delta R_1 = 0$
$\Delta m_{l1} = 0,\pm1$	$\Delta m_{l1} = 0$
$\Delta m_{l2} = 0$	$\Delta m_{l2} = 0,\pm1$
$\Delta M_{R1} = 0,\pm1$	$\Delta M_{R1} = 0$
$\Delta M_{R2} = 0$	$\Delta M_{R2} = 0,\pm1$
$\Delta(M_{R1}+m_{l1}) = 0$	$\Delta(M_{R2}+m_{l2}) = 0$

The expected splittings of the ν_3-level due to the rotational part of the Hamiltonian are small with respect to the splittings caused by H_{dd}. Consequently, in first order approximation we can treat the $+\lambda$-level and the -2λ-level separately. As is clear from the eigenfunctions ($|+\lambda_a\rangle$, $|+\lambda_b\rangle$ and $|-2\lambda\rangle$), H_{dd} does not mix $(m_{l1}+m_{l2})=0$ (-2λ-level) with $(m_{l1}+m_{l2})=\pm1$ ($+\lambda$-level), in agreement with the selection rule $\Delta(m_{l1}+m_{l2})=0$ for H_{dd}. In combination with the above selection rules this yields $\Delta m_{li}=0$ and $\Delta M_{Ri}=0$. As a consequence, the only matrix elements of interest are the diagonal elements

$$\langle l_1,m_{l1},R_1,M_{R1};l_2,m_{l2},R_2,M_{R2}|H_{rot1}+H_{rot2}|l_1,m_{l1},R_1,M_{R1};l_2,m_{l2},R_2,M_{R2}\rangle =$$

$$\sum_{i=1}^{2} BR_i(R_i+1)+2B(1-\zeta)m_{li}M_{Ri}+B(1-2\zeta)l_i(l_i+1)$$

These matrix elements yield the following energy splittings for, respectively, $|+\lambda_a\rangle$, $|+\lambda_b\rangle$, $|-2\lambda\rangle$ and $|0\rangle$, due to the rotational Hamiltonian

$$\langle+\lambda_a,R_1,M_{R1},R_2,M_{R2}|H_{rot1}+H_{rot2}|+\lambda_a,R_1,M_{R1},R_2,M_{R2}\rangle =$$

$$= BR_1(R_1+1)+BR_2(R_2+1)+2B(1-\zeta)(M_{R1}+M_{R2})+2B(1-2\zeta)$$

$$\langle +\lambda_b, R_1, M_{R1}, R_2, M_{R2} | H_{rot1} + H_{rot2} | +\lambda_b, R_1, M_{R1}, R_2, M_{R2} \rangle =$$

$$= BR_1(R_1+1) + BR_2(R_2+1) - 2B(1-\zeta)(M_{R1}+M_{R2}) + 2B(1-2\zeta)$$

$$\langle -2\lambda, R_1, M_{R1}, R_2, M_{R2} | H_{rot1} + H_{rot2} | -2\lambda, R_1, M_{R1}, R_2, M_{R2} \rangle =$$

$$= BR_1(R_1+1) + BR_2(R_2+1) + 2B(1-2\zeta)$$

$$\langle 0 | H_{rot1} + H_{rot2} | 0 \rangle = BR_1(R_1+1) + BR_2(R_2+1)$$

Because of the absence of a permanent dipole moment for the SF_6-monomers only $\Delta R_1=0$, $\Delta R_2=0$ transitions (Q-branches) from the vibrational groundstate to the ν_3-excited states are allowed. As a consequence the $|0\rangle \rightarrow |-2\lambda\rangle$ transition is not smeared out by the introduction of the rotational Hamiltonian. In contrast the $|0\rangle \rightarrow |+\lambda_a\rangle$ and the $|0\rangle \rightarrow |+\lambda_b\rangle$ transitions are smeared out. This effect is proportional to $2B(1-\zeta)(M_{R1}+M_{R2})$.

For $(SiH_4)_2$ the blue peak is substantially broader than the red peak (9.6 cm^{-1} vs. 6.1 cm^{-1}) [12], suggesting an important contribution of the Coriolis interaction to the observed spectrum. Indeed, for this dimer the effect of introducing the rotational Hamiltonian is expected to be large because of the relatively big B-constant for SiH_4 (2.859 cm^{-1}) and the smearing out process being proportional to $2B(1-\zeta)(M_{R1}+M_{R2})$.

ACKNOWLEDGEMENTS

The authors would like to thank dr. Jon Hougen for helpful discussions concerning section 4, dr. Marcel Snels for calculating the $^{32}SF_6$-trimer spectra for different geometrical configurations and drs. Nico Dam for providing us with plotprog. The authors also want to thank Cor Sikkens for his work on the design of the apparatus and his technical advice and assistance, and Frans van Rijn and John Holtkamp for electronic support. We thank dr. H.

Bluyssen and A. van Etteger for designing our lasers and for lending us the third laser for the three-laser experiments. The support of A. van Etteger during the three-laser measurements is gratefully appreciated. This work was financially supported by the Stichting Fundamenteel Onderzoek der Materie (FOM) and the Nederlandse Organisatie voor Wetenschappelijk Onderzoek (NWO).

REFERENCES

[1] W.R. Gentry, Am. Chem. Soc. Symp. Ser. 263 (1984) 289

[2] K.C. Janda, Adv. Chem. Phys. 60 (1985) 201

[3] F.G. Celii and K.C. Janda, Chem. Rev. 86 (1986) 507

[4] R.E. Miller, J. Phys. Chem. 90 (1986) 3301

[5] U. Buck and H. Meyer, Phys. Rev. Lett. 52 (1984) 109

[6] F. Huisken and T. Pertsch, J. Chem. Phys. 86 (1987) 106

[7] U. Buck, Ch. Lauenstein, H. Meyer and R. Sroka, J. Phys. Chem., to be published

[8] U. Buck, Ch. Lauenstein, A. Rudolph, B. Heijmen, S. Stolte and J. Reuss, Chem. Phys. Lett. 144 (1988) 396

[9] J. Geraedts, S. Stolte and J. Reuss, Z. Phys. A 304 (1982) 167

[10] J. Geraedts, M. Waayer, S. Stolte and J. Reuss, Faraday Disc. Chem. Soc. 73 (1982) 375

[11] J. Geraedts, M. Snels, S. Stolte and J. Reuss, Chem. Phys. Lett. 106 (1984) 377

[12] M. Snels and R. Fantoni, Chem. Phys. 109 (1986) 67

[13] B. Heijmen, C. Liedenbaum, S. Stolte and J. Reuss, accepted for publication in Laser Chemistry

[14] B. Heijmen, A. Bizzarri, S. Stolte and J. Reuss, to be published in Chem. Phys.

[15] G. Herzberg, "Spectra of diatomic molecules" (van Nostrand Reinhold Company, 1950)

[16] H.P. Godfried and I.F. Silvera, Phys. Rev.. A 27 (1983) 3008

[17] E.A. Colbourn and A.E. Douglas, J. Chem. Phys. 65 (1976) 1741

[18] J. Hirschfelder, C. Curtiss, R. Byron Bird, "Molecular theory of gases and liquids" (John Wiley and Sons Inc., 1954)

[19] K. Hecht, J. Mol. Spectrosc. 5 (1960) 355

[20] R.T. Pack, J.J. Valentini and J.B. Cross, J. Chem. Phys. 77 (1982) 5486

CHAPTER 6

IR-EXCITATION AND DISSOCIATION OF $(NH_3)_n$ (n=2,3,4,5) AND $ArNH_3$

B. Heijmen, A. Bizzarri, S. Stolte and J. Reuss
Department of Molecular and Laser Physics, University of Nijmegen
Toernooiveld, 6525 ED Nijmegen, The Netherlands

ABSTRACT

By means of IR-IR double resonance experiments with CO_2-lasers correlations and homogeneous linewidths have been determined in the predissociation spectrum of ammonia dimers. Excitation with a CO_2-laser photon without dissociation has been observed for ammonia trimers and some heavier ammonia clusters (n=4,5), yielding broad (6.5 cm^{-1} for the trimers) homogeneous excitation peaks. In these cases absorption of a second (red-shifted) photon yields dissociation. Due to quenching of the inversion motion the observed ν_2-anharmonicity-red-shifts (10 cm^{-1} for the ammonia trimer and 17 cm^{-1} for $(NH_3)_n$, n=4,5) are much smaller than the shift for the free ammonia molecule (329 cm^{-1}). In case of the ammonia trimer sharp holes (1 MHz FWHM) have been burnt into the broad (6.5 cm^{-1} FWHM) excitation peak. We have measured a (still instrumental) FWHM linewidth of 2 MHz for a predissociation-line of $ArNH_3$.

As was shown independently by Snels et al. [1,2] and the Pauly group, Huisken et al. [3], the $(NH_3)_2$-predissociation spectrum connected with the ν_2-umbrella excitation consists of two main maxima, one around 975 cm^{-1} (peak b), the other around 1005 cm^{-1} (peak a), see fig. 1. Both peaks are strongly shifted towards the blue with respect to the inversion-free ν_2 band origin of free NH_3 at 950.3 cm^{-1}. The appearance of two peaks in the spectrum is due to the fact that the two monomers in the complex are not equivalent [1].

Snels et al. measured the $(NH_3)_n$ predissociation spectrum using a cw CO_2 laser and bolometric detection of the induced attenuation of the molecular beam. By varying the source conditions and the concentration of NH_3 in the seeding gas helium, they demonstrated convincingly that the peaks a and b both belong to the ammonia dimer [1]. In combination with a pulsed CO_2-laser Huisken et al. used the method of cluster-size-selection by means of scattering, which was developed by Buck et al. in Göttingen [4]. By choosing the proper detector angle and detection mass, a pure ammonia dimer spectrum could be measured [3].

Fraser et al. and Snels et al. discovered that peak b arises from partially overlapping peaks [1,5,6], see fig. 1. Microwave-IR double resonance experiments showed that b_2 and b_3 (see fig. 1) are related to J=0→1, K=0 microwave transitions, belonging to different initial levels [5]. According to Snels et al. a tunneling motion of the monomers in the complex could be partly responsible for the observed structure in peak b [1].

Several theoretical as well as experimental studies on the dissociation energy have suggested that dissociation of the ammonia dimer after absorption of a single CO_2-laser photon is unlikely [7,8]. Other experiments, however, show that dissociation with a single photon of 970 cm^{-1} is indeed possible [1,5]. It has been reported that only dimers with a relatively high internal energy can dissociate after absorption of a single CO_2-laser photon [9], but an alternative interpretation of the last experiment has been proposed in which the existence of the undissociable complexes is attributed to the presence of higher clusters in the molecular beam [1].

It has been observed that the small ammonia clusters (n=3,4,5,6) have permanent dipole moments smaller than 0.3 D [10]. A cyclic configuration of the monomers in the clusters is in agreement with these observations. In such a geometry each monomer is bound to two neighbours in the complex, possibly

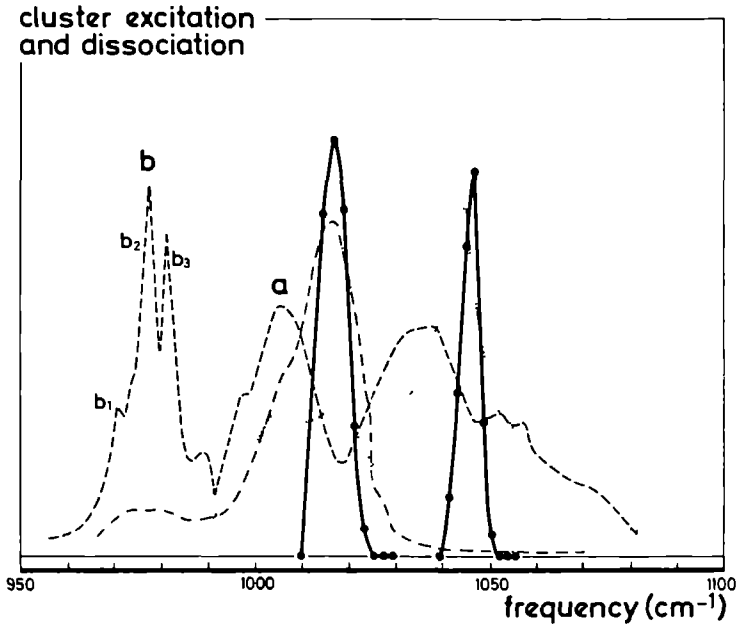

Figure 1

------- IR predissociation spectrum of ammonia clusters measured by means of bolometric detection [1]

-·-·-·- IR predissociation spectrum for $(NH_3)_{2,3}$ [3]

····· IR predissociation spectrum for $(NH_3)_{4,5}$ [3]

The solid curves around 1016 cm^{-1} and 1045 cm^{-1} are excitation curves for $(NH_3)_3$ and $(NH_3)_{4,5}$, respectively; the clusters absorb a photon but do not dissociate. The spectrum for $(NH_3)_2$ in [3] which is not depicted in this figure consists of the peaks a and b.

yielding a higher dissociation energy for the trimers and the tetramers than for the dimers.

Using an electrostatic model and the assumption of a cyclic structure Snels et al. estimated the bonding energies for small ammonia clusters (n=3,4,5,6) [1]. They reported an energy per bond of about 700 cm^{-1} for all small clusters. Dissociation of a cyclic cluster requires rupture of at least two bonds, i.e. one CO_2-laser photon would not suffice for dissociation of trimers and tetramers.

In fig. 1 cluster spectra of Huisken et al. [3] for selected cluster-sizes are compared with the cluster dissociation spectrum obtained by Snels et al. The experiments of Huisken et al. have been performed with a pulsed line-tunable CO_2 laser, whereas Snels et al. used a cw line-tunable CO_2 laser. The laser power in the pulsed laser experiment is several orders of magnitude higher than in the cw laser experiment, providing the possibility of multiphoton transitions in the first case. Fig. 1 shows that in Huisken's experiment trimers dissociate after absorption at 1016 cm^{-1}. However, the cw laser experiment shows a dip around 1016 cm^{-1}. The same phenomenon appears around 1045 cm^{-1}; a peak due to $(NH_3)_n$ with n=4 or 5 is accompanied by a dip in the cw laser spectrum. These observations, together with the expected high binding energy for cyclic clusters suggest that in the pulsed laser experiment dissociation of clusters due to multiphoton transitions plays a role. The low power in the cw laser experiment makes such transitions improbable.

In this paper we report on excitation and dissociation of ammonia clusters in two- and three-laser experiments.

2. EXPERIMENTAL

The measurements were performed with a molecular beam apparatus, similar to the one described in [11,12]. The apparatus is sketched in fig. 2. The molecular beam is produced by supersonic expansion of a gas mixture through a platinum-iridium electron microscope diaphragm (Siemens) with a diameter of 30 μm. After passing through the skimmer (diameter 1 mm) the molecules enter the laser chamber. Here interaction with three home-built cw CO_2 lasers is possible. In the last chamber the molecular beam is detected by a bolometer.

The pump system of the source chamber consists of a water baffled oil diffusion pump (6000 l/s) backed by a mechanical booster pump (500 m^3/h) and a

rotary pump (16 m^3/h). The buffer chamber is pumped by a water baffled oil diffusion pump (3100 l/s) backed by a rotary pump (16 m^3/h). The pumping of the bolometer chamber is performed partly by a water baffled oil diffusion pump (400 l/s) backed by a rotary pump (4 m^3/h) and partly by the bolometer dewar that acts as a cryopump. Typical operating pressures are $2 \cdot 10^{-4}$ torr, 10^{-6} torr and 10^{-7} torr in, respectively, the source chamber, the laser chamber and the bolometer chamber.

For the experiments on the ammonia dimer and trimer a 2% NH_3 in helium mixture was used. For the higher cluster measurements we chose a 5% NH_3 in helium mixture. The stagnation pressure was 5 atm. The measurements on $ArNH_3$ were performed with a mixture consisting of 2% NH_3, 10% Ar and 88% He. The stagnation pressure was 9 atm in this case. The source temperature was always 295 K.

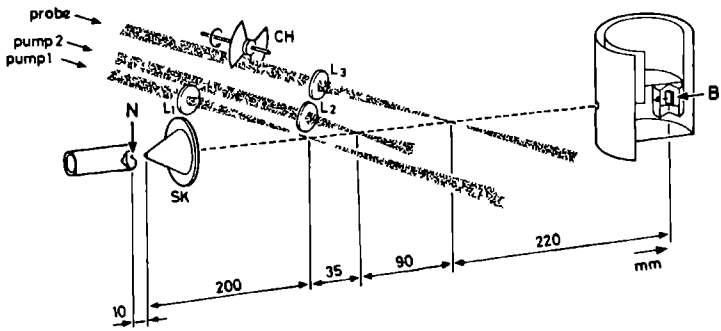

Figure 2

A schematic picture of the apparatus. The lenses L1, L2 and L3 have focal lengths of 37.5 cm, 25 cm and 37.5 cm, respectively. Pump laser 1, pump laser 2 and the probe laser have spot diameters of, respectively, 0.8 mm, 0.5 mm and 0.8 mm at the molecular beam. N=nozzle (30 microns), SK=skimmer, B=bolometer, CH=chopper. The bolometer is shielded by screens at 4.2 K and 77 K, respectively. The nozzle temperature can be varied between 100 K and 300 K.

The bolometer (Infrared Lab.) was operated at 4.2 K. It consists of a doped Si detector (1x1 mm^2) on a substrate of sapphire (2x5 mm^2).

In all experiments the probe-laser-beam is mechanically chopped (67 Hz). Irradiation of the molecular beam by the probe laser initiates dissociation of clusters in the beam. The fragments leave the molecular beam, yielding a reduction of energy flux onto the bolometer, which results in a change of bolometer signal. This probe-laser-dissociation-signal is measured by means of phase sensitive detection. Switching on one or both of the unchopped pump lasers can lead to an attenuated (hole burning) or to an enhanced probe-laser-dissociation-signal. If the pump and the probe lasers dissociate clusters in the same initial state, pumping will lead to an attenuation of probe-laser-dissociation-signal. However, if the beam contains clusters that do not dissociate after absorption of a single CO_2-laser-photon, the following process can occur. The (unchopped) pump laser excites clusters without dissociating them. Next, absorption of a second (probe laser) photon leads to dissociation, yielding an enhanced probe-laser-dissociation-signal.

The line tunable cw CO_2 lasers have a fine-tunability of 75 MHz around the laser lines. Scanning of the lasers around the laser-line-centres was perfomed by applying a high voltage ramp to a PZT that controls the length of the laser cavity. The lasers were operated with $^{12}CO_2$ and with $^{13}CO_2$.

The laser beams were focused onto the molecular beam by means of lenses (see fig. 2). The resulting spots were always bigger than the effective dimensions of the molecular beam. The effective profile of the molecular beam is determined by the dimensions of the bolometer, the source-to-bolometer distance and the source-to-laser distance.

Most experiments described below are two-laser experiments. In these cases pump laser 1 is not used (see fig. 2). Three-laser experiments will be announced explicitly in the text. In all other cases two lasers have been employed.

3. RESULTS

3.1. THE AMMONIA DIMER

Fig. 3 shows two-laser predissociation spectra. Figs. 3a and 3b clearly demonstrate that the peaks b_2 and b_3 originate from different initial states,

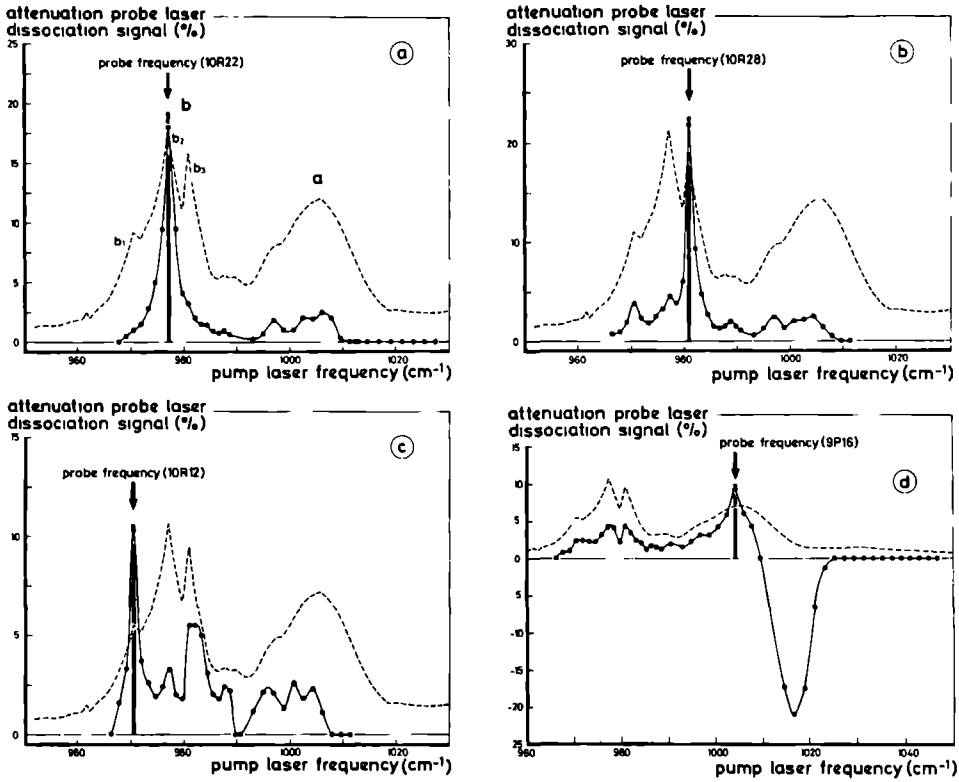

Figure 3

Two-laser predissociation spectra of the ammonia dimer. Irradiation with the pump laser yields a reduction in probe-laser-dissociation-signal. The big negative peak in 3d is due to ammonia trimers. The probe (pump) laser power was 5 Watt (7.5 Watt). The probe laser frequencies are indicated in the figures. The dashed curves indicate the one-laser predissociation spectrum.

in agreement with the microwave-IR double resonance measurements [5] and a tentative assignment of the structure of peak b [13]. From figs. 3b and 3c we deduce a correlation between b_1 and the blue side of b_3, again in agreement with the above mentioned assignment, the K=1→0 transition at 970 cm^{-1} (b_1) is correlated to the K=1→2 transition around 984 cm^{-1}, see fig. 3c. Figs. 3a, 3b and 3c show that the peaks b_1, b_2 and b_3 are all correlated with peak a. In agreement with this observation the top of peak a is correlated to b_1, b_2 and b_3, see fig. 3d. The big negative peak around 1015 cm^{-1} in fig. 3d is due to ammonia trimers and will be discussed in the next section.

For b_1, b_2 and b_3 the linewidths are, respectively, 2.3 cm^{-1}, 2.9 cm^{-1} and 2.3 cm^{-1} FWHM. From their IR-microwave double resonance experiments Fraser et al. deduce the somewhat larger linewidths 5.2 cm^{-1} and 3.5 cm^{-1} for b_2 and b_3, respectively. Another difference concerns the strongly asymmetric double resonance lineshapes of Fraser et al. for b_2 and b_3 as compared to our lineshapes. The origin of the observed widths can be due to a complicated rotation-vibration excitation spectrum, a lifetime effect or a combination of the two.

According to Howard et al. [9] only the ammonia dimers with a relatively high internal energy can dissociate after absorption of a single CO_2-laser-photon. In our experiments no evidence has been found for the existence of dimers that absorb a CO_2-laser-photon and do not dissociate; for all laser frequencies around the peaks a and b irradiation yields a reduction in the heat transferred to the bolometer. Moreover, in the two-laser experiments, enhanced dimer-dissociation-signal of the probe laser due to excitation of dimers (without dissociation) by the pump laser was not observed. For the ammonia trimer enhanced probe-laser-dissociation-signal due to excitation by the pump laser has been observed, see section 3.2.

In order to find evidence for the existence of long-living (narrow line) dimers, we have also searched for narrow hole-burning lines (1 MHz) in two-laser spectra (see section 3.4.3 and section 5), however, again without success. The absence of narrow structures in the two-laser-spectra indicates that the linewidth due to the finite lifetime of the dimer is much larger than 1 MHz.

As is shown in fig. 3d an enhanced probe-laser-dissociation-signal is detected, if the probe laser is set to 1004.28 cm^{-1} and the pump laser to 1016 cm^{-1}. This enhanced probe-laser-dissociation-signal is observed while pumping in the frequency region where Huisken et al. measured dissociation of ammonia trimers (see fig. 1). In our experiment the pump laser at 1016 cm^{-1} excites trimers without dissociating them. Next the excited trimers absorb a probe-laser-photon which causes dissociation. The frequency of this second photon is shifted towards the red with respect to the excitation frequency. For the probe-laser-frequency set to 1004.28 cm^{-1} the (pump laser) excitation curve is also depicted in fig. 1.

Fig. 5 displays similar excitation curves for several probing frequencies; enhanced dissociation due to pumping is only observed after excitation around 1015 cm^{-1}. The power dependence of the trimer excitation is displayed in fig. 4.

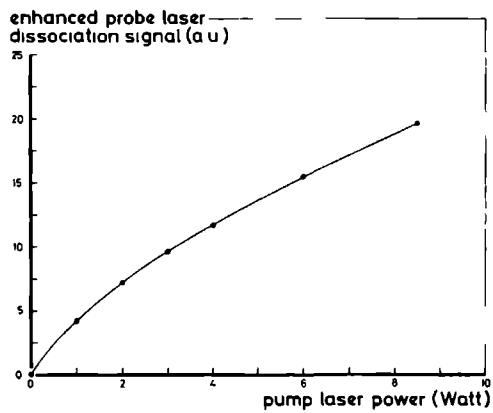

Figure 4

Power dependence of the ammonia trimer excitation. Excitation yields an enhanced probe-laser-dissociation-signal. The probe laser was fixed at 1004.28 cm^{-1}. The pump laser was tuned to the 9P50 laser transition (1016.72 cm^{-1}), near to the trimer excitation maximum (see fig. 5). The spot diameter of the pump laser was about 0.5 mm.

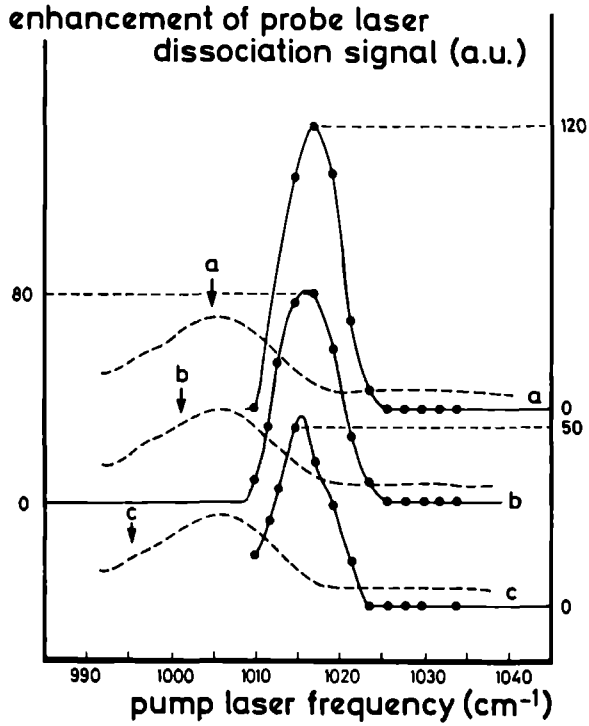

Figure 5

Excitation spectra of the ammonia trimer. The trimers are excited by the pump laser. Next, absorption of a second (probe laser) photon yields dissociation. The probe-laser-frequencies for the three spectra are indicated by arrows. The probe (pump) laser power was 3 Watt (8 Watt). The dashed curves indicate the one-laser predissociation spectrum.

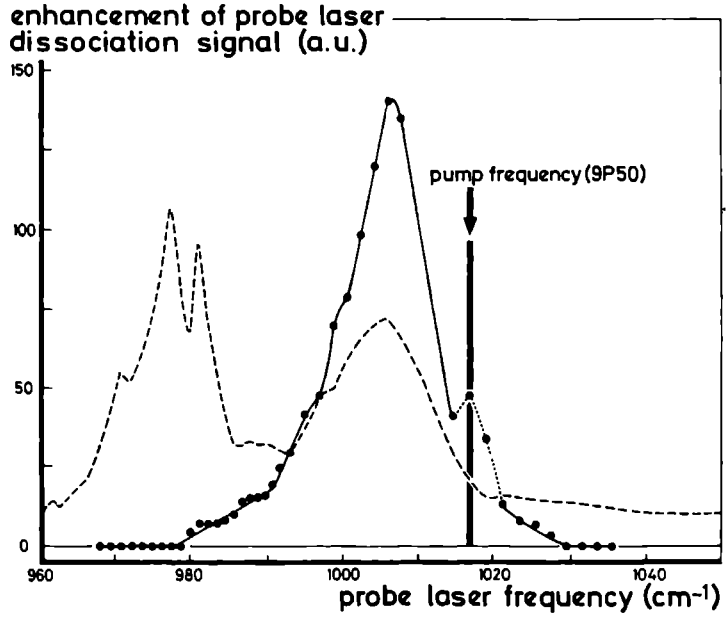

Figure 6

Two-step dissociation of ammonia trimers. First the trimers are excited by the pump laser but do not dissociate. Next, absorption of a second (probe-laser) photon yields dissociation. The pump laser was fixed near to the trimer excitation maximum (see fig. 5). The dotted shoulder around the excitation frequency is mainly attributed to depletion of trimer levels by the pump laser, yielding a reduction in the probe-laser-excitation-signal. The probe laser (pump laser) power was 3 Watt (9 Watt). The dashed curve indicates the one-laser predissociation spectrum.

Fig. 6 shows the enhanced probe-laser-dissociation-signal due to pumping as a function of probe-laser-frequency. The pump laser was fixed at 1016.72 cm^{-1}, the maximum of the trimer excitation peak (see fig. 5). The observed dissociation peak around 1006 cm^{-1} is shifted 10 cm^{-1} towards the red with respect to the excitation maximum. This shift reflects the anharmonicity of the potential of the ν_2-excitation of the complex. The here observed 10 cm^{-1} red shift is much smaller than the 329 cm^{-1} found for the free ammonia molecule [14,15]. This is not at all surprising since the umbrella mode is greatly altered in a cyclic bound trimer, containing hydrogen bonds which entirely suppress the inversion-motion.

The anharmonicity shift of 10 cm^{-1} is not reflected by the two-photon predissociation peak, measured by Huisken et al. [3], see fig. 1. For sharp transitions in long living complexes a red shift for the two-photon $2\nu_2$-excitation of about 5 cm^{-1} with respect to the ν_2-excitation frequency would have been expected. However, dissociating $2\nu_2$-excited states are rather smeared out in energy (see fig. 6). Therefore, the best trade-off between detuning of the intermediate ν_2 level and high transition probability to the final state leads here to a two-photon transition, essentially unshifted with respect to the one-photon excitation peak. The larger anharmonicity shift of 17 cm^{-1} yields a slightly red shifted two-photon peak for heavier clusters, see section 3.3.

The observation of a pump laser enhanced probe-laser-dissociation-signal implies that ν_2-excited trimers live longer than the travelling time of the trimer from pump- to probe-laser-beam, which is about 0.1 ms.

The dotted shoulder at 1016 cm^{-1} in fig. 6 will be discussed in section 3.4.

3.3. HIGHER AMMONIA CLUSTERS (n=4,5)

As was already pointed out in the introduction, the dip in the cw laser dissociation spectrum at 1045 cm^{-1} (see fig. 1) is accompanied by a sharp maximum in the pulsed-laser dissociation spectrum. This maximum is due to dissociation of tetramers and/or pentamers [3].

As in the case of the trimers (see section 3.2), an enhanced probe-laser-dissociation-signal has been observed in a two-laser experiment if the pump laser is tuned near to this dip (see fig. 1 and fig. 8). The pump laser

excites clusters without dissociating them. Next, absorption of a second (probe laser) photon leads to dissociation. The excitation curve has been measured for several probe-laser-frequencies. In all cases its maximum was around 1045 cm^{-1}. The power dependence of the excitation is depicted in fig. 7.

Fig. 9 shows the enhanced probe-laser-dissociation-signal as a function of probe-laser-frequency. The pump laser was fixed at the 9P20 laser line (1046.85 cm^{-1}), the maximum of the excitation curve (see fig. 8). The observed dissociation curve is shifted 17 cm^{-1} to the red with respect to the excitation maximum, again reflecting the anharmonicity of the potential of the ν_2-excitation of the complex. The dotted peak in fig. 9 will be discussed in the next section.

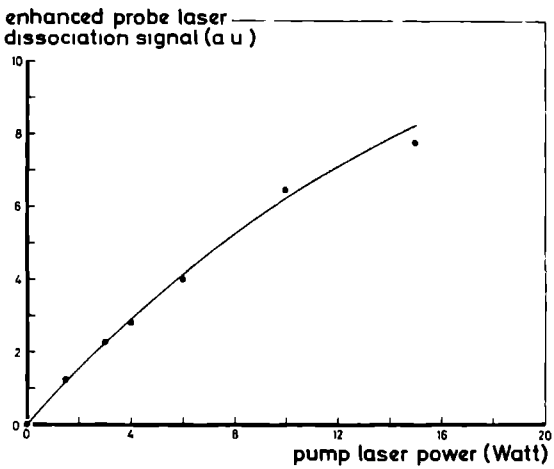

Figure 7

Power dependence of the excitation of $(NH_3)_{4,5}$. Excitation yields an enhanced probe-laser-dissociation-signal. The probe laser was fixed at 1031.48 cm^{-1}. The pump laser was tuned to the 9P20 laser transition (1046.48 cm^{-1}), near to the excitation maximum (see fig. 8). The spot diameter of the pump laser was about 0,8 mm.

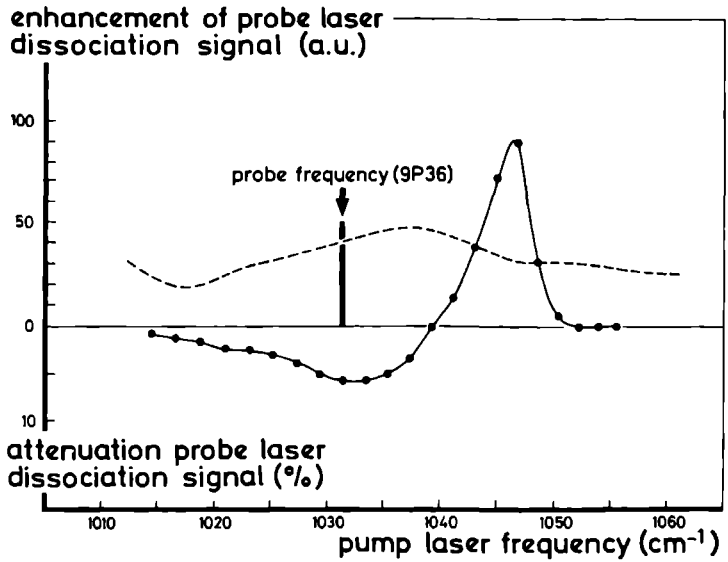

Figure 8

Excitation spectrum of $(NH_3)_{4,5}$. First the clusters are excited by the pump laser but do not dissociate. Next, absorption of a second (probe laser) photon yields dissociation. The broad negative peak around the probe-laser-frequency is due to hole burning in the spectrum of clusters that do dissociate after absorption of a single CO_2-laser photon. The probe laser (pump laser) power was 5 Watt (10 Watt). The dashed curve indicates the one-laser predissociation spectrum.

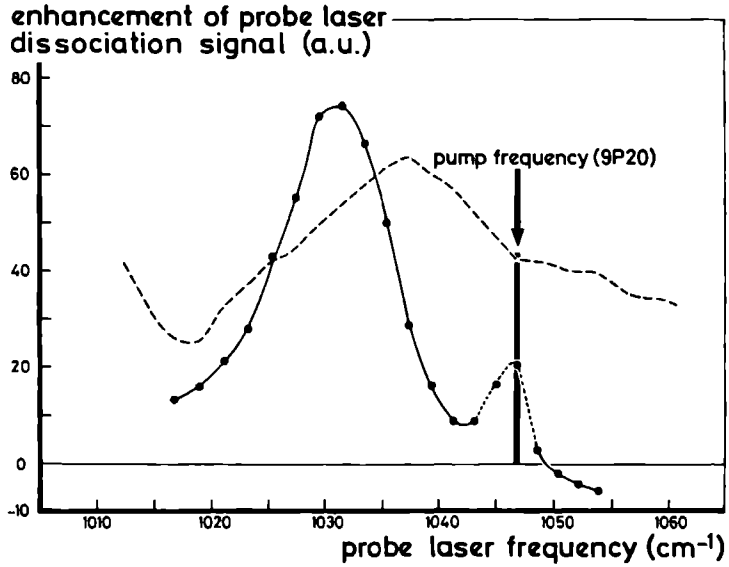

Figure 9

Two-step dissociation of $(NH_3)_{4,5}$. The pump laser was fixed near to the excitation maximum (see fig. 8). The dotted peak around the excitation frequency is mainly attributed to depletion of cluster levels by the pump laser, yielding a reduction in the probe-laser-excitation-signal. The probe laser (pump laser) power was 4 Watt (10 Watt). The dashed curve indicates the one-laser predissociation spectrum.

3.4. EXCITATION (WITHOUT DISSOCIATION) OF $(NH_3)_n$ (n=3,4,5)

3.4.1. Two-laser experiments

In general, irradiation of the molecular beam by infrared radiation leads to two processes. Some clusters absorb a photon and dissociate, others absorb but do not dissociate. In the first case irradiation yields a reduction of energy detected by the bolometer. However, excitation without dissociation leads to an increase of energy detected by the bolometer.

For ammonia clusters, excitation without dissociation is observed in two frequency regions, one around 1016 cm^{-1} and the other around 1045 cm^{-1} (see sections 3.2 and 3.3). However, at these frequencies other clusters also absorb a CO_2-laser-photon and do dissociate. For both above mentioned frequency regions the net effect of irradiation in a one-laser experiment is a reduction of energy at the bolometer (see the spectrum of Snels et al. in fig. 1).

Fig. 10 shows the result of a two-laser experiment on ammonia trimers with laser frequencies around 1016 cm^{-1}. The (chopped) probe laser is fixed at the trimer excitation maximum (1016.72 cm^{-1}). Switching on the (unchopped) pump laser yields an increased probe-laser-induced reduction of the molecular beam energy, i.e. a seemingly enhanced probe-laser-dissociation-signal. Note, however, that both enhancement of dissociation and reduction of excitation yield a decrease of energy delivered to the bolometer. In this experiment the pump laser excites trimers. Due to a reduction of the number of non-excited trimers the excitation signal of the probe laser diminishes. Moreover, the probe laser might produce stimulated de-excitation of pump-laser-excited trimers, also yielding a reduced probe-laser-excitation-signal. Stimulated de-excitation has been observed before in SF_6 and C_2H_4 [16,17]. The dotted features in figs. 6 and 9 at 1016 and 1045 cm^{-1}, respectively, are attributed to the here described phenomenon.

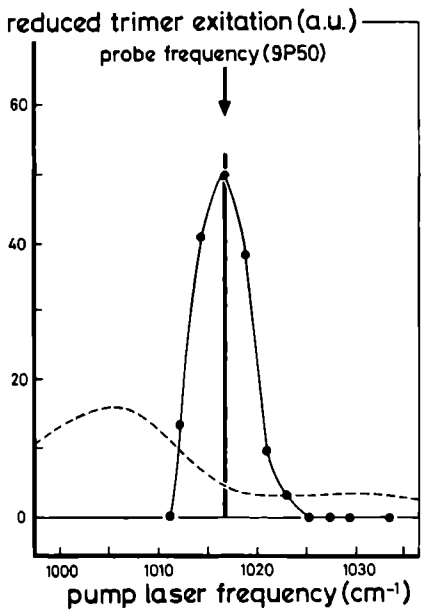

Figure 10

Depletion of trimer levels by the pump laser yields a reduction in probe-laser-excitation-signal. The probe (pump) laser power was 4 (8) Watt. The dashed line indicates the one-laser dissociation spectrum.

3.4.2. Three-laser experiments

In order to confirm this interpretation of our measurements two three-laser experiments have been performed (see figs. 2 and 11). In both experiments the probe laser was fixed at 1031.48 cm^{-1} (see fig. 8). Pump laser 1 was fixed at 1046.85 cm^{-1} (fig. 11a) or at 1048.66 cm^{-1} (fig. 11b). Pump laser 2 was scanned around the excitation peak (1045 cm^{-1}) with and without pump laser 1 on. The dashed lines in fig. 11 indicate the enhanced probe-laser-dissociation-signal due to pump laser 2 with pump laser 1 off (see also fig. 8). The solid lines connecting the heavy dots indicate the enhancement of probe-laser-dissociation-signal due to pumping with both pump lasers. This enhanced dissociation signal is built up in two steps. First only pump laser 1 is switched on at the 9P20 (fig. 11a) or 9P18 (fig. 11b) CO_2-laser transition. The effect on the probe-laser-dissociation-signal is in both figures indicated by a solid horizontal line. Next, pump laser 2 is switched on too, yielding a further enhancement of the probe-laser- dissociation-signal for all pumping frequencies of pump laser 2 (see fig. 11).

The observations in the three-laser experiments are in agreement with the interpretation of the dotted features in figs. 6 and 9, given in section 3.4.1. Pump laser 1 excites part of the clusters in the beam. Due to depletion of intial states, less clusters can be excited by pump laser 2. Furthermore pump laser 1 populates upper levels which might be partially de-populated by pump laser 2. Because of this depletion of initial levels and de-excitation of excited levels, if both pump laser 1 and pump laser 2 are switched on, the enhancement of probe-laser-dissociation-signal is smaller than the sum of the effects on the probe-laser-dissociation-signal of pump laser 1 and pump laser 2, (see fig. 11). This feature is observed for all frequencies of pump laser 2 and is strongest in fig. 11a for which pump laser 1 is at the maximum of the excitation profile.

3.4.3. Fine tuned spectra

Fig. 12a shows the result of a different type of double resonance experiment. Both the pump laser and the probe laser are tuned to the 9P50 CO_2-laser transition (1016.72 cm^{-1}), near to the trimer excitation maximum (see fig. 5). The probe laser is fixed in frequency, while the pump laser is piezo-electrically scanned around the 9P50 laser transition. As before (see

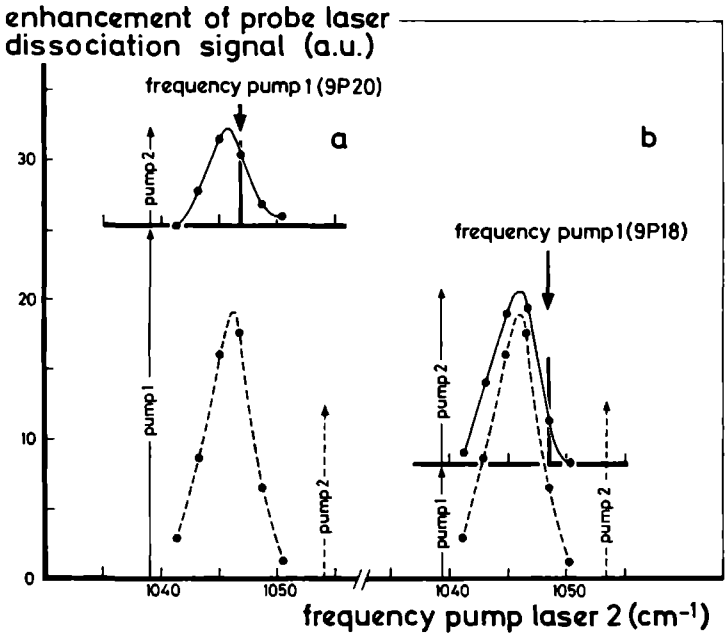

Figure 11

Three-laser experiments. The probe laser was fixed at 1031.48 cm^{-1} (see fig. 8). Pump laser 1 was fixed at 1046.85 cm^{-1} (fig. 11a) or at 1048.66 cm^{-1} (fig. 11b). Pump laser 2 was scanned around the excitation peak (1045 cm^{-1}) with (solid lines) and without (dashed lines) pump laser 1 on. Both in 11a and 11b the solid horizontal line indicates the enhanced probe-laser-dissociation-signal with only pump laser 1 on. The powers for the probe laser, pump laser 1 and pump laser 2 were 4 Watt, 15 Watt and 10 Watt, respectively.

fig. 10 and section 3.4.1), switching on the pump laser yields a reduction in energy transferred to the bolometer, independently of the fine tuning of the pump laser. However, if the two lasers are at precisely the same frequency one observes a sharp extra reduction in energy delivered to the bolometer. Apparently depletion and de-excitation processes occur mainly if the pump and the probe laser coincide in frequency. This feature will be discussed in section 5.

Narrow peaks in two-laser spectra have been observed at the 9P52 (1014.52 cm^{-1}), the 9P50 (1016.72 cm^{-1}), the 9P48 (1018.9 cm^{-1}) and the 9P46 (1021.06 cm^{-1}) CO_2 laser transitions. These are the pumping frequencies that lead to an enhanced probe-laser-dissociation-signal (see fig. 5). The intensities of the sharp peaks at the different above mentioned laser lines are roughly proportional to the intensities in the trimer excitation spectrum (see fig. 5).

Fig. 12b was measured with the set-up sketched in fig. 13. The pump laser was scanned, whereas the probe laser was fixed in frequency. Narrow features are observed for two pump-laser-frequencies. The two peaks belong to the two pump-laser-beams, pump 1 and pump 2 (see fig. 13). For the peak in the middle of the spectrum the pump and the probe-laser-frequencies coincide. This peak is produced by the pump-laser-beam perpendicular to the molecular beam (pump 2). The other sharp feature is due to the non-perpendicular pump-laser-beam (pump 1). Because of the Doppler shift for this laser beam, a narrow peak is produced if the frequencies of the probe laser and the pump laser differ by the amount of the Doppler shift. The linewidth of the sharp lines in figs. 12a and 12b is about 10 MHz, which is determined by laser instabilities.

A set-up can be chosen which avoids broadening by laser instabilities [16]. Only one laser is used which is split into a probe-laser-beam and a pump-laser-beam. The probe laser in fig. 13 is removed and instead of this laser, pump 2 is chopped and serves as probe-laser-beam. Pump 1 is the only pump-laser-beam. In this set-up the laser is not scanned in frequency. The frequency of pump 1 experienced by the clusters is tuned by scanning the tilt-angle of mirror M_2. In order to avoid that for zero tilt-angle laser-power is coupled back into the laser cavity a $\lambda/4$ plate in combination with a Brewster window had to be used. Fluctuations of the laser frequency affect the pump-beam-frequency and the probe-beam-frequency equally, thus avoiding line broadening due to laser instabilities.

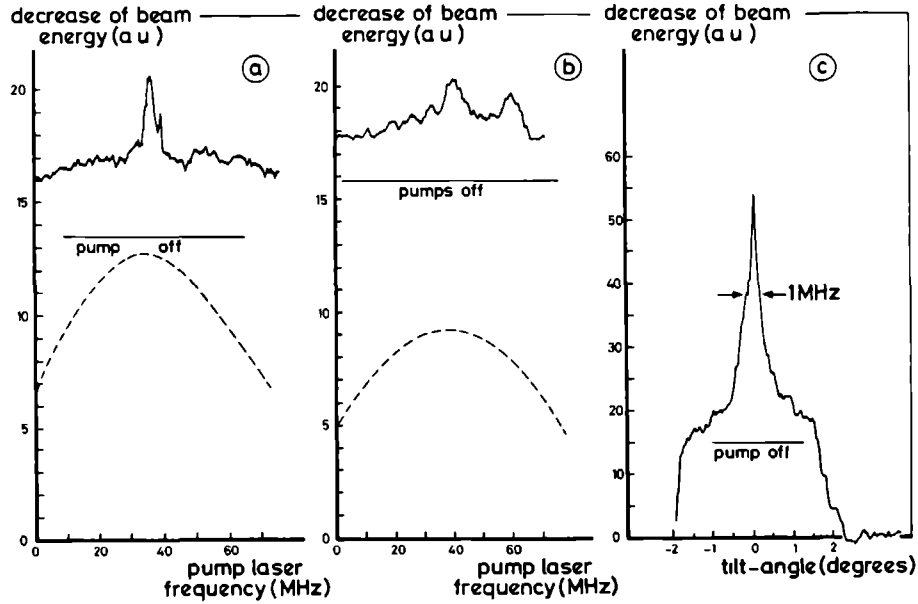

Figure 12

The pump and the probe laser were both tuned to the 9P50 laser transition (1016.72 cm^{-1}) near to the trimer excitation maximum.

a. The probe laser was fixed in frequency and the pump laser was scanned around the laser line.

b. The pump laser beam was split into two beams (see fig. 13). Again the pump laser was scanned.

c. The probe laser was removed and pump 2 (see fig. 13) was chopped. The tilt-angle of pump 1 was scanned.

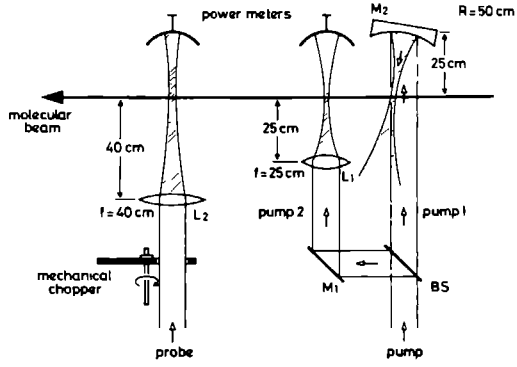

Figure 13

Experimental set-up for fig. 12b. The contribution to cluster excitation of the first (unfocused) passage of pump 1 through the molecular beam is negligible with respect to the contribution of the second (focused) passage. BS is a beam splitter and M_1 is a flat mirror.

Scanning the tilt-angle of the curved mirror M_2 (see fig. 13) yields the sharp line as a function of the pump-beam-tilt-angle, see fig. 12 c. The FWHM of the angle-tuned peak can be transferred to a corresponding FWHM in the frequency domain by calculating the Doppler shifts. In this way the FWHM could be reduced to about 1 MHz. This width is due to the residual Doppler width of a transition in the molecular beam. The big reduction in linewidth (from 10 MHz to 1 MHz) is accompanied by a corresponding increase in intensity of the narrow peak (compare figs. 12a and 12b with fig. 12c).

For the higher ammonia clusters (n=4,5) narrow peaks have not been observed. A higher level density with respect to the trimer level density is held responsible for the absence of sharp features, see section 5.

4. $ArNH_3$

By employing a very stable home-built waveguide CO_2-laser (scanning range 230 MHz) [11] we measured a (still instrumental) linewidth of 2 MHz for a predissociation transition in $ArNH_3$, yielding a minimum lifetime of 80 ns. Considerable line broadening has been observed at high laser powers. The line is situated 32±5 MHz towards the blue with respect to the 10P26 laser line centre (938.68826 cm^{-1}). Predissociation of $ArNH_3$ following excitation at the 10P26 laser line frequency has been reported before [5] and the linewidth was estimated to be about 100 MHz.

The waveguide laser was scanned at CO_2-laser lines around 940 cm^{-1} to search for more $ArNH_3$ transitions, however, without success. This hunt has been extended employing a long (1.8 m), high gain CO_2-laser (scanning range 83 MHz). This laser was operated on $^{13}CO_2$- and N_2O-transitions, again to no avail. Further work is in progress.

5. DISCUSSION

The experiments described in section 3 show that from initial states of the ammonia trimer transitions can be made to a band of non-dissociating final states, yielding a broad homogeneous excitation peak (see fig. 5). The width of this peak is 6.5 cm^{-1}. Its homogeneity is derived from the fact that the depletion/de-excitation-curve for the trimers in fig. 10 has essentially the same shape and width as the excitation curve (see fig. 5). The situation is schematically indicated in fig. 14, which displays the transition frequencies to ν_2-excited states for two different groundstate trimer levels. The sticks represent narrow (FWHM ≤ 1 MHz) peaks with transition strengths proportional to the stick-heights. For both levels the overall excitation bandwidth is about 6.5 cm^{-1}. The observation of the narrow peaks described in section 3.4.3 is attributed to the in fig. 14 suggested excitation spectra, consisting of in principle different sets of narrow lines for all groundstate trimer levels. Only if the pump and the probe laser coincide in frequency, all groundstate trimer levels from which probe-laser-excitation occurs can be (partially) depleted by the pump laser. Moreover, for equal probe- and pump-laser-frequencies all pump-laser-excited levels can be partially de-excited by the probe laser. Both these processes yield a sharp (FWHM ≤ 1 MHz) reduction

in the probe-laser-induced heat transfer to the bolometer for equal probe- and pump-laser-frequencies.

Comparing the dotted depletion/de-excitation peak for $(NH_3)_n$, n=4 or 5, in fig. 9 with the excitation peak in fig. 8 yields the same conclusions as for the trimers; from initial states of the tetramers and/or pentamers transitions can be made to a band of non-dissociating final states. The width of this band is about 4 cm^{-1}. The non-dissociating character of the final states excludes the contribution of lifetime effects to the widths of the observed peaks. If the density of narrow transitions in fig. 14 becomes very high, for every pump laser frequency around the excitation peak the majority of initial levels is depleted. In this case, a coincidence in frequency of pump and probe laser does not lead to an observable enhanced hole burning effect, i.e. no sharp peaks occur. This situation prevails for $(NH_3)_n$, n=4,5.

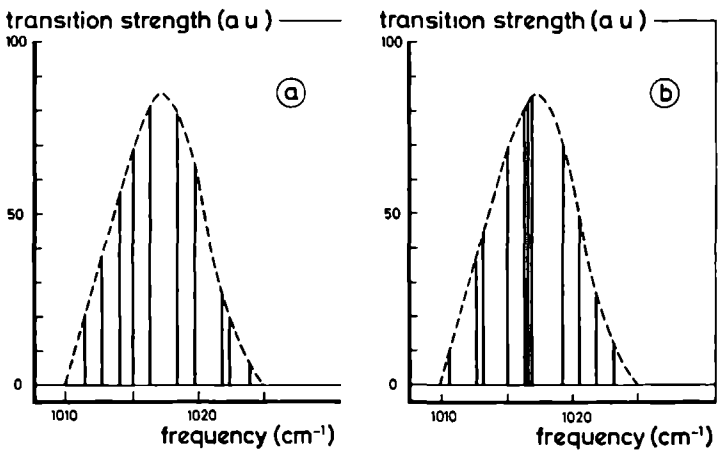

Figure 14

Transitions starting from two (14a and 14b) imaginary trimer groundstate levels. The sticks represent narrow (FWHM ≤ 1 MHz) lines.

6. CONCLUSIONS

Excitation with a CO_2-laser photon (1000 cm^{-1}) without dissociation has been observed for ammonia trimers and ammonia tetramers and/or pentamers, yielding broad (6.5 cm^{-1}, respectively, 4 cm^{-1}) homogeneous excitation peaks. For these clusters absorption of a second (red-shifted) photon yields dissociation. The red shifts (10 cm^{-1} for the trimer and 17 cm^{-1} for n=4,5) reflect the anharmonicity of the ν_2-potential of the complexes. The observed shifts are much smaller than the shift in the free ammonia molecule (329 cm^{-1}); the hydrogen bonds in the clusters quench the inversion motion. In case of the ammonia trimer sharp holes (1 MHz FWHM) were burnt into the broad (6.5 cm^{-1} FWHM) excitation peak.

ACKNOWLEDGEMENTS

The authors would like to thank Cor Sikkens, Frans van Rijn and John Holtkamp for technical and electronical support and advice. We thank dr. H. Bluyssen and A. van Etteger for designing our lasers and for lending us the third laser for the three-laser experiments. The support of A. van Etteger during the three-laser measurements is gratefully appreciated. This work is financially supported by the Stichting voor Fundamenteel Onderzoek der Materie (FOM) and the Nederlandse Organisatie voor Wetenschappelijk Onderzoek (NWO).

REFERENCES

[1] M. Snels, R. Fantoni, R. Sanders en W. Leo Meerts, Chem. Phys. 115 (1987) 79

[2] M. Snels, R. Fantoni and W.L. Meerts, in "Structure and Dynamics of Weakly Bound Molecular Complexes", NATO Advanced Research Workshop, ed. A. Weber (1986)

[3] F. Huisken and T. Pertsch, Book of Abstracts, XIth International Symposium on Molecular Beams, Edinburgh 1987

[4] U. Buck and H. Meyer, Phys. Rev. Lett. 52 (1984) 109

[5] G.T. Fraser, D.D. Nelson, A.C. Charo and W. Klemperer, J. Chem. Phys. 82 (1985) 2535

[6] D.D. Nelson, Jr., G.T. Fraser and W. Klemperer, J. Chem. Phys. 83 (1985) 6201

[7] Z. Latajka and S. Scheiner, J. Chem. Phys. 84 (1986) 341

[8] G. Duguette, T.H. Ellis, G. Scoles, R.O. Watts, and M.L. Klein, J. Chem. Phys. 68 (1978) 2554

[9] M.J. Howard, S. Burdenski, C.F. Giese and W.R. Gentry, J. Chem. Phys. 80 (1984) 4137

[10] J.A. Odutola, T.R. Dyke, B.J. Howard and J.S. Muenter, J. Chem. Phys. 70 (1979) 4884

[11] B. Heijmen, C. Liedenbaum, S. Stolte and J. Reuss, Z. Phys. D 6 (1987) 199

[12] B. Heijmen, C. Liedenbaum, S. Stolte and J. Reuss, accepted for publication in Laser Chemistry

[13] M. Snels, PhD thesis, Katholieke Universiteit Nijmegen 1986

[14] G. Herzberg, "IR and Raman Spectra of Polyatomic Molecules" (van Nostrand Reinhold Company, 1959)

[15] F.W. Taylor, J. Quant. Spectrosc. Radiat. Transfer 13 (1973) 1181

[16] C. Liedenbaum, S. Stolte and J. Reuss, submitted to Chem. Phys.

[17] C. Liedenbaum, B. Heijmen, N. Dam, S. Stolte and J. Reuss, Ber. Bunsenges. Phys. Chem. (in press)

CHAPTER 7

A MOLECULAR BEAM STUDY OF A VAN DER WAALS COMPLEX; THE LINEWIDTH OF A VIBRATION-INVERSION TRANSITION IN NH_3-Ar AT 938.69 CM^{-1}

B. Heijmen, A. Bizzarri, S. Stolte and J. Reuss
Physics Laboratory, University of Nijmegen
Toernooiveld, 6525 ED Nijmegen, The Netherlands

ABSTRACT

The linewidth of a ν_2-vibration transition of NH_3-Ar at 938.69 cm^{-1} has been found to be smaller than 2 MHz FWHM. This result yields a minimum lifetime of 80 ns.

Van der Waals complexes of NH_3 with NH_3 [1], HCCH [2], HCN [3], N_2O [4], CO_2 [5], HF [6], CF_3H [7], CO [8], N_2 [8], H_2O [9] and Ar [10,11] have been studied in the past; structural information has been mainly derived from high resolution microwave spectroscopy using the molecular beam electric resonance technique. Of all these complexes only NH_3-Ar shows unquenched inversion transitions. Evidence for this fact comes from the observed microwave transitions (especially those clustering between 19 and 20 GHz) and from the somewhat fortunate discovery of a narrow IR-transition at 938.69 cm^{-1} [10]. The linewidth of this transition was estimated to be 100 MHz FWHM [10].

The 8 transitions between 19 and 20 GHz were interpreted as perturbed inversion transitions, red-shifted with respect to the 23 GHz observed for the ammonia molecule [10]. An unquenched inversion would mean a nearly isotropic Ar-NH_3 potential, i.e. the NH_3-subunit is nearly freely rotating. A more detailed analysis of the $\Delta J=1$, $K=0$ progression supports this qualitative picture [11].

An unquenched inversion implies an inversion doublet for ν_2-vibrational transitions as in the free molecule, split by about 36 cm^{-1} and centered around 950 cm^{-1}. The single narrow transition at 938.69 cm^{-1} is interpreted as a lower doublet line [10]; the search for other lines has been unsuccessful. The odds to find a (FWHM=100 MHz) transition with a line-tunable CO_2-laser are about 1:600, considering about 100 CO_2-laser transitions which are distributed over a range of 200 cm^{-1}. Since we have found a considerably smaller FWHM, the odds were actually about 1:10000.

A 100 MHz linewidth of the 938.69 cm^{-1} transition yields a minimmum lifetime of about 1 ns. Except for NH_3-Ar and NH_3-HCCH, all other binary systems containing NH_3 have been found to possess much larger linewidths.

$(NH_3)_2$ was originally reported to form a stable ν_2-vibrationally excited complex, one 1000 cm^{-1} photon lacking sufficient energy to dissociate this supposed hydrogen bonded system [12]. This expectation was not borne out by other experiments [10,13,14]. Stable ν_2-vibrationally excited ammonia trimers and heavier ammonia clusters have been observed recently [14].

It is the purpose of this paper to actually measure the up to now only estimated linewidth of the 938.69 cm^{-1} vibration-inversion transition of NH_3-Ar and to obtain a sharper lower lifetime limit.

2. EXPERIMENTAL

The experimental set-up was similar to one described before [15]. As for the $(C_2H_4)_2$-IR-predissociation measurements [16], the complexes were vibrationally excited utilizing a small 62.5 cm long waveguide CO_2-laser with a tunability of about 230 MHz around the laser transitions. This laser has good frequency and intensity stability yielding a minimum instrumental linewidth of about 2 MHz FWHM.

The complex NH_3-Ar was produced in a supersonic expansion from a 9 bar source through a 30 μm diameter nozzle. The molecular beam was detected by means of a bolometer, operated at 4.2 K. The source chamber (laser chamber) is equipped with a 6000 l/s (3100 l/s) water baffled oil diffusion pump; the bolometer chamber is pumped by a 400 l/s oil diffusion pump aiding the cryopump, formed by the cold surfaces of the bolometer dewar.

The gas mixture consists of 2% NH_3, 10% Ar and 88% He. The bolometer deteriorates because of condensation of Ar at its surface; therefore, the mixture was prepared with only 10% Ar.

As mentioned in the introduction, NH_3-Ar has an unquenched ammonia inversion-motion; therefore, in the frequency range of the lower level of the inversion-doublet, transitions can be induced in NH_3-Ar as well as in NH_3. The here discussed 938.69 cm^{-1} transition disappears at lower stagnation pressures; moreover, absorption of a photon yields a reduction of beam energy transferred to the bolometer. These observations indicate that the observed transition is due to NH_3-Ar.

The absorption strength is comfortably high; already at a laser intensity of $I_{1/2}$=2 W/cm^2 the dissociation peak as detected by the bolometer reaches one half of its saturation value.

3. RESULTS AND DISCUSSION

The 938.69 cm^{-1} transition coincides with the 10P26 CO_2-laser transition. By putting a high voltage ramp on the PZT that controlled the cavity length of the laser, the frequency was scanned to determine the position and the linewidth of the transition. The line is situated (32±5) MHz towards the blue with respect to the 10P26 laser line centre (938.68826 cm^{-1}). A still instrumental FWHM of $\gamma/2\pi \simeq 2$ MHz was observed, corresponding to a minimum

lifetime of 80 ns and a minimum flight-path after absorption of a photon of about 0.1 mm. Considerable line broadening has been observed at higher laser powers.

The effective transition dipole moment can be estimated from the half-saturation at $I_{\frac{1}{2}}=2$ W/cm^2. On resonance half-saturation is reached at $\Omega^2_{Rabi}=\gamma^2$, yielding $\mu_{01}=0.07$ debye, in reasonable agreement with the expectation. Note that the ν_2-vibration of NH_3 has a transition dipole moment of 0.24 debye [17]. For γ, we have used the experimental FWHM value of $4\pi\cdot10^6$ Hz.

The laser has been scanned at CO_2-laser transitions around 940 cm^{-1} to search for more NH_3-Ar transitions, however, without success. This hunt has been extended employing a long (1.8 m), high gain, CO_2-laser which can be scanned over 83 MHz around the laser lines. This laser was operated on $^{13}CO_2$- and N_2O-transitions, again to no avail.

Further work with the waveguide laser is in progress. Moreover, in view of the large transition strength and because optimalization is possible due to the known narrow 938.69 cm^{-1} transition, NH_3-Ar is a good candidate for diode laser measurements which will be undertaken in the near future.

ACKNOWLEDGEMENTS

The measurements have greatly profited from the skilful assistance of Cor Sikkens and Frans van Rijn. This work has been supported by the Dutch Foundation for Fundamental Research (FOM) and has been made possible by financial support from the Dutch Organization for Scientific Research (NWO).

REFERENCES

[1] D.D. Nelson, G.T. Fraser and W. Klemperer, J. Chem. Phys. 83 (1985) 6201

[2] G.T. Fraser, K.R. Leopold and W. Klemperer, J. Chem. Phys. 80 (1984) 1423

[3] G.T. Fraser, K.R. Leopold, D.D. Nelson, A. Tung, and W. Klemperer, J. Chem. Phys. 80 (1984) 3073

[4] G.T. Fraser, D.D. Nelson, G. Gerven, and W. Klemperer, J. Chem. Phys. 83 (1985) 5442

[5] G.T. Fraser, K.R. Leopold and W. Klemperer, J. Chem. Phys. 81 (1984) 2577

[6] B.J. Howard, private communications

[7] G.T. Fraser, F.J. Lovas, R.D. Suenram, D.D. Nelson and W. Klemperer, J. Chem. Phys. 84 (1986) 5983

[8] G.T. Fraser, D.D. Nelson, K.I. Peterson and W. Klemperer, J. Chem. Phys. 84 (1986) 2472

[9] P. Herbine and T.R. Dyke, J. Chem. Phys. 83 (1985) 3768

[10] G.T. Fraser, D.D. Nelson, A.C. Charo and W. Klemperer, J. Chem. Phys. 82 (1985) 2535

[11] D.D. Nelson, G.T. Fraser, K.I. Peterson, K. Zhao, W. Klemperer, F.J. Lovas and R.D. Suenram, J. Chem. Phys. 85 (1986) 5512

[12] M.J. Howard, S. Burdenski, C.F. Giese, W.R. Gentry, J. Chem. Phys. 80 (1984) 4137

[13] M. Snels, R. Fantoni, R. Sanders and W.L. Meerts, Chem. Phys. 115 (1987) 79

[14] B. Heijmen, A. Bizzarri, S. Stolte and J. Reuss, to be published in Chem. Phys.

[15] M. Snels, R. Fantoni, M. Zen, S. Stolte and J. Reuss, Chem. Phys. Lett. 124 (1986) 1

[16] B. Heijmen, C. Liedenbaum, S. Stolte and J. Reuss, Z. Phys. D 6 (1987) 199

[17] T. Shimizu, F.U. Shimizu, R. Turner and T. Oka, J. Chem. Phys. 55 (1971) 2822

FOTO-EXCITATIE EN DISSOCIATIE VAN KLEINE MOLEKULAIRE KLUSTERS

Dit proefschrift beschrijft een systematische studie van infrarood-excitatie en dissociatie van $(C_2H_4)_2$ (Hoofdstukken 2 en 3), $(^{32}SF_6)_2$ (Hoofdstukken 4 en 5), $(^{32}SF_6)_3$, $^{34}SF_6(^{32}SF_6)_{1,2}$ en $(SiF_4)_2$ (Hoofdstuk 5), $(NH_3)_{2,3,4,5}$ (Hoofstuk 6) en NH_3Ar (Hoofdstuk 7). Deze van der Waals molekulen werden geëxciteerd door energie (een foton) te stoppen in een monomeer vibrationele mode van de molekulen in het kluster. Als de foton-energie groter is dan de bindingsenergie van het kluster leidt excitatie tot verbreking van de van der Waals binding. In dat geval spreekt men van dissociatie.

De klusters werden gevormd in een molekuulbundel door supersone expansie van een gasmengsel in vakuum. De sterke koeling van het gas in zo'n expansie is gunstig voor de vorming van deze zwakgebonden systemen. De molekuulbundel werd (behalve bij de experimenten beschreven in hoofdstuk 3) gedetekteerd met behulp van een cryogene bolometer met een werktemperatuur van 4.2 K. In geval van dissociatie ten gevolge van excitatie met een infrarood-foton verlaten de fragmenten de molekuulbundel met als gevolg een afname van de energie-overdracht aan de bolometer. Excitatie zonder dissociatie leidt tot een toename van overgedragen (vibrationele) energie.

De infraroodstraling werd geproduceerd door verschillende types CO_2-lasers. Om zeer smalle (1 MHz) lijnen te kunnen meten werd een stabiele CO_2-waveguide laser ontwikkeld met een verstembaarheid van 230 MHz rondom de CO_2-laser lijncentra. Ter vergroting van het aan de C_2H_4-clusters aangeboden laservermogen werd een lijnverstembare CO_2-laser zodanig om de molekuulbundel gebouwd dat de klusters door de laser cavity bewogen. Een extra vergroting van de laserintensiteit ter plaatse van de molekuulbundel werd verkregen met behulp van een lens in de laser cavity. Hiermee werd een intracavity focus gevormd ter plaatse van de molekuulbundel (zie hoofdstuk 2). Verder werd gewerkt met lijnverstembare, twee meter lange CO_2-lasers (maximum vermogen 50 W). Veel van de in dit proefschrift beschreven experimenten zijn "pomp en probe" experimenten met behulp van twee (dubbelresonantie) of drie lasers.

Er wordt aangetoond dat zowel de brede (12 cm^{-1}) homogene piek als de smalle (3.5 MHz) lijnen in het dissociatiespektrum van ethyleenklusters

afkomstig zijn van het dimeer. Aanwijzingen zijn gevonden dat de smalle lijnen afkomstig zijn van dimeren met een lage interne energie, terwijl de brede achtergrond te wijten is aan dimeren met hogere interne energieën. De gevonden niet-instrumentele lijnbreedte van 3.5 MHz korrespondeert met een minimum levensduur van 45 ns.

Voor $(^{32}SF_6)_2$ en $(^{28}SiF_4)_2$ geven dubbelresonantie experimenten inzicht in de breedtes van de pieken in de predissociatiespektra. De waargenomen korrelaties duiden op een distributie in de gemiddelde intermolekulaire afstand. Een model, gebaseerd op centrifugale distortie, dat een verdeling in intermolekulaire afstand oplevert wordt uiteengezet. Aangetoond wordt dat Coriolis-interaktie extra verbreding oplevert voor slechts één van de pieken in de spektra, in overeenstemming met de waarnemingen. De dubbelresonantiespektra voor $(^{32}SF_6)_2$ en $(^{28}SiF_4)_2$ zijn onafhankelijk van de relatieve polarisatie van de twee lasers. Met behulp van de dubbelresonantietechniek werden predissociatiespektra van $^{32}SF_6$-trimeren en van $(^{32}SF_6)_n{}^{34}SF_6$ (n=1,2) gemeten. Deze spektra worden vergeleken met berekeningen, gebaseerd op een model voor excitatie van een drievoudig ontaarde monomeer-mode in een kluster.

Voor ammonia dimeren zijn korrelaties en homogene lijnbreedtes bepaald voor de pieken in het predissociatiespektrum. Ammoniaktrimeren en enkele zwaardere ammoniakklusters kunnen geëxciteerd worden met een CO_2-laser foton zonder dat dissociatie optreedt. In het geval van het trimeer werd een homogene excitatie bandbreedte van 6.5 cm^{-1} gevonden. Zowel voor de trimeren als voor de zwaardere klusters leidt absorptie van een tweede (roodverschoven) foton tot dissociatie. Ten gevolge van demping van de inversiebeweging in deze ammoniakklusters zijn de waargenomen ν_2-anharmoniciteits-roodverschuivingen (10 cm^{-1} voor $(NH_3)_3$ en 17 cm^{-1} voor $(NH_3)_{4,5}$) veel kleiner dan voor het vrije ammoniakmolekuul (329 cm^{-1}). In de brede (6.5 cm^{-1}) excitatiepiek van het ammoniaktrimeer konden smalle (1 MHz) gaten gebrand worden.

Voor NH_3Ar werd een (instrumentele) lijnbreedte van 2 MHz gevonden voor een predissociatielijn, duidend op een minimale levensduur van 80 ns.

CURRICULUM VITAE

B.J.M. Heijmen

geboren 22 mei 1959 te Westervoort

1971-1976 : HAVO, RK Scholengemeenschap Presikhaaf, Arnhem

1976-1978 : VWO (Atheneum B), Thomas a Kempis College, Arnhem

1978 : begin natuurkundestudie aan de Katholieke Universiteit Nijmegen

1981 : kandidaatsexamen natuurkunde met bijvak informatika

1982 : begin afstudeeronderzoek op de afdeling Molekuul en Laserfysika onder leiding van prof.dr. J. Reuss

maart 1984 : doktoraalexamen natuurkunde

april 1984 : begin promotieonderzoek (in dienst van stichting FOM) op de afdeling Molekuul en Laserfysika onder leiding van prof.dr. J. Reuss

mei 1987 : in het kader van het promotieonderzoek werkzaam bij het Max Planck Institut für Strömungsforschung te Göttingen (West-Duitsland) bij prof.dr. U. Buck

STELLINGEN

1. De door Bokor et al. waargenomen piek in het multifoton UV fotodissociatie-spektrum van CO is, in tegenstelling tot wat de auteurs beweren, niet te wijten aan een overgang in het C-fragment; deze struktuur is de omhullende van rotationele lijnen van de spin-verboden $a^3\Pi, v'=2 \leftarrow X^1\Sigma^+, v''=0$ één-foton overgang.

   J. Bokor, J. Zavelovich and C.K. Rhodes, J. Chem. Phys. 72 (1980) 965

2. De onafhankelijkheid van het orientatie-effekt voor de aangelegde zespoolspanning in de experimenten van Novakoski en McClelland impliceert dat de kwantitatieve uitkomst van hun experimenten door andere parameters dan de orientatieparameter bepaald wordt.

   L.V. Novakoski and G.M. McClelland, Phys. Rev. Lett. 56 (1987) 1259

3. De bevinding van Novakoski en McClelland dat HCF_3 vanaf een Ag(111)-oppervlak bij voorkeur desorbeert met het H-atoom gericht naar het oppervlak maakt, in tegenstelling tot beweringen van bovengenoemde auteurs, de bindingskonfiguratie HCF_3-Ag(111) aannemelijk.

   L.V. Novakoski and G.M. McClelland, Phys. Rev. Lett. 56 (1987) 1259

4. In geval van een singlet-triplet koppeling moet, bij vergelijking van de toestandsdichtheid verkregen uit spektra met rotationele resolutie met de toestandsdichtheid volgens de Haarhoff-vergelijking, kernspin-statistiek buiten beschouwing gelaten worden.

   B.J. van der Meer, H.Th. Jonkman, J. Kommandeur, W.L. Meerts and W.A. Majewski, Chem. Phys. Lett. 92 (1982) 565;
   P.C. Haarhoff, Mol. Phys. 7 (1963) 101

5. De kortere stijgtijd van de ν_{12}-fluorescentie ten opzichte van de ν_7-fluorescentie in de experimenten van Häger et al. is waarschijnlijk eerder een gevolg van de bijna-resonantie tussen de $2\nu_{12}$-band en de gepompte ν_{11}-band dan van het door de auteurs veronderstelde verschil in energie-uitwisselingsmechanisme.

   J. Häger, W. Krieger, T. Rüegg and H. Walther, J. Chem. Phys. 70 (1979) 2859

6. Multifoton overgangen spelen mogelijkerwijs een rol in Zeeman-spektra van het O_2-Ne dimeer. Recent werk toont het optreden van dergelijke overgangen in andere systemen aan.

7. Het fitten van een Lorentziaan aan een min of meer op een Lorentziaan lijkende piek in het predissociatiespektrum van een kluster heeft in bepaalde gevallen slechts een geringe fysische betekenis.

   M. Snels and R. Fantoni, Chem. Phys. 109 (1986) 67;
   dit proefschrift

8. Voor het C_2H_4-SF_6 dimeer is een niet-lokale excitatie (één foton verdeeld over 2 molekulen) zoals waargenomen voor het SF_6 dimeer te verwachten.

9. Het uitvoeren van drie-laser experimenten is soms lastig. Het duidelijk overbrengen van wat gemeten is lijkt vaak onmogelijk.

10. Het verdergaand fakultatief stellen van het bestuderen van vreemde talen op middelbare scholen zou een situatie scheppen die in meerdere opzichten vergelijkbaar zou zijn met die van een vrije keuze voor kinderen om al dan niet regelmatig hun tanden te poetsen.

11. De voordelen van een alfabetische ordening in de lijst van auteurs van een publikatie worden vaak onderschat.

    "Private communications" with A. Aaba

Ben Heijmen

22 juni 1988